

INTERNATIONAL JOURNAL OF RESEARCH CULTURE SOCIETY

ISSN: 2456-6683

Monthly Peer-Reviewed, Refereed, Indexed Research Journal

UGC approved Journal with Global Indexing

Publishes original research papers/articles, reviews, mini-reviews, case studies, synopsis, research project and short research communications of all subjects/topics

Special Issue of IJRCS

Proceedings of the **National Seminar**

GREEN CHEMISTRY FOR SUSTAINABLE DEVELOPMENT

(GCSD -2017)

6th & 7th APRIL, 2017



Benefits to publish the Paper in IJRCS

- IJRCS is an Open-Access, peer reviewed, Indexed, Refereed International Journal.
- Author Research Guidelines & Support.
- Platform to researchers and scholars of different field.
- Reliable and Rapidly growing Publication with nominal publication fees.
- Prestigious Editorials from different Institutes of the world.
- Communication of authors to get the manuscript status time to time.
- Quick and Speedy Review Process.
- Full text of all articles in the form of PDF format.
- Individual copy of "Certificate of Publication" to all Authors of Paper.
- Indexing of paper in all major online journal databases like Google Scholar, Academia, Scribd, Mendeley, and Internet Archive.
- Open Access Journal Database for High visibility and promotion of your article with keyword and abstract.
- Provides ISSN to Conference / Seminar Proceeding papers.



RESEARCH CULTURE SOCIETY & PUBLICATION

Email: editorijrcs@gmail.com

Web Email: editor@ijrcs.com

Cont. No: +91 9033767725

WWW.IJRCS.ORG



Research Culture Society & Publication



UGC Sponsored

National Seminar
on

**GREEN CHEMISTRY FOR SUSTAINABLE
DEVELOPMENT**
(GCSD -2017)

6th & 7th APRIL, 2017



Organized by

Department of Chemistry
Government Degree College, Jammikunta
Re-accredited by NAAC with 'B' Grade (Cycle 2)
Dist. Karimnagar, Telangana State

INAUGURAL FUNCTION

The Students, staff and organizing committee cordially invites
you to the inaugural function of (GCSD -2017) on 6th
April, 2017 at 10.00 a.m.

Dr. K. Ramakrishna

Chairman & Principal
Government Degree College, Jammikunta
President of the Function

Chief Guest

Prof. T. Papi Reddy

Chairman
Telangana State Council of Higher Education (TSCHE), Hyderabad

Key Note Speaker

Dr. G. Narahari Shastry

Shanti Swarup Bhatnagar Awardee,
DST JC Bose National Fellow, FNASc
CSIR-Indian Institute of Chemical Technology (IICT), Hyderabad

Guest of Honour

Prof. M. Komal Reddy

Registrar
Satavahana University, Karimnagar

Dr. B. Ramesh

Vice-Principal & Head, Department of Chemistry
Convener

Scientific Programme: Day-I (6th April, 2017, Thursday)		Scientific Programme: Day-II (7th April, 2017, Friday)	
9.00 - 10.00 am	Registration	09.30 - 11.00 am	Technical Session-IV: Lead Lecture_IV Dr. K. Laxma Reddy, FAPAS, FTAS Dean, Research & Consultancy and Professor of Chemistry National Institute of Technology (NIT), Warangal & Paper presentations
10.00 - 11.15 am	Inauguration	11.00 - 12.00 noon	Technical Session-V: Lead Lecture_V Dr Shirish Sonawane DST BOYSCAST FELLOW, FNASc, Associate Professor, Department of Chemical Engineering National Institute of Technology (NIT), Warangal
11.15 - 11.45 am	Key Note Address Dr. G.Narahari Shastry Shanti Swarup Bhatnagar Awardee, DST JC Bose National Fellow, FNASc CSIR-Indian Institute of Chemical Technology (IICT), Hyderabad	12.00 - 12.15 pm	Tea Break
11.45 - 12.00 noon	Tea Break	12.15 - 1.15 pm	Technical Session-VI: Lead Lecture_VI Dr. Bhaskar Tallada Principal Scientist CSIR-Indian Institute of Petroleum (IIP), Dehradun
12.00 - 01.30 pm	Technical Session-I: Lead Lecture_I Dr. K. Rajender Reddy Principal Scientist CSIR-Indian Institute of Chemical Technology (IICT), Hyderabad & Paper presentations	1.15 - 2.00 pm	Lunch Break
01.30 - 02.30 pm	Lunch Break	02.00 - 03.00 pm	Technical Session-VII: Lead Lecture_VII Dr. S. Prabhakar Principal Scientist National Centre for Mass Spectrometry CSIR-Indian Institute of Chemical Technology (IICT), Hyderabad
02.30 - 04.00 pm	Technical Session-II: Lead Lecture_II Dr. Dhurke Kashinath Assistant Professor National Institute of Technology (NIT), Warangal & Paper presentations	03.00 - 03.15 pm	Tea Break
04.00 - 04.15 pm	Tea Break	03.15 - 04.30 pm	Valedictory Function Cheif Guest: Prof.CH. Sanjeeva Reddy Registrar, NIPER, Hyderabad
04.15 - 05.30 pm	Technical Session-III: Lead Lecture_III Dr. V. Chandrasekhar Head & Associate Professor Department of Pharmaceutical Chemistry Telangana University, Nizamabad & Poster presentations		

INDEX

SR.NO	TITLE - AUTHOR	PAPER ID	PAGE.NO
1	Aerobic Oxidative Cross-Coupling Of O-Phenylenediamines And 2-Aryl/Heteroarylethylamines: A Direct Approach To Construct Quinoxalines - D. Chenna Rao, Gopalaiah Kovuru	GCSD001	1-6
2	A Mild And Efficient Method For The Cleavage Of Primary T-Butyldimethylsilyl (TBS) Ethers In Presence Of Secondary T-Butyldimethylsilyl (TBS) Ethers By Zirconium (IV) Chloride - B. Sreenivas, Prashanth Thodupunuri & Gangavaram V. M. Sharma	GCSD002	7-11
3	Molecular Docking Approach To Evaluate The Antibacterial Effect Of Pyridinyl-3-Aminophenylmethane Sulphonamides On 1fxv: A Comparative Study With Pencillin G. - Venkata Bharat Nishtala, Vinaypogaku And Srinivasbasavoju	GCSD003	12-15
4	Solvent-Free Microwave Assisted Synthesis Of (E)-1-(2,4-Dihydroxy-5-{(E)-3-[3-(4-Aryl)-1-Phenyl-1h-4-Pyrazolyl]-2-Propenoyl}-Phenyl)-3-[3-(4-Aryl)-1-Phenyl-1h-4-Pyrazolyl]-2-Propene-1-Ones - Ramesh Banothu, V. Ravinder Reddy And Veerabathini Manohar	GCSD004	16-19
5	Novel Three-Component One-Pot Synthesis Of 1,2-Dihydro-1-Aryl-Naphtho[1,2-E] [1,3]Oxazin-3-One Derivatives Catalyzed By Cu(II)-Nay Zeolite And Their Evaluation Of Biological Activity K. Sudhakar, Y. Hemasri, Y. Jayaprakash Rao, K. Arundhathi & Thota Anupama Yadav	GCSD005	20-25
6	A Structure-Based Qsar And Docking Studies On Donepzil Derivatives As Selective Ache Inhibitors - Dr. B. Venkateshwarlu	GCSD006	26-35
7	Noval Method Devevelopment Of Ertapenem By Spectrophotometric Determination In Bulk And Injection Formulations By Cobalt Thio Cyanate - N. Aruna Kumari, A.Vasundhra	GCSD007	36-41
8	Solvent Effects In The Reaction Between Allyl Bromide And Thioacetamide - B. Ramesh, B. Kavitha , D. Vijaya Bharathi And P. Manikyamba	GCSD008	42-46
9	Synthesis Of Multifunctional Nanocomposites Of Superparamagnetic (Fe ₃ O ₄) /Sio ₂ Nanoparticles K.Anjaneyulu, Gundu.Mallikarjun	GCSD009	47-52
10	Cellulase Production By Trichoderma Sp. Under Solid State Fermentation Using Delignified Rice Straw - J Sridevi	GCSD010	53-56
11	Insect Growth Regulating Activity Of Betulinic Acid In Controlling Coreyra Cephalonica - N. Sridevi, S. Sabita Raja, N. Shilaja Yougender	GCSD011	57-61

UGC Sponsored Two Day National Seminar on GREEN CHEMISTRY FOR SUSTAINABLE DEVELOPMENT (GCSD -2017)

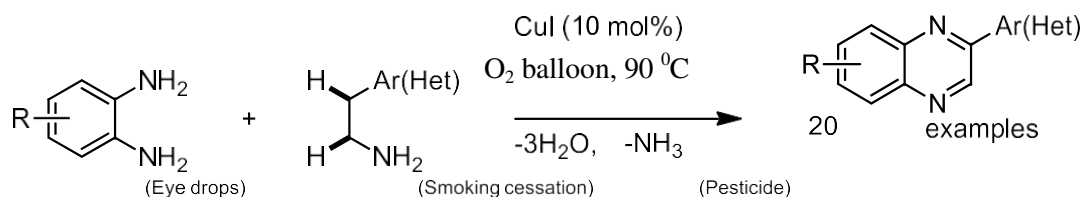
April 06 - 07, 2017 at Government Degree College,
Jammikunta, Karimnagar, Telangana State, India

Aerobic Oxidative Cross-Coupling of *o*-Phenylenediamines and 2-Aryl/Heteroarylethylamines: A Direct approach to construct Quinoxalines

D. Chenna Rao¹, Gopalaiah Kovuru²

^{1 & 2} Organic Synthesis and Catalysis Laboratory, Department of Chemistry, University of Delhi
Delhi-110 007, India

Email - dchennarao@yahoo.co.in



Abstract: Quinoxaline, which is one of the well-known and important classes of nitrogen heterocyclic compounds, exhibits extensive biological and pharmaceutical properties. This scaffold is also an active core unit of several antibiotics, pesticides, herbicides, fungicides, and advanced functional materials. Owing to these important applications, a large number of synthetic methods have been developed to construct quinoxalines. Our study commenced with the reaction of *o*-phenylenediamine and 2-phenylethylamine catalyzed by Copper salts. In air, 2-phenylquinoxaline was obtained in 73% isolated yield upon treatment of a 1 : 1.2 mixture with 20 mol% CuI in chlorobenzene at room temperature for 12 h. Other Cu salts, also showed catalytic activity, but they were found to be less effective. Finally, the reaction conditions described in the scheme were chosen as the standard conditions for further exploration.

1. INTRODUCTION:

Quinoxaline derivatives are an important class of nitrogen-containing heterocycles as they represent useful intermediates in organic synthesis. They received paramount importance from the pharmaceutical industry because of their active therapeutic properties viz., anti-inflammatory, antiviral, antibacterial, antiprotozoal and kinase inhibitors.¹ They also acts as antifungal, anticancer, anthelmintic, and insecticidal agents.² Commercially, the quinoxaline moiety is a part of several antibiotics such as levomycin, echinomycin, olaquinox, carbadox and actinoleutin that are known to inhibit the growth of gram-positive bacteria and are active against various transplantable tumors.³ Furthermore, they have found applications as dyes, cavitands, organic semiconductors, electroluminescent materials, chemically controllable switches, and DNA cleaving agents.^{4,5} As they exhibit a broad spectrum of biological properties, they are considered as privileged structures in combinatorial drug discovery. Drug formulations containing quinoxalines such as brimonidine, varenicline, quinalphos, clofazimine, carbadox, cyadox and quizalofop-ethyl are currently available (Figure 1).

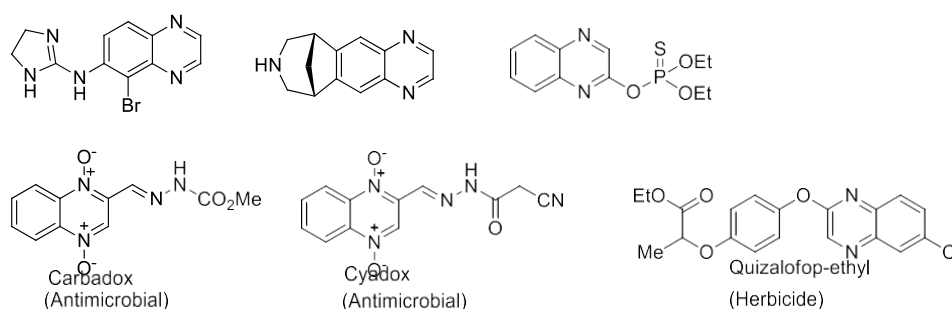
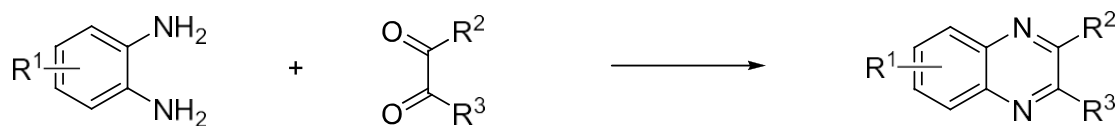


Figure 1 Some Biologically Active Quinoxaline Compounds

Conventionally, Quinoxaline synthesis has been carried out by a double condensation between 1,2-dicarbonyl compounds and *o*-phenylenediamines (Scheme 1). The reaction is catalyzed by indium(III) chloride,⁶ copper(II) sulfate,⁷ *o*-iodoxybenzoic acid, ceric ammonium nitrate,⁸ phosphorus oxychloride,⁹ iodine,¹⁰ silica gel,¹¹ gallium(III) tri-flate and clayzic.¹²

Nevertheless, the handling of highly reactive dicarbonyl compounds is an important drawback in this method.

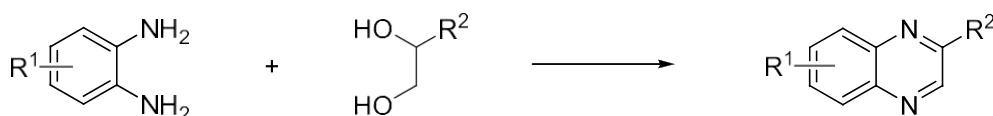


R^1 = aryl, alkyl, alkoxy, CN, NO_2

$R^2 = R^3$ = aryl, alkyl, heteroaryl

Scheme 1 Classical method to prepare quinoxalines

There have been several creditable approaches for the quinoxaline syntheses in the literature, and some of them are briefly discussed here. One of the approaches involve the oxidative trapping of vicinal diols with *o*-phenylenediamines in the presence of metal catalysts (Scheme 2). Cho^{13a} and Kempe^{13b} independently developed ruthenium and iridium catalysts, respectively, for this transformation. These reactions were promoted in the presence of strong bases such KOH and *t*-BuOK.

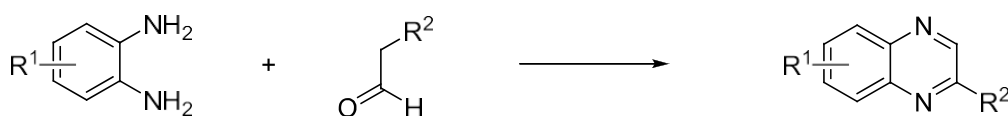


R^1 = H, alkyl

R^2 = aryl, alkyl, heteroaryl

Scheme 2 Synthesis of quinoxalines from vicinal diols and *o*-phenylenediamines

Recently, Chen and co-workers reported the synthesis of quinoxalines via transition-metal-free cyclization of arylacetaldehydes and *o*-phenylenediamines (Scheme 3).¹⁴ In this process, an inorganic base (K_2CO_3) is the only reagent required, and the reaction proceeded smoothly under air atmosphere.



R^1 = H, alkyl, alkoxy, halogen

R^2 = aryl, alkyl

Scheme 3 Preparation of quinoxalines from arylacetaldehydes and *o*-phenylenediamines

In this protocol, we report an efficient and practical approach for synthesis of quinoxaline derivatives from the oxidative condensation of 2-arylethylamines with 2-aminoanilines in the presence of copper catalyst and molecular oxygen. This route is an attractive and environmentally friendly for a variety of functionalized quinoxaline in a simple and one-pot procedure.

2. RESULTS AND DISCUSSION:

The optimization study has been initiated by conducting the reaction of 2-phenylethylamine (**1a**, 1.2 equiv) with 2-aminoaniline (**2a**, 1 equiv). Initially, **1a** and **2a** were treated with iron(II) bromide (5 mol %) at 110 °C in chlorobenzene and the reaction system was equipped with an oxygen balloon (Table 1, entry 1). This resulted the formation of 2-phenylquinoxaline (**3a**) in 53% after 24 hours. Motivating by these results, we further tested several other commercially available iron compounds such as FeCl_2 , FeCl_3 and FeBr_3 (Table 1, entries 2-4). Although the formation of 2-phenylquinoxaline was observed with many iron salts, the yields were lower as compared with the reaction of iron(II) bromide.

To enhance the yields, copper catalysts such as CuBr₂, Cu(OAc)₂, CuO, CuCl and CuI were screened with molecular oxygen in the reaction (Table 1, entries 5-9). The catalytic system with copper and oxygen has been demonstrated to be very effective for the aerobic oxidation of benzylic methylene group.¹⁵ Elatedly, the reaction is progressive when CuI was used, and the yield of **3a** rose to 75% (Table 1, entry 9). The yield of **3a** was further enhanced by the increase of catalyst loading to 10 mol% (entry 10). There was no effect on yield by further increase of the catalyst loading (entry 11). Among the various solvents screened, chlorobenzene gave the best results (entries 10 and 12-14). Lower yields of **3a** were observed when the reactions are carried out either at a lower temperature or under air atmosphere (entries 15 and 16). However, perceptibly no desired product was obtained when the reaction was performed under nitrogen atmosphere in the same conditions, demonstrating that oxygen is the terminal oxidant (entry 17). The conditions identified in the entry 10, Table 1 were therefore used for further reactions.

To explore the applicability of this method, the scope of the oxidative coupling reaction was examined under the optimized conditions (Table 2 and Table 3). A variety of 2- arylethylamines were allowed to react with 2-aminoaniline in the presence of 10 mol % of CuI in chlorobenzene under molecular oxygen (Table 2). 2-Phenylethylamines bearing different substitution patterns and electronic properties were proven to be suitable substrates, giving products in good yields. With unsubstituted 2-phenylethylamine, the desired product 2-phenylquinoxaline (**3a**) was isolated in high yield (Table 2, entry 1). Amine substrates possessing electron-withdrawing groups (eg. -Br) (Table 2, entry 2) produced a slightly higher yields of desired product than their analogues bearing an electron-donating substituents (eg. -OMe, -OH) (Table 2, entries 3 and 4). Additionally, heteroaryl ethylamines, such as 2-(2-pyridyl)ethylamine (**1e**), 2-thiopheneethylamine (**1f**) and 3-(2-aminoethyl)indole (**1g**) could also be used as substrates, leading to formation of the corresponding 2-(pyridin-2-yl)quinoxaline (**3e**), 2-(thiophen-2-yl)quinoxaline (**3f**) and 2-(1H-Indol-3-yl)quinoxaline (**3g**) in 81%, 86% and 84% yields, respectively (Table 2, entries 5-7). Ostensibly, an aliphatic amine such as 1-(2- aminoethyl)piperazine (**1h**) has been appears to be a suitable substrate which gave the quinoxaline (**3h**) in 75% yield (Table 2, entry 8).

Subsequently, we studied the effect of various 2-aminoanilines **2b-2j** with 2- phenylethylamine (**1a**) under the standard conditions (Table 3). The reaction of 4,5-disubstituted symmetrical 2-aminoanilines **2b-d** gave the corresponding cyclized products **4b-d** as single isomers in each case in high yields (Table 3, entries 1-3). On the other hand, the monosubstituted 2-aminoanilines **2e-j** obtained in a mixture of two possible regioisomers in good yields. Most of these regioisomers were easily isolable by column chromatography (Table 3, entries 4-9).

Lastly, the synthetic utility of the reaction protocol was examined by preparing certain biologically active compounds. For instance, 6,7-dimethyl-2-phenylquinoxaline (**4b**) and 2- phenylbenzo[g]quinoxaline (**4d**) are EGFR tyrosine kinase inhibitors.¹⁶

3. CONCLUSIONS:

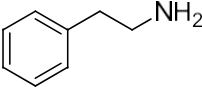
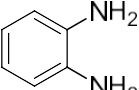
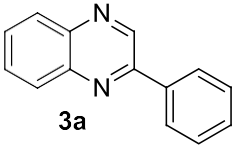
The development a novel and efficient protocol for the synthesis of quinoxalines from 2- arylethylamines with 2-aminoanilines is a simple and one-pot approach with wide substrate scope. Several structurally diverse 2-arylethylamines and 2-aminoanilines were potentially effective for the reaction, leading to the formation of quinoxalines in high yields. Simple, inexpensive and commercially available copper(I) iodide promoted the reaction in the presence of molecular oxygen as a sole oxidant, which makes the process more economical and practically viable. We have also tested the reaction protocol to synthesize 6,7-dimethyl-2-phenylquinoxaline and 2-phenylbenzo[g]quinoxaline, which are EGFR tyrosine kinase inhibitors.

REFERENCES:

1. He, W.; Meyers, M. R.; Hanney, B.; Sapada, A.; Blider, G.; Galzeinski, H.; Amin, D.; Needle, S.; Page, K.; Jayyosi, Z.; Perrone, H. *Bioorg. Med. Chem. Lett.* **2003**, 13, 3097.
2. Sakata, G.; Makino, K.; Kuraswa, Y. *Heterocycles* **1988**, 27, 2481.
3. Dell, A.; William, D. H.; Morris, H. R.; Smith, G. A.; Feeney, J.; Roberts, G. C. K. *J. Am. Chem. Soc.* **1975**, 97, 2497.
4. Katoh, A.; Yoshida, T.; Ohkanda, J. *Heterocycles* **2000**, 52, 911. (b) Thomas, K. R. J.; Velusamy, M.; Lin, J. T.; Chuen, C. H.; Tao, Y. T. *Chem. Mater.* **2005**, 17, 1860.
5. Sessler, J. L.; Maeda, H.; Mizuno, T.; Lynch, V. M.; Furuta, H. *J. Am. Chem. Soc.* **2002**, 124, 13474. (b) Crossley, M. J.; Johnston, L. A. *Chem. Commun.* **2002**, 1122.
6. Hazarika, P.; Gogoi, P.; Konwar, D. *Synth. Commun.* **2007**, 37, 3447.
7. Heravi, M. M.; Taheri, S.; Bakhtiari, K.; Oskooie, H. A. *Catal. Commun.* **2007**, 8, 211. (8). More, S. V.; Sastry, M. N. V.; Yao, C.-F. *Green Chem.* **2006**, 8, 91.
8. Venkatesh, C.; Singh, B.; Mahata, P. K.; Iia, H.; Junjappa, H. *Org. Lett.* **2005**, 7, 2169.
9. Bhosale, R. S.; Sarda, S. R.; Ardhapure, S. S.; Jadhav, W. N.; Bhusare, S. R.; Pawar, R. P. *Tetrahedron Lett.* **2005**, 46, 7183.
10. Nandi, G. C.; Samai, S.; Kumar, R.; Singh, M. S. *Synth. Commun.* **2011**, 41, 417.

11. Cai, J.-J.; Zou, J.-P.; Pan, X.-Q.; Zhang, W. *Tetrahedron Lett.* **2008**, 49, 7386. (b) Dhakshinamoorthy, A.; Kanagaraj, K.; Pitchumani, K. *Tetrahedron Lett.* **2011**, 52, 69.
12. Hille, T.; Irrgang, T.; Kempe, R. *Chem. – Eur. J.*, **2014**, 20, 5569. (b) Cho, C. S.; Oh, S. *G. Tetrahedron Lett.*, **2006**, 47, 5633.
14. Song, J.; Li, X.; Chen, Y.; Zhao, M.; Dou, Y.; Chen, B. *Synlett* **2012**, 2416.
15. Allara, D. L. *J. Org. Chem.* **1972**, 37, 2448. (b) Dhakshinamoorthy, A.; Alvaro, M.; Garcia, H. J. *Catal.* **2009**, 267, 1.
16. Ibrahim, M. M.; Grau, D.; Hampel, F.; Tsogoeva, S. B. *Eur. J. Org. Chem.* **2014**, 1401.

Table 1 Optimization of Reaction Conditions for the Synthesis of Quinoxalines^a

<div style="display: flex; justify-content: space-around; align-items: center;"> <div style="text-align: center;">  <p>1a</p> </div> <div style="text-align: center;">  <p>2a</p> </div> <div style="text-align: center;"> <p>catalyst</p> </div> <div style="text-align: center;">  <p>3a</p> </div> </div>				
Entry	Catalyst	Solvent	Time (h)	Yield (%) ^b
1	FeBr ₂	chlorobenzene	24	53
2	FeCl ₂	chlorobenzene	24	38
3	FeCl ₃	chlorobenzene	24	31
4	FeBr ₃	chlorobenzene	24	36
5	CuBr ₂	chlorobenzene	24	65
6	Cu(OAc) ₂	chlorobenzene	24	49
7	CuO	chlorobenzene	24	35
8	CuCl	chlorobenzene	24	68
9	CuI	chlorobenzene	24	75
10 ^c	CuI	chlorobenzene	18	92
11 ^d	CuI	chlorobenzene	18	92
12 ^c	CuI	toluene	24	79
13 ^c	CuI	anisole	24	74
14 ^c	CuI	DMSO	24	59
15 ^{c,e}	CuI	chlorobenzene	24	23
16 ^{c,f}	CuI	chlorobenzene	24	68
17 ^{c,g}	CuI	chlorobenzene	24	trace

^a Reaction conditions: **2a** (2.0 mmol), **1a** (2.4 mmol), catalyst (5 mol %), solvent (2 mL), 110 °C, molecular oxygen. ^b Isolated yield. ^c Using 10 mol % of catalyst. ^d Using 20 mol % of catalyst. ^e Reaction was carried out at 80 °C. ^f Reaction was carried out in air atmosphere. ^g Reaction carried out in inert atmosphere.

Table 2 Substrate Scope of 2-Arylethylamines^a

Entry	Amine (1)	Time (h)	Product (3)	Yield (%) ^b	
1	1a	18	3a	92	
2	1b	21	3b	95	
3	1c	20	3c	90	
4	1d	23	3d	89	
5	1e	24	3e	81	
6	1f	21.5	3f	86	
7	1g	18.0	3g	84	
8	1h	24	3h	75	

^a Reaction conditions: **1a** (1.3 mmol), **2a** (1.0 mmol), CuI (10 mol %), chlorobenzene (1 mL), 110 °C, O₂ balloon.^b Isolated yield.

Table 3 Substrate Scope of 2-Aminoanilines^a

Entry	Amine (2)	Time (h)	Product (4) ^b	Ratio ^c
1		21	 4b, 70	
2		24	 4c, 79	
3		24	 4d, 73	
4		21	 4e, 41	 4e', 32
5		24	 4f, 47	 4f', 30
6		22	 4g, 47	 4g', 22
7		20	 4h 74 ^d	 4h' 1:1
8		20	 4i 76 ^d	 4i' 2:1
9		25	 4j 65 ^d	 4j' 0.9:1

^a 1a (1.2 mmol), 2 (1.0 mmol), CuI (10 mol %), chlorobenzene (1 mL), 100 °C, O₂ balloon.^b Isolated yield. ^c NMR ratio of regioisomers. ^d Yield of both regioisomers.^a Reaction conditions:

UGC Sponsored Two Day National Seminar on GREEN CHEMISTRY FOR SUSTAINABLE DEVELOPMENT (GCSD -2017)

April 06 - 07, 2017 at Government Degree College,
Jammikunta, Karimnagar, Telangana State, India

A Mild and Efficient Method for the cleavage of primary *t*-butyldimethylsilyl (TBS) ethers in presence of secondary *t*-butyldimethylsilyl (TBS) ethers by Zirconium (IV) chloride

B. Sreenivas¹, Prashanth Thodupunuri² & Gangavaram V. M. Sharma³

^{1, 2, 3} Organic and Biomolecular Chemistry Division, CSIR-Indian Institute of Chemical Technology, Hyderabad – 500 007, India

Email - ¹vasujith@gmail.com; ²sreenivasbommagani@gmail.com

Abstract: A very mild and efficient method for removal of primary *t*-butyldimethylsilyl (TBS) ethers in the presence of secondary *t*-butyldimethylsilyl (TBS) ethers using catalytic amount of ZrCl₄ (20 mol %) as Lewis acid in isopropanol at room temperature in short time. Various functional groups such as TPS, Bn, Allyl, Bz, Ac, PMB and isopropylidene acetals are found to be stable under the reaction conditions.

Keywords: Deprotection, *t*-butyldimethylsilyl (TBS) ethers, zirconium (IV) chloride, isopropanol, protecting groups.

1. INTRODUCTION

Protection and deprotection of functional groups plays a very prominent role in organic synthesis. A large number of protecting groups are available for free hydroxyl groups¹. Silyl protecting groups are widely used as hydroxyl group protecting agents in organic synthesis due to their stability towards many reagents and reaction conditions^{1c}. Though a wide variety of reagents have been developed² for their removal, still there is a need to develop better alternatives, which might work under mild conditions. Although protic acids and fluoride sources continue to be widely used for the removal of silyl protecting groups, a number of Lewis acids have been introduced to mediate desilylation reactions. Some examples from the literature: BF₃-OEt₂³, BCl₃⁴, Sc(OTf)₃⁵, InCl₃⁶, ZnBr₂⁷, CeCl₃-7H₂O/NaI⁸, BiOClO₄-xH₂O⁹ and FeCl₃¹⁰. Only few methods are available for the selective deprotection of primary TBS ethers in the presence of secondary TBS ethers¹¹.

In our previous studies on the protection and deprotection¹²⁻¹⁵ of alcoholic functional groups by using Lewis acids, we have successfully deprotected, selectively the primary TBS in the presence of secondary TBS and PMB groups by using 20 mol% of ZrCl₄ in isopropanol at ambient temperature (Figure 1).

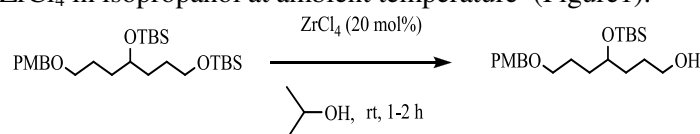


Figure 1

A variety of TBS ethers were prepared from aliphatic and sugar alcohols, in addition to diols possessing other different protecting groups. Out of those protecting groups only primary TBS was deprotected using 20 mol% of ZrCl₄ in isopropanol at room temperature for 60 min gave **1a** in 92% yield, while secondary TBS remained unaffected. A similar study on **2**, **3** and **4** possessing TPS, benzylic and allylic protecting groups, when treated with 20 mol% of ZrCl₄ at room temperature in isopropanol gave the expected products **2a** (89%), **3a** (92%) and **4a** (91%), respectively, in which the TPS, benzylic and allylic groups remained unaffected during the primary desilylation.

In a further study with **5** and **6**, which possess the base sensitive acetate and benzoate groups gave the respective alcohols **5a** (92%) and **6a** (88%), respectively. Earlier our group reported^{14a} a facile deprotection of *p*-methoxybenzyl (PMB) group with ZrCl₄ in CH₃CN. However, the reaction of **7** with ZrCl₄ in isopropanol resulted in **7a** while PMB remained unaffected. Even though, both the PMB and TBS are known to undergo cleavage in CH₃CN, in isopropanol PMB and secondary TBS remained unchanged. In addition TBS ether **8** was subjected to desilylation with 20 mol% ZrCl₄ in isopropanol at room temperature to give **8a** in 89% yield. The study was then extended to the sugar substrates **9** and **10** possessing 1,3-dioxolane protecting groups. Initially, reaction of **9** with 20 mol% of ZrCl₄ at room temperature gave **9a** in 79% yield, while desilylation of **10** at room temperature gave **10a** in 90% yield in 6 h.

2. EXPERIMENTAL SECTION:

General: Solvents were dried over standard drying agents and freshly distilled prior to use. ^1H -NMR (200 MHz, 300 MHz and 400 MHz) spectra were measured with a Varian Gemini FT-200 MHz spectrometer, Bruker-Avance 300 MHz and Varian Unity FT-400 MHz with tetramethylsilane as internal standard for solutions in deuteriochloroform. J values are given in Hz. Mass spectra were recorded on CEC-21-11013 or Finnigan Mat 1210 double focusing mass spectrometers operating at a direct inlet system. IR spectra were recorded on Nicolet 740-FT spectrometer as neat liquids. Organic solutions were dried over anhydrous Na_2SO_4 and concentrated below 40°C in *vacuo*.

***tert*-Butyl[(4-[1-(*tert*-butyl)-1,1-dimethylsilyl]oxyheptyl)oxy]dimethylsilane, 1:** To a stirred solution of 4-[1-(*tert*-butyl)-1,1-dimethylsilyl]oxy-1-heptanol (**1a**; 0.2 g, 0.86 mmol) in CH_2Cl_2 (10 mL), imidazole (0.087 g, 1.29 mmol) and TBSCl (0.129 g, 0.86 mmol) were added and stirred at room temperature for 2 h. The reaction mixture was diluted with water (20 mL) and extracted with CH_2Cl_2 (20 mL). Organic layer was washed with brine (20 mL), dried (Na_2SO_4), concentrated under reduced pressure and purified by column chromatography (silica gel, EtOAc: hexane, 0.5:9.5) to afford **1** (0.336 g, 85%) as a colourless syrup. IR (neat): 2921, 2835, 1527, 1117, 698, 612, 502 cm^{-1} ; ^1H NMR (300 MHz, CDCl_3): δ 0.03 (s, 12H), 0.82-0.9 (m, 21H), 1.21-1.47 (m, 8H), 3.52-3.61 (m, 3H); FABMS (m/z %): 361 ($\text{M}+\text{H}$)⁺, 345 (12), 244 (8), 147 (32), 111 (22), 73 (100), 55 (26).

***tert*-Butyl[(4,7-di[1-(*tert*-butyl)-1,1-dimethylsilyl]oxyheptyl)oxy]diphenylsilane, 2:** To a stirred solution of 4,7-di[1-(*tert*-butyl)-1,1-dimethylsilyl]oxy-1-heptanol (0.2 g, 0.53 mmol) in CH_2Cl_2 (10 mL), imidazole (0.054 g, 0.79 mmol) and TPSCl (0.12 mL, 0.53 mmol) were added and stirred at room temperature for 2 h. The reaction mixture was worked up as described for **1** and purified by column chromatography (silica gel, EtOAc: hexane, 0.5:9.5) to afford **2** (0.27 g, 83%) as a colourless syrup. IR (neat): 2940, 2851, 1417, 1017, 845, 612, 521 cm^{-1} ; ^1H NMR (300 MHz, CDCl_3): δ 0.02 (s, 12H), 0.87 (s, 18H), 1.02 (s, 9H), 1.42-1.52 (m, 8H), 3.51-3.62 (m, 5H), 7.28-7.39 (m, 6H, Ar-H), 7.57-7.64 (m, 4H, Ar-H); FABMS (m/z %): 500 ($\text{M}-114$)⁺, 374 (21), 318 (14), 244 (12), 188 (15), 147 (45), 73 (100).

[(7-(benzyloxy)-4-[1-(*tert*-butyl)-1,1-Dimethylsilyl]oxyheptyl)oxy](*tert*-butyl) dimethylsilane, 3: To a stirred solution of 4,7-di[1-(*tert*-butyl)-1,1-dimethylsilyl]oxy-1-heptanol (0.2 g, 0.53 mmol) in anhydrous THF (10 mL), NaH (0.025 g, 1.06 mmol, 60% suspension) was added in portions with constant stirring at 0°C . After 10 min, benzyl bromide (0.075 mL, 0.63 mmol), was added and stirred at room temperature for 6 h. Excess NaH was quenched by slow and careful addition of MeOH (5 mL), diluted with water (10 mL) and extracted into ether (2 X 20 mL). Combined ether extracts were washed with brine solution (10 mL), dried (Na_2SO_4), concentrated under reduced pressure and purified by column chromatography (silica gel, EtOAc: hexane, 0.5:9.5) to afford **3** (0.2 g, 81%) as a pale yellow syrup. IR (neat): 2943, 2892, 1466, 1253, 1087, 845, 778 cm^{-1} ; ^1H NMR (200 MHz, CDCl_3): δ 0.06 (s, 12H), 0.88 (s, 18H), 1.42-1.7 (m, 8H), 3.42 (t, 2H, $J = 5.71$ Hz), 3.6 (t, 2H, $J = 5.71$ Hz), 3.63-3.71 (m, 1H), 4.48 (s, 2H, $\text{Ph}-\text{CH}_2$), 7.15-7.37 (m, 5H, Ar-H); FABMS (m/z %): 466 (M)⁺, 281 (7), 240 (14), 136 (24), 91 (100), 69 (41), 57 (83).

[(7-(allyloxy)-4-[1-(*tert*-butyl)-1,1-Dimethylsilyl]oxyheptyl)oxy](*tert*-butyl) dimethyl silane, 4: To a stirred solution of 4,7-di[1-(*tert*-butyl)-1,1-dimethylsilyl]oxy-1-heptanol (0.2 g, 0.53 mmol) in anhydrous THF (10 mL), NaH (0.025 g, 1.06 mmol, 60% suspension) was added in portions with constant stirring at 0°C . After 10 min, allyl bromide (0.054 mL, 0.63 mmol), was added and stirred at room temperature for 6 h. The reaction mixture was worked up as described for **3** and purified by column chromatography (silica gel, EtOAc: hexane, 0.5:9.5) to afford **4** (0.19 g, 86%) as a pale yellow syrup. IR (neat): 2952, 2831, 1504, 1121, 911, 601, 507 cm^{-1} ; ^1H NMR (400 MHz, CDCl_3): δ 0.09 (s, 12H), 0.92 (s, 18H), 1.42-1.68 (m, 8H), 3.4 (t, 2H, $J = 5.55$ Hz), 3.54 (t, 2H, $J = 5.55$ Hz), 3.62-3.69 (m, 1H), 3.92 (d, 2H, $J = 8.8$ Hz), 5.16 (d, 1H, $J = 11.2$ Hz), 5.27 (d, 1H, $J = 18.8$ Hz), 5.8-5.92 (m, 1H); FABMS (m/z %): 359 ($\text{M}-57$)⁺, 285 (9), 185 (16), 133 (21), 95 (58), 73 (100), 59 (19).

4,7-Di[1-(*tert*-butyl)-1,1-dimethylsilyl]oxyheptyl benzoate, 5: To a stirred solution 4,7-di[1-(*tert*-butyl)-1,1-dimethylsilyl]oxy-1-heptanol (0.2 g, 0.53 mmol) in CH_2Cl_2 (10 mL), triethylamine (0.22 mL, 1.5 mmol) and benzoyl chloride (0.06 mL, 0.53 mmol) were added at 0°C , stirred at room temperature for 2 h. The reaction mixture was diluted with water (20 mL) and extracted with CH_2Cl_2 (20 mL). Organic layer was washed with brine (20 mL), dried (Na_2SO_4), concentrated under reduced pressure and purified by column chromatography (silica gel, EtOAc: hexane, 0.5:9.5) to afford **5** (0.23 g, 90%) as a colourless syrup. IR (neat): 2942, 2896, 1723, 1462, 1267, 1104, 837, 712 cm^{-1} ; ^1H NMR (300 MHz, CDCl_3): δ 0.02 (s, 12H), 0.82 (s, 18H), 1.38-1.62 (m, 6H), 1.69-1.82 (m, 2H), 3.62 (t, 2H, $J = 5.62$ Hz), 3.61-3.72 (m, 1H), 4.24 (t, 2H, $J = 5.62$ Hz), 7.3-7.51 (m, 3H, Ar-H), 7.96 (d, 2H, Ar-H, $J = 6.25$ Hz); FABMS (m/z %): 423 ($\text{M}-57$)⁺, 207 (12), 179 (15), 136 (18), 105 (64), 73 (100).

4,7-Di[1-(*tert*-butyl)-1,1-dimethylsilyl]oxyheptyl acetate, 6: To a stirred solution 4,7-di[1-(*tert*-butyl)-1,1-dimethylsilyl]oxy-1-heptanol (0.2 g, 0.53 mmol) in CH_2Cl_2 (10 mL), triethylamine (0.22 mL, 1.5 mmol) and acetic anhydride (0.05 mL, 0.53 mmol) were added at 0°C , stirred at room temperature for 3 h. The reaction mixture was worked up as described for **5** and purified by column chromatography (silica gel, EtOAc: hexane, 1.0:9.0) to afford **6** (0.19 g, 87%) as a pale yellow syrup. IR (neat): 2921, 2836, 1736, 1237, 1104, 690 cm^{-1} ; ^1H NMR (300 MHz, CDCl_3): δ 0.02 (s, 12H), 0.79 (s, 18H), 1.39-1.72 (m, 8H), 2.02 (s, 3H, CH_3-CO), 3.59 (t, 2H, $J = 8.57$ Hz), 3.63-3.69 (m, 1H), 4.1 (t, 2H, $J = 8.57$ Hz); FABMS (m/z %): 361 ($\text{M}-57$)⁺, 306 (8), 288 (12), 185 (16), 95 (86), 73 (100).

tert-Butyl(4-[1-(tert-butyl)-1,1-dimethylsilyl]oxy-1-3-[(4-methoxybenzyl)oxy] propylbutoxy)dimethylsilane, 7: To a stirred solution of 4-[1-(tert-butyl)-1,1-dimethylsilyl]oxy-7-[(4-methoxybenzyl)oxy]-1-heptanol (**7a**; 2.5 g, 6.5 mmol) in CH_2Cl_2 (25 mL), imidazole (0.66 g, 9.8 mmol) and TBSCl (1.17 g, 7.8 mmol) were added and stirred at room temperature for 2 h. The reaction mixture was worked up as described for **1** and purified by column chromatography (silica gel, EtOAc: hexane, 1.0:9.0) to afford *tert*-butyl(4-[1-(tert-butyl)-1,1-dimethylsilyl]oxy-1-3-[(4-methoxybenzyl)oxy] propylbutoxy)dimethylsilane **7** (3.12 g, 96%) as a colourless syrup. IR (neat): 2930, 2833, 1517, 1100, 689, 612, 517 cm^{-1} ; ^1H NMR (300 MHz, CDCl_3): δ 0.02 (s, 12H), 0.85 (s, 18H), 1.4-1.7 (m, 8H), 3.38 (t, 2H, $J = 8.57$ Hz), 3.55 (t, 2H, $J = 8.57$ Hz), 3.61-3.68 (m, 1H), 3.73 (s, 3H, OCH_3), 4.36 (s, 2H, Ar- CH_2), 6.79 (d, 2H, Ar-H, $J = 10.55$ Hz), 7.15 (d, 2H, Ar-H, $J = 10.55$ Hz); FABMS (m/z %): 496 (M^+), 133 (9), 121 (100), 95 (8), 73 (32), 58 (10).

tert-Butyl(4-[1-(tert-butyl) 1,1dimethylsilyl]oxy-4 phenylbutoxy)dimethylsilane, 8: To a stirred solution of 1-phenyl-1,4-butanediol (0.1 g, 0.6 mmol) in CH_2Cl_2 (10mL), imidazole (0.122 g, 1.8 mmol) and TBSCl (0.216 g, 1.44 mmol) were added and stirred at room temperature for 12 h. The reaction mixture was worked up as described for **1** and purified by column chromatography (silica gel, EtOAc: hexane, 0.5:9.5) to afford **8** (0.21 g, 89%) as a colourless syrup. IR (neat): 3042, 2921, 2835, 1517, 1127, 691, 612, 507 cm^{-1} ; ^1H NMR (300 MHz, CDCl_3): δ 0.1 (s, 12H), 0.98 (s, 18H), 1.5-1.88 (m, 4H), 3.67 (t, 2H, $J = 5.8$ Hz), 4.74 (t, 1H, $J = 5.8$ Hz), 7.28-7.37 (m, 5H, Ar-H); FABMS (m/z %): 303 ($\text{M}-91$) $^+$, 245 (16), 171 (19), 113 (58), 95 (72), 73 (100), 55 (42).

tert-Butyl4-[1-(tert-butyl)-1,1dimethylsilyl]oxy-4-[(4R)-2,2-dimethyl-1,3-dioxolan-4-yl]butoxydimethylsilane, 9: To a stirred solution of 4-[1-(tert-butyl)-1,1-dimethylsilyl]oxy-4-[(4R)-2,2-dimethyl-1,3-dioxolan-4-yl]-1-butanol (0.25 g, 0.82 mmol) in CH_2Cl_2 (25 mL), imidazole (0.083 g, 1.23 mmol) and TBSCl (0.148 g, 0.98 mmol) were added and stirred at room temperature for 2 h. The reaction mixture was worked up as described for **1** and purified by column chromatography (silica gel, EtOAc: hexane, 0.25:9.75) to afford **9** (0.3 g, 87%) as a colourless syrup. IR (neat): 2928, 2834, 1517, 1127, 693, 614, 517 cm^{-1} ; ^1H NMR (300 MHz, CDCl_3): δ 0.03 (s, 12H), 0.86 (s, 18H), 1.3 (s, 3H), 1.38 (s, 3H), 1.42-1.57 (m, 4H), 3.58 (t, 2H, $J = 4.61$ Hz), 3.63-3.68 (m, 1H), 3.82-3.91 (m, 3H); FABMS (m/z %): 403 ($\text{M}-15$) $^+$, 361 (10), 303 (14), 171 (21), 133 (14), 101 (18), 73 (100).

[(3aR,5R,6S,6aR)-6-[1-(tert-butyl)-1,1 Dimethylsilyl]oxy-2,2-dimethylperhydro furo[2,3-d][1,3]dioxol-5-yl)methoxy](tert-butyl)dimethylsilane, 10: To a stirred solution of (3aR,5R,6S,6aR)-5-(hydroxymethyl)-2,2-dimethylperhydrofuro[2,3-d][1,3]dioxol-6-ol (0.2 g, 1.05 mmol) in CH_2Cl_2 (10 mL), imidazole (0.214 g, 3.15 mmol) and TBSCl (0.315 g, 2.1 mmol) were added and stirred at room temperature for 12 h. The reaction mixture was worked up as described for **1** and purified by column chromatography (silica gel, EtOAc: hexane, 1.0:9.0) to afford **10** (0.363 g, 82%) as a pale yellow syrup. IR (neat): 2943, 2859, 1507, 1102, 892, 615, 507 cm^{-1} ; ^1H NMR (300 MHz, CDCl_3): δ 0.06 (s, 6H), 0.08 (s, 6H), 0.85 (s, 18H), 1.24 (s, 3H), 1.45 (s, 3H), 3.62-3.74 (m, 2H, H-5), 3.96-4.06 (m, 1H, H-3), 4.1 (d, 1H, H-4, $J = 4.2$ Hz), 4.22 (d, 1H, H-2, $J = 4.2$ Hz), 5.73 (d, 1H, H-1, $J = 4.2$ Hz); FABMS (m/z %): 403 ($\text{M}-15$) $^+$, 361 (12), 303 (10), 261 (12), 89 (25), 73 (100).

General experimental procedure for deprotection of primary t-butyl dimethylsilyl (TBS) ethers in presence of secondary t-butyl dimethylsilyl (TBS) ethers: A solution of silyl ether (1.0 mmol) in isopropanol (10 mL) was treated with ZrCl_4 (0.2 mmol) and stirred at room temperature until the starting material completely disappeared (tlc analysis). The solvent was removed under reduced pressure and the residue treated with EtOAc (20 mL), washed with water (10 mL), brine (10 mL), dried (Na_2SO_4) and evaporated under reduced pressure. The residue was purified by column chromatography (60-120 mesh silica gel, EtOAc: hexane) to furnish the desilylated products, which were characterized by IR, ^1H NMR and Mass spectra.

4-[1-(tert-butyl)-1,1-Dimethylsilyl]oxy-1-heptanol, 1a: Colourless syrup, 60 min, 92% yield. IR (neat): 2941, 2843, 1407, 1247, 842, 531 cm^{-1} ; ^1H NMR (300 MHz, CDCl_3): δ 0.02 (s, 6H), 0.81-0.92 (m, 12H), 1.31-1.44 (m, 8H), 3.54-3.62 (m, 3H); EIMS (m/z %): 231 ($\text{M}-15$) $^+$, 187 (21), 73 (100), 55 (46).

4-[1-(tert-butyl)-1,1-Dimethylsilyl]oxy-7-[1-(tert-butyl)-1,1-diphenylsilyl]oxy-1 heptanol, 2a: Pale yellow syrup, 105 min, 89% yield. IR (neat): 2923, 2831, 1503, 1117, 792, 614, 521 cm^{-1} ; ^1H NMR (200 MHz, CDCl_3): δ 0.03 (s, 6H), 0.9 (s, 9H), 1.09 (s, 9H), 1.5-1.61 (m, 8H), 3.52-3.74 (m, 5H), 7.36-7.41 (m, 6H, Ar-H), 7.59-7.64 (m, 4H, Ar-H); FABMS (m/z %): 485 ($\text{M}-15$) $^+$, 427 (16), 189 (51), 147 (12), 96 (100), 76 (72).

7-(benzyloxy)-4-[1-(tert-butyl)-1,1-Dimethylsilyl]oxy-1-heptanol, 3a: Colourless syrup, 105 min, 92% yield. IR (neat): 2938, 2852, 1463, 1243, 1081, 805, 678 cm^{-1} ; ^1H NMR (300 MHz, CDCl_3): δ 0.07 (s, 6H), 0.87 (s, 9), 1.45-1.69 (m, 8H), 3.39 (t, 2H, $J = 5.82$ Hz), 3.62 (t, 2H, $J = 5.82$ Hz), 3.69-3.73 (m, 1H), 4.52 (s, 2H, Ph- CH_2), 7.21-7.41 (m, 5H, Ar-H); FABMS (m/z %): 352 (M^+), 281 (7), 240 (14), 136 (24), 91 (100), 69 (41), 57 (83).

7-(allyloxy)-4-[1-(tert-butyl)-1,1-Dimethylsilyl]oxy-1-heptanol, 4a: Pale yellow syrup, 90 min, 91% yield. IR (neat): 2925, 2832, 1514, 1021, 911, 601, 504 cm^{-1} ; ^1H NMR (400 MHz, CDCl_3): δ 0.09 (s, 6H), 0.91 (s, 9H), 1.52-1.66 (m, 8H), 3.41 (t, 2H, $J = 6.66$ Hz), 3.56-3.67 (m, 2H), 3.73-3.8 (m, 1H), 3.96 (d, 2H, $J = 8.88$ Hz), 5.28 (d, 1H, $J = 11.3$ Hz), 5.28 (d, 1H, $J = 16.7$ Hz), 5.82-5.93 (m, 1H); FABMS (m/z %): 303 ($\text{M}+\text{H}$) $^+$, 215 (12), 187 (19), 171 (28), 137 (12), 113 (74), 73 (100).

4-[1-(*tert*-butyl)-1,1-Dimethylsilyl]oxy-7-hydroxyheptyl benzoate, 5a: Colourless syrup, 75 min, 92% yield. IR (neat): 2941, 2891, 1726, 1467, 1261, 1114, 834, 722 cm^{-1} ; ^1H NMR (300 MHz, CDCl_3): δ 0.06 (s, 6H), 0.86 (s, 9H), 1.48-1.6 (m, 6H), 1.69-1.8 (m, 2H), 3.52-3.58 (m, 2H), 3.7-3.78 (m, 1H), 4.25 (t, 2H, $J = 8.2$ Hz), 7.36 (t, 2H, Ar-H, $J = 8.2$ Hz), 7.45 (t, 1H, Ar-H, $J = 8.2$ Hz), 7.94 (d, 2H, Ar-H, $J = 9.3$ Hz); FABMS (m/z %): 367 ($\text{M}+\text{H}$) $^+$, 207 (8), 179 (11), 136 (19), 105 (64), 73 (100), 55 (36).

4-[1-(*tert*-butyl)-1,1-Dimethylsilyl]oxy-7-hydroxyheptyl acetate, 6a: Pale yellow syrup, 120 min, 88% yield. IR (neat): 2922, 2834, 1517, 1127, 691, 617, 527 cm^{-1} ; ^1H NMR (300 MHz, CDCl_3): δ 0.09 (s, 6H), 0.89 (s, 9H), 1.45-1.71 (m, 8H), 2.04 (s, 3H, $\text{CH}_3\text{-CO}$), 3.6 (t, 2H, $J = 6.34$ Hz), 3.7-3.8 (m, 1H), 4.05 (t, 2H, $J = 6.34$ Hz); FABMS (m/z %): 306 ($\text{M}+2$) $^+$, 288 (12), 185 (16), 137 (27), 133 (28), 95 (84), 73 (100), 57 (32).

4-[1-(*tert*-butyl)-1,1-Dimethylsilyl]oxy-7-[(4-methoxybenzyl)oxy]-1-heptanol, 7a: Colourless syrup, 110 min, 91% yield. IR (neat): 2930, 2858, 1517, 1461, 1249, 1042, 832, 733, 507 cm^{-1} ; ^1H NMR (400 MHz, CDCl_3): δ 0.08 (s, 6H), 0.84 (s, 9H), 1.2-1.29 (m, 4H), 1.46-1.68 (m, 4H), 3.47 (t, 2H, $J = 3.42$ Hz), 3.5-3.57 (m, 2H), 3.64-3.71 (m, 1H), 3.78 (s, 3H, OCH_3), 4.35 (s, 2H, Ph-CH_2), 6.78 (d, 2H, Ar-H, $J = 11.42$ Hz), 7.15 (d, 2H, Ar-H, $J = 11.42$ Hz); FABMS (m/z %): 367 ($\text{M}-15$) $^+$, 325 (14), 133 (23), 121 (100), 93 (18), 58 (12).

4-[1-(*tert*-butyl)-1,1-dimethylsilyl]oxy-4-phenyl-1-butanol, 8a: Pale yellow syrup, 105 min, 89% yield. IR (neat): 2943, 2859, 1501, 1257, 695, 614, 517 cm^{-1} ; ^1H NMR (400 MHz, CDCl_3): δ 0.18 (s, 6H), 1.08 (s, 9H), 1.62-1.79 (m, 2H), 1.82-1.97 (m, 2H), 3.7-3.76 (m, 2H), 4.82-4.87 (m, 1H), 7.31-7.45 (m, 5H, Ar-H); FABMS (m/z %): 281 ($\text{M}+\text{H}$) $^+$, 181 (22), 131 (58), 105 (13), 91 (19), 73 (100), 59 (18).

4-[1-(*tert*-butyl)-1,1-Dimethylsilyl]oxy-4-[(4*R*)-2,2-dimethyl-1,3-dioxolan-4-yl]-1-butanol, 9a: Pale yellow syrup, 110 min, 79% yield. IR (neat): 2923, 2836, 1527, 1177, 698, 614, 517 cm^{-1} ; ^1H NMR (300 MHz, CDCl_3): δ 0.03 (s, 6H), 0.81 (s, 9H), 1.26 (s, 3H), 1.3 (s, 3H), 1.44-1.62 (m, 4H), 3.57 (t, 2H, $J = 4.6$ Hz), 3.63-3.68 (m, 1H), 3.8-3.91 (m, 3H); EIMS (m/z %): 247 ($\text{M}-57$) $^+$, 171 (18), 133 (24), 73 (100).

((3*aR*,5*R*,6*S*,6*aR*)-6-[1-(*tert*-butyl)-1,1-Dimethylsilyl]oxy-2,2-dimethylperhydro furo[2,3-*d*][1,3]dioxol-5-yl)methanol, 10a: Colourless syrup, 6 h, 90% yield. IR (neat): 2943, 2835, 1517, 1121, 874, 612, 501 cm^{-1} ; ^1H NMR (300 MHz, CDCl_3): δ 0.04 (s, 6H), 0.84 (s, 9H), 1.19 (s, 3H), 1.37 (s, 3H), 3.6 (dd, J 8.3, 6.46 Hz, 1H, H-3), 3.7 (dd, J 8.3, 6.46 Hz, 1H, H-4), 4.05-4.1 (m, 2H, H-5, 5'), 4.19 (d, J 6.46 Hz, 1H, H-2), 5.78 (d, J 6.46 Hz, 1H, H-1); FABMS (m/z %): 305 ($\text{M}+\text{H}$) $^+$, 289 (9), 247 (39), 185 (31), 133 (42), 93 (57), 73 (100).

3. ACKNOWLEDGEMENTS:

The authors BS and TP are thankful to CSIR and CSC-0108 (ORIGIN), New Delhi, India, for the award of research fellowships.

4. CONCLUSIONS:

In conclusion, our present studies achieved high regeoselectivity in the deprotection of primary TBS ethers in the presence of secondary TBS ethers with ZrCl_4 in isopropanol under mild conditions. This study also demonstrated that both acid and base sensitive groups and allylic and benzylic groups were unaffected. Thus, ZrCl_4 (20 mol %) in isopropanol is an efficient catalyst with simple reaction conditions, shorter reaction times, high selectivity and high yields.

REFERENCES:

- Greene T W & Wuts P G M, *Protective groups in organic Synthesis*, 2nd ed.; John Wiley and Sons: New York, 1999; pp. 17-292. (b) Calvin E W, *Chem Soc Rev*, 1978, 7, 35. (c) Corey, E. J.; Venkateswarlu, A. *J Am Chem Soc*, 1972, 94, 6190. (c) Barton T J & Tully C R, *J Org Chem*, 1978, 43, 3649. (e) Prakash C, Roberts L J, Satesh S, Taber D F & Blair I A, *Adv Prost Thromb Leuk Res*, 1987, 17, 781.
- (a) Greene T W & Wuts P G M, *Protective groups in Organic Synthesis*, 3rd ed.; John Wiley and Sons: New York, 1999, 127-144 (b) Clark J H, *Chem Rev*, 1980, 80 429.
- Jackson S R, Johnson M G, Mikami M, Shiokawa S & Carreira E M, *Angew Chem Intl Ed*, 2001, 40, 2694.
- Yang Y-Y, Yang W-B, Teo C-F & Lin C-H, *Synlett*, 2000, 11, 1634.
- Oriyama T, Kobayashi Y & Noda K, *Synlett*, 1998, 1047.
- Yadav J S, Subba Reddy B V & Madan C, *New J Chem.*, 2000, 24 853.
- Crouch R D, Polizzi J M, Cleiman R A, Yi J & Romany C A, *Tetrahedron Lett*, 2002, 43, 7151.
- Bartoli G, Basco M, Marcantoni E, Sambri L & Torregiani E, *Synlett*, 1998, 209.
- Crouch R D, Romany C A, Kreshock A C Menconi K A & Zile J L, *Tetrahedron Lett*, 2004, 45 1279.
- Yang Q-Y, Cui J-R, Zhu L-G, Sun Y-P & Wu Y, *Synlett*, 2006, 1260.
- (a) Chen M-Y, Lu K-C, Lee A S-Y & Lin C-C, *Tetrahedron Lett*, 2002, 43, 2777. (b) Yang Y-Y, Yang W-B, Teo C-F & Lin C-H, *Synlett*, 2000, 11, 1634. (c) Feixas J, Capdevila A & Guerrero A, *Tetrahedron*, 1994, 50, 8539.

- 12 (a) Sharma G V M, Mahalingam A K, Nagarajan M, Ilangoan A & Radha Krishna P, *Synlett*, 1999, 8, 1200. (b) Sharma G V M & Mahalingam A K, *J Org Chem*, 1999, 64,8943. (c) Sharma G V M & Illangoan A *Synlett*, 1999,12,1963. (d) Sharma G V M, Lavanya B, Mahalingam A K & Radha Krishna P, *Tetrahedron Lett*, 2000, 41, 10323. (e) Sharma G V M, Prasad T R & Mahalingam A K, *Tetrahedron Lett*, 2001, 42 759. (f) Sharma G V M & Rakesh K, *Tetrahedron Lett*, 2001, 42, 5571.
- 13 Sharma G V M, Srinivas B & Radha Krishna P, *Tetrahedron Lett*, 2003, 44,4689.
- 14 (a) Sharma G V M, Goverdhan Reddy Ch & Radha Krishna P, *J Org Chem*, 2003,45,6874. (b) Sharma G V M, Goverdhan Reddy Ch & Radha Krishna P, *Synlett*, 2003, 11,1728.
- 15 Sharma G V M, Srinivas B & Radha Krishna P, *Letters in Organic Chemistry*, 2005,2 297.

Table 1. ZrCl₄ (20 mol%) Catalysed Deprotection of 1⁰ TBS Ethers in IPA

ENTRY	STARTING MATERIAL	PRODUCT	TIME (min)	YIELD (%)
1.			60	92
2.			105	89
3.			105	92
4.			90	91
5.			75	92
6.			120	88
7.			110	91
8.			105	89
9.			110	79
10.			6 (h)	90

UGC Sponsored Two Day National Seminar on GREEN CHEMISTRY FOR SUSTAINABLE DEVELOPMENT (GCSD -2017)

April 06 - 07, 2017 at Government Degree College,
Jammikunta, Karimnagar, Telangana State, India

Molecular Docking Approach to Evaluate the Antibacterial Effect of Pyridinyl-3-Aminophenylmethane Sulphonamides on 1fxv: A Comparative Study with Pencillin G.

Venkata Bharat Nishtala¹, Vinay Pogaku² and Srinivas Basavoju³

^{1, 2, 3} Department of Chemistry, National Institute of Technology Warangal, Warangal -506 004, Telangana, India.
Email - basavoju_s@yahoo.com

Abstract: A molecular docking study was carried out to evaluate *insilico* antibacterial activity of pyridinyl-3-aminophenylmethanesulphonamides using Argus Lab software version 4.0. We have screened the binding affinity of pre-existing drug penicillin G and pyridinyl-3-aminophenylmethanesulphonamide derivatives against *E. Coli*:1FXV (PDB ID). The results indicate that ethyl and isopropyl derivatives of pyridinyl-3-aminophenylmethanesulphonamides (ligand binding energy -9.64249 kcal/mol and -9.93369) show good antibacterial activity than the other derivatives (ligand binding energy varies from +4.013 kcal/mol to -9.56832 kcal/mol) and also with standard drug Penicillin G (ligand binding energy -8.82863 kcal/mol). The study suggests that pyridinyl-3-aminophenylmethanesulphonamides shows potent antibacterial activity than penicillin G.

Keywords: pyridinyl-3-aminophenylmethanesulphonamides, *E. Coli*:1FXV, Antibacterial, Molecular docking, Argus lab version 4.0.

1. INTRODUCTION:

There is an urgency in recent days that the development of novel antibacterial drugs with enhanced activity as the microbial infections are becoming the most important issue for global health and economy. These infections are transmittable in nature that can range from common cold, cough, typhoid, malaria, cholera to even some severe diseases like TB and AIDS [1]. Due to the emergence of higher frequency antibiotic resistance in broad range of pathogenic bacterial strains, there is a need to design more potent and effective drugs. Sulphonamide moiety plays a vital role in the medicinal chemistry which constitutes an important class of drugs used mainly as pharmaceutical and agricultural agents [2,3]. These sulphonamide derivatives show various biological properties such as antibacterial, antithyroid, antidiabetics, diuretics and carbonic anhydrase (CA) inhibitors etc. [4,5].

Molecular docking plays an important role in the rational design of drugs [6]. For comparative molecular docking studies, the designed sulphonamide derivatives were docked using Argus Lab software version 4.0. In the present study, we explored the potential of sulphonamide derivatives as an antibacterial agent through inhibition of *E. Coli* protein, 1FXV using *in silico* docking approach.

2. RESULTS AND DISCUSSION:

MOLECULAR DOCKING STUDIES

Molecular docking is an important research area which is used to understand about the drug receptor interactions. Docking is frequently used to predict the binding alignment of drug candidates to their protein targets in order to predict the affinity and activity of the drug molecule. The crystal structure of 1FVX protein for antibacterial activity was obtained from the Protein Data Bank. The inhibitor (pyridinyl-3-aminophenylmethanesulphonamides) and target protein (PDB ID: 1FVX) was geometrically optimized and docked using docking engine Argus Dock. Argus lab consists of a user interface that supports OpenGL graphics display of molecule structures and runs quantum mechanical calculations using the Argus computer server.

Initially it was designed a compound containing sulphonamide group in the core moiety to study the ligand pose energy through docking. After that the ligands were designed by substituting various functional groups at the *meta*-position to the sulphonamide group (Fig. 1). The designed compounds were docked against with *E. Coli*:1FVX

(fig.2) using Argus Lab software. The results indicate that pyridinyl-3-aminophenylmethanesulphonamides show good antibacterial activity than the drug penicillin G against 1FVX. Among the 20 derivatives, the ethyl and isopropyl derivatives of designed molecules possess the best ligand pose energy (-9.64249 kcal/mol and -9.93369 kcal/mol). The results of the binding energies were shown in table 1. The ethyl substituted pyridinyl-3-aminophenylmethanesulphonamide form four strong hydrogen bonds with protein with in a range of 2.5 - 3.0 Å (Fig. 3) where as the isopropyl substituted derivative form two strong hydrogen bonds with protein in a range of 2.5 - 3.0 Å (Fig. 4). However, penicillin G forms one strong hydrogen bonds with the protein lie within the range of 2.5 - 3.0 Å (Fig. 5). The iodine substituted derivative shows large deviation in the ligand pose energy $+4.019$ and this may be due to its large size to fit in the binding site of the protein.

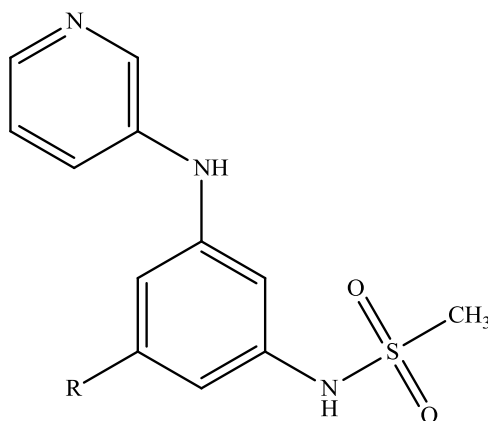


Fig. 1. Designed molecules containing sulphonamide group.

Table 1. Best ligand pose energies of the pyridinyl-3-aminophenylmethanesulphonamide derivatives.

S.No.	Substituent (R)	E (Kcal/mol)
1	-H	-8.48
2	-CH ₃	-8.96339
3	-CH ₃ -CH ₂	-9.64249
4	-CH(CH ₃) ₂	-9.93369
5	-OCH ₃	-8.10849
6	-OCH ₂ -CH ₃	-8.66218
7	-OCH(CH ₃) ₂	-8.97643
8	-Cl	-8.97643
9	-Br	-9.56832
10	-I	+4.0913
11	-NH ₂	-8.64893
12	-NH-CH ₃	-8.64893
13	-N(CH ₃) ₂	-8.41016
14	-NO ₂	-8.90728
15	-CN	-9.00518
16	-CONH ₂	-8.68221
17	-CO-NH-CH ₃	-9.17232
18	-CO-N(CH ₃) ₂	-9.17232
19	-COOH	-8.81869
20	-COOCH ₃	-8.82863
21	Penicillin G	-8.82863

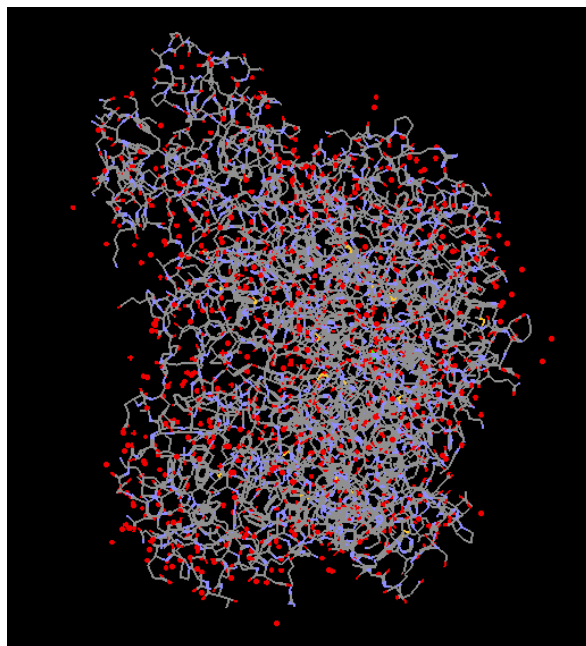


Fig. 2.Crystal structure of the protein 1fvx.

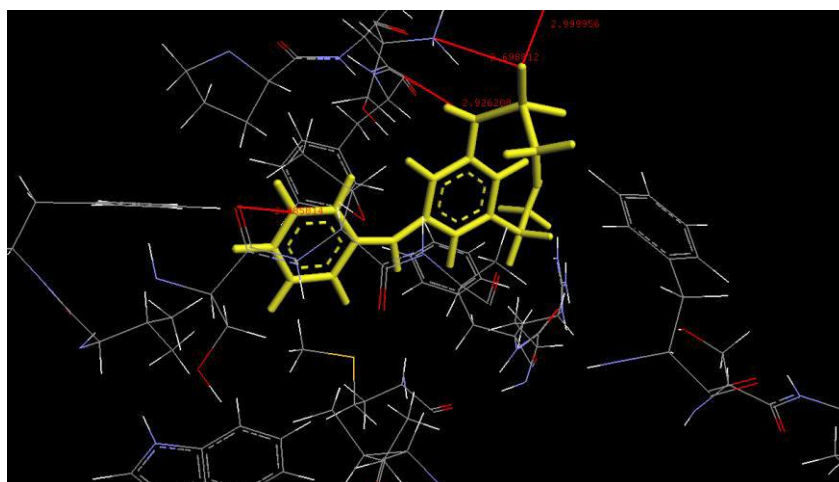


Fig. 3.Docking complex of the ethyl substituted pyridinyl-3-aminophenyl methanesulphonamidewith 1FVX.

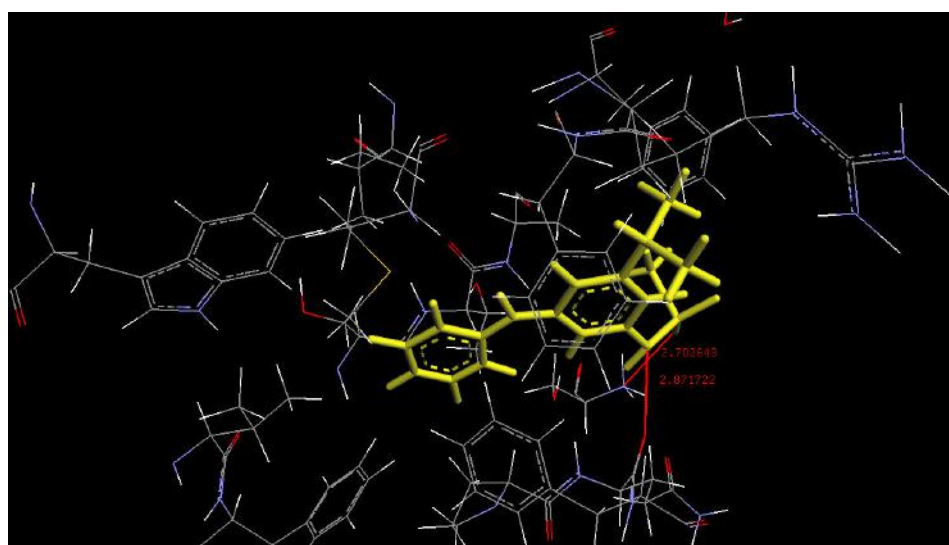


Fig. 4.Docking complex of the isopropyl substituted pyridinyl-3-aminophenyl methanesulphonamidewith 1FVX.

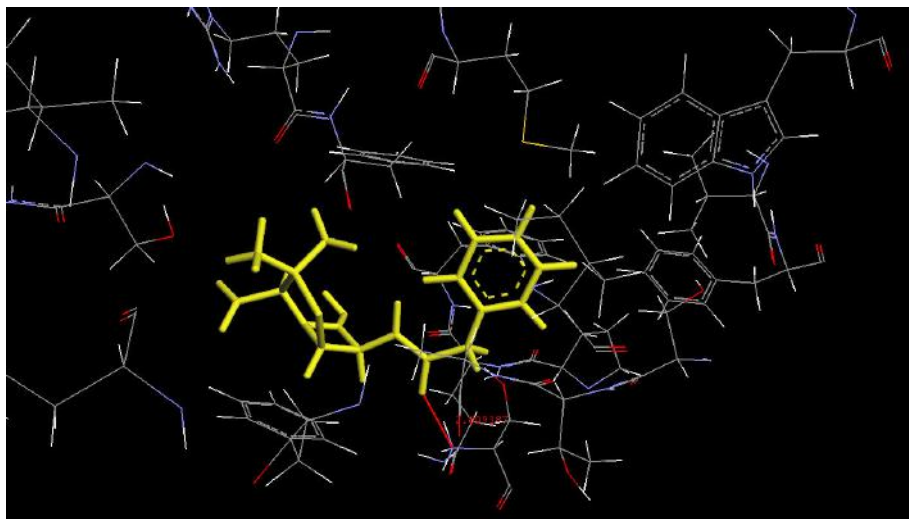


Fig. 5.Docking complex of the penicillin G with 1FVX.

3. CONCLUSION:

The binding pattern of pyridinyl-3-aminophenylmethanesulphonamide derivatives with *E. Coli* protein model 1FVX may provide a clue for designing a new potent drug to control the diseases caused by newly evolved antibiotic resistant pathogenic bacterial strains.

4. ACKNOWLEDGEMENTS:

SB thanks the MHRD, India for the Research Seed Grant. VBN thanks the MHRD, India for fellowship. The authors thank the ArgusLab for providing the free software.

REFERENCES:

1. Sindhu T. J.; Meena Chandran.; Krishnakumar, K.; Bhat A. R.; *An International Journal*. **2013**, 1(11), 992-996.
2. Ugwu. D.I.; Okoro. U.C.; Ukoha. P.O.; Okafor. S.; Ibezim. A.; Kumar. N.M.; *Eur. J. Med. Chem.* **2017**, 135, 349-369.
3. Jain. P.; Saravanan. C.; Singh. S. K.; *Eur. J. Med. Chem.* **2013**, 60, 89-100.
4. Scozzafava. A.; Menabuoni. L.; Mincione. F.; Briganti. F.; Mincione. G.; Supuran. C.T.; *J. Med. Chem.* **1999**, 42, 2641-2650.
5. Majumdar. K.C.; Mondal. S.; *Chem. Rev.* **2011**, 111, 7749-7773.
6. Chandran. M.; George. S.; Ganewar. P.; Santhalingam. K.; Rajasekar. D.; *Asian J. Res. Chem.* **2011**, 4(8), 1254-1257.

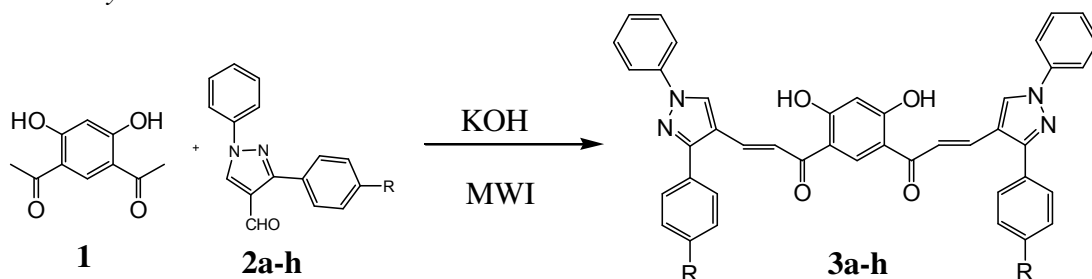
**UGC Sponsored Two Day National Seminar on
GREEN CHEMISTRY FOR SUSTAINABLE DEVELOPMENT (GCSD -2017)
April 06 - 07, 2017 at Government Degree College,
Jammikunta, Karimnagar, Telangana State, India**

Solvent-Free Microwave Assisted Synthesis Of (*E*)-1-(2,4-Dihydroxy-5-[(*E*)-3-[3-(4-Aryl)-1-Phenyl-1*H*-4-Pyrazolyl]-2-Propenoyl]-Phenyl)-3-[3-(4-Aryl)-1-Phenyl-1*H*-4-Pyrazolyl]-2-Propene-1-Ones

Ramesh Banothu¹, Dr. V. Ravinder Reddy² and Veerabathini Manohar³

^{1, 2, 3} Department of Chemistry, Government Degree College - Siddipet(A), Telangana, India - 502103
Email - rameshgdchem@gmail.com

Abstract: A series of new (*E*)-1-(2,4-dihydroxy-5-[(*E*)-3-[3-(4-Aryl)-1-phenyl-1*H*-4-pyrazolyl]-2-propenoyl]phenyl)-3-[3-(4-Aryl)-1-phenyl-1*H*-4-pyrazolyl]-2-propene-1-ones have been synthesized by a microwave-promoted solvent-free condensation of 1-(5-acetyl-2,4-dihydroxy phenyl)-1-ethanone and 1-phenyl-3-aryl-1*H*-4-pyrazole carbaldehydes. The synthesized compounds have been characterized by Elemental analysis and spectral data such as IR, ¹H-NMR, ¹³C-NMR and Mass. All the compounds were screened for their antimicrobial activity.



Scheme 1. Microwave assisted synthesis of bis-chalcones, 3a-h.

Keywords: Bis-chalcones; Green synthesis; Solvent-free; Eco-friendly and Microwave irradiation.

1. INTRODUCTION

Chalcones undergo a variety of chemical reactions and are found useful in synthesis of variety of heterocyclic compounds. Green or sustainable chemistry has now attained the status of a major scientific discipline [1] and the studies in this area have led to the development of cleaner and relatively benign chemical processes with many new technologies being developed in recent years. Among them, much effort has been devoted towards the solvent free microwave assisted organic synthesis. Traditional aprotic solvents are often expensive, toxic and difficult to remove due to their high boiling points. Further the use of microwave irradiation is a step towards green synthesis, which can offer many advantages such as high yields, enhanced reaction rates, shorter reaction times due to their uniform heating effect, eco-friendly and economical. Chalcones have great existence in the plant kingdom. It is well-known that most of the natural or synthetic chalcones are highly biologically active with a great pharmaceuticals and medicinal applications [2]. The compounds with the backbone of chalcones have been reported to possess various biological activities such as antimicrobial [3], anti-inflammatory [4], analgesic [5], antiplatelet [6], antiulcerative [7], antimalarial [8], anticancer [9], antiviral [10], antileishmanial [11], antioxidant [12], antitubercular [13], antihyperglycemic [14], immunomodulatory [15], inhibition of chemical mediators release [16], inhibition of leukotriene B4 [17], inhibition of tyrosinase [18] and inhibition of aldose reductase [19] activities. Geiger and Conn [20] during their chemical studies on the structure of clavacin found that a structural feature which was responsible for antibacterial activity was α , β unsaturated keto functional group. Many of the chalcones are used as agrochemicals and drugs [21]. More recently, there has been strong interest in the potential antimalarial [22] activity of chalcones and bis-chalcones. The antimalarial activity of chalcones was first noted when lipochalcone-A, a natural product isolated from Chinese liquorice roots, was reported to exhibit potent *in vivo* and *in vitro* antimalarial activity [23]. Recently they are used as anti-AIDS [24] agents, cytotoxic with antiangiogenic activity [25]. Pyrazoles have attracted much

attention in the last 30years as their diverse properties appreciated [26]. Pyrazole derivatives are well established in the literature as important biologically active heterocyclic compounds. These derivatives are the subject of many research studies due to their widespread potential biological activities such as anti-inflammatory [27], Antipyretic [28], antimicrobial [29], antiviral [30], antitumour [31, 32], anticonvulsant [33], antihistaminic [34], antidepressant [35], insecticides [36] and fungicides [37]. Due to biopotentiality of bischalcones and pyrazoles and to know the effect of bischalcone and pyrazole moieties on biological activity we have taken up the synthesis of bischalcones containing pyrazole moiety.

2. RESULTS AND DISCUSSION:

Synthesis of (E)-1-(2,4-dihydroxy-5-((E)-3-[3-(4-methylphenyl)-1-phenyl-1*H*-4-pyrazolyl]-2-propenoyl)phenyl)-3-[3-(4-methylphenyl)-1-phenyl-1*H*-4-pyrazolyl]-2-propene-1-one (3a-h) was carried out by condensation of 1-(5-acetyl-2,4-dihydroxy phenyl)-1-ethanone (1) and 1-phenyl-3-aryl-1*H*-4-pyrazole carbaldehydes.

In the IR spectrum (KBr) of **3b** 3397 (OH), 1634(>C=O) and 1566 cm⁻¹ (C=C). In the ¹H-NMR spectrum: (300 MHz, CDCl₃) **3b** exhibited two singlets at δ 13.7 integrating for two protons was assigned to two hydroxyl groups. Two singlets at δ 8.17 & 6.48 integrating for one proton was assigned to H-5' and H-4 respectively. Four doublets each at δ 8.02 and δ 7.2 four protons each was assigned to α and β protons and remaining two doublets at δ 7.78 and δ 7.58 four protons each was assigned to methyl substituted phenyl ring. At δ 8.3 singlets integrating for two protons was assigned two pyr-H. Two methyl protons appeared at δ 2.2 as singlets for six protons. N-Ar appeared as two multiplets at δ 7.42-7.52 and δ 7.30-7.40 was assigned to four meta and six ortho para protons respectively. In the ¹³C NMR spectrum (75 MHz, CDCl₃) the >C=O of **3b** appeared at δ 191.69 and the methyl carbon at δ 21.35 remaining peaks observed at δ 170.22, 154.07, 139.34, 139.02, 136.89, 134.93, 133.49, 129.78, 129.64, 129.33, 127.77, 127.58, 119.51, 118.49, 117.94, 113.86 and 105.35. The ESI MS of **3b** showed [M+H]⁺ peak at m/z = 683 (100%).

Table 1

Physical data of the compound synthesized(3a-h).

Compound	R	M.P.(°C)	Time(min)	Yield(%)
3a	-H	214	5	85
3b	-CH ₃	223	5	90
3c	-OCH ₃	230	5	85
3d	-Cl	245	5	90
3e	-OH	241	5	80
3f	-F	239	5	85
3g	-Br	256	5	80
3h	-NO ₂	251	5	80

3. EXPERIMENTAL:

Melting point determinations was in open capillaries and was uncorrected. TLC was carried out using merck brand silicagel Gel-G and spotting was done using iodine or UV light. IR spectra were recorded in Perkin-Elmer 577 IR spectrophotometer. ¹H and ¹³C NMR spectra were conducted on Bruker (300 MHz) spectrometer in CDCl₃ with tetramethylsilane as the internal standard. The chemical shifts are reported in ppm scale.

General procedure for synthesis of (E)-1-(2,4-Dihydroxy-5-((E)-3-[3-(4-aryl)-1-phenyl-1*H*-4-pyrazolyl]-2-propenoyl)-phenyl)-3-[3-(4-aryl)-1-phenyl-1*H*-4-pyrazolyl]-2-propene-1-one

Microwave irradiation:

To a mixture of 1(0.05mole) and 2a-h (0.1mole) was added catalytic amount of KOH and swirled thoroughly. The mixture was irradiated in microwave oven at 200W for 5 min. Then to the reaction mixture add some amount of ice cold water, then neutralized with dil.HCl and filter the yellow solid, dried, and recrystallized from methanol to afford pure 3a-h in good yield (Table 1)

(E)-3-(1,3-Diphenyl-1*H*-4-pyrazolyl)-1-[5-[(E)-3-(1,3-diphenyl-1*H*-4-pyrazolyl)-2-prop-enoyl]-2,4-dihydroxy phenyl]-2-propen-1-one (3a). Yellow solid, mp 214°C. IR (KBr, cm⁻¹) 3432(ν_{OH}), 1635($\nu_{C=O}$), 1533($\nu_{C=C}$). ¹H-NMR: (300 MHz, CDCl₃): δ 8.15 (1H, s, H-5), 6.50 (1H, s, H-10), 8.3 (2H, s, PyH), 7.25-7.46 (20H, m, Ar-H), 8.01 (2H, d, =C β -H), 7.7 (2H, d, C=C α -H), 13.65 (s, 2XOH). ¹³C-NMR (75 MHz, CDCl₃): δ 191.58, 170.01, 153.67, 139.13, 136.49, 136.15, 134.73, 133.39, 129.59, 129.27, 128.98, 127.94, 119.69, 118.73, 117.93, 113.71 and 105.16. MS: m/z = 655 [M+H]⁺.

(E)-1-(2,4-Dihydroxy-5-((E)-3-[3-(4-methylphenyl)-1-phenyl-1H-4-pyrazolyl]-2-propen-oyl)-phenyl)-3-[3-(4-methylphenyl)-1-phenyl-1H-4-pyrazolyl]-2-propene-1-one (3b). Yellow solid, mp 223°C. IR (KBr, cm^{-1}) 3440.2(ν_{OH}), 1635($\nu_{\text{C=O}}$), 1565.1($\nu_{\text{C=C}}$). ^1H NMR (300MHz, CDCl_3): δ 13.72(s, 2H, -OH), 8.3(s, 2H, pyrazol-H), 8-8.5(d, 2H, $=\text{C}_\beta\text{-H}$, $J=15\text{MHz}$), 7.5-8.1(d, 4H, Ar), 7.56-7.62(d, 4H, Ar), 7.41-7.52(m, 5H, Ar), 7.29-7.38(m, 5H, Ar), 7.18-7.23(d, 2H, $=\text{C}_\alpha\text{-H}$, $J=15\text{MHz}$), 6.48(s, 1H, Ar), 2.3(s, 6H, $-\text{CH}_3$). ^{13}C -NMR (75MHz, CDCl_3): δ 191.69(C=O), 170.22(C-OH), 154.07, 139.3, 139.1, 136.9, 133.5, 129.7, 129.6, 129.3, 128.7, 127.7, 127.5, 119.4, 118.4, 117.9, 113.8, 105.3 and 21.35(CH_3). MS: m/z 683[$\text{M}+\text{H}$] $^+$.

(E)-1-(2,4-Dihydroxy-5-((E)-3-[3-(4-methoxyphenyl)-1-phenyl-1H-4-pyrazolyl]-2-prop-enoyl)-phenyl)-3-[3-(4-methoxyphenyl)-1-phenyl-1H-4-pyrazolyl]-2-propene-1-one (3c). Yellow solid, mp 230°C. IR (KBr, cm^{-1}) 3419(ν_{OH}), 1640($\nu_{\text{C=O}}$), 1469($\nu_{\text{C=C}}$), 1250. ^1H -NMR (300MHz, CDCl_3): δ 13.76(s, 2H, -OH), 8.27(s, 2H, pyrazol-H), 8.0(d, 2H, $=\text{C}_\beta\text{-H}$, $J=15\text{MHz}$), 7.74(d, 4H, Ar), 7.57(d, 4H, Ar), 7.42-7.57(m, 5H, Ar), 7.31-7.40(m, 5H, Ar), 7.18-7.23(d, 2H, $=\text{C}_\alpha\text{-H}$, $J=15\text{MHz}$), 6.45(s, 1H, Ar), 3.71(s, 6H, 2XOCH_3). ^{13}C -NMR (75 MHz, CDCl_3): δ 184.7(C=O), 160.7(C-OH), 154.36, 139.2, 139.1, 136.9, 131.1, 130.2, 129.5, 129.3, 128.7, 127.7, 127.7, 124, 122.5, 119.9, 114.2, 105.3 and 55.3(OCH_3). MS: m/z 715 [$\text{M}+\text{H}$] $^+$.

(E)-3-[3-(4-Chlorophenyl)-1-phenyl-1H-4-pyrazolyl]-1-5-((E)-3-[3-(4-chlorophenyl)-1-phenyl-1H-4-pyrazolyl]-2-propenoyl)-2,4-dihydroxyphenyl)-2-propen-1-one (3d). Yellow solid, mp 241°C. IR (KBr, cm^{-1}) 3423(ν_{OH}), 1641($\nu_{\text{C=O}}$), 1534($\nu_{\text{C=C}}$), 1500. ^1H -NMR (400MHz, CDCl_3): δ 13.65(s, 2H, -OH), 8.28(s, 2H, pyrazol-H), 7.9(d, 2H, $=\text{C}_\beta\text{-H}$, $J=16\text{MHz}$), 7.79(d, 4H, Ar), 7.63(d, 4H, Ar), 7.34-7.4(m, 6H, Ar), 7.43-7.49(m, 5H, Ar), 6.86(d, 2H, $=\text{C}_\alpha\text{-H}$, $J=15\text{MHz}$), 6.75(s, 1H, Ar). ^{13}C -NMR (75 MHz, CDCl_3): δ 188.15(C=O), 152.63(C-OH), 139.42, 134.96, 133.43, 130.92, 130.12, 129.78, 129.17, 127.59, 126.97, 125.44, 123.57, 119.53, 118.21, 117.90, 113.75 and 102.65. MS: m/z 723 [$\text{M}+\text{H}$] $^+$.

(E)-1-(2,4-Dihydroxy-5-((E)-3-[3-(4-hydroxyphenyl)-1-phenyl-1H-4-pyrazolyl]-2-prop-enoyl)-phenyl)-3-[3-(4-hydroxyphenyl)-1-phenyl-1H-4-pyrazolyl]-2-propene-1-one (3e). Yellow solid, mp 241°C. IR (KBr, cm^{-1}) 3418(ν_{OH}), 1634.6($\nu_{\text{C=O}}$), 1566($\nu_{\text{C=C}}$)1535. ^1H -NMR (300MHz, CDCl_3): δ 13.7(s, 2H, -OH), 8.31(s, 2H, pyrazol-H), 8.02(d, 2H, $=\text{C}_\beta\text{-H}$, $J=15\text{MHz}$), 7.8(d, 4H, Ar), 7.61(d, 4H, Ar), 7.32-7.45(m, 6H, Ar), 7.43-7.51(m, 5H, Ar), 6.86(d, 2H, $=\text{C}_\alpha\text{-H}$, $J=15\text{MHz}$), 7.0(s, 1H, Ar), 4.9(s, 2H, -OH). ^{13}C -NMR (75MHz, CDCl_3): δ 187.95(C=O), 157.73(C-OH), 140.62, 135.06, 134.23, 130.22, 130.17, 129.58, 129.28, 127.40, 126.37, 125.74, 123.40, 120.53, 119.21, 115.90, 114.65 and 103.55. MS: m/z 687[$\text{M}+\text{H}$] $^+$.

(E)-3-[3-(4-Fluorophenyl)-1-phenyl-1H-4-pyrazolyl]-1-5-((E)-3-[3-(4-fluoro phenyl)-1-phenyl-1H-4-pyrazolyl]-2-propenoyl)-2,4-dihydroxy phenyl)-2-propen-1-one (3f). Yellow solid, mp 239°C. IR (KBr, cm^{-1}) 3415(ν_{OH}), 1641($\nu_{\text{C=O}}$), 1471($\nu_{\text{C=C}}$), 1260. ^1H -NMR (300MHz, CDCl_3): δ 13.7(s, 2H, -OH), 8.3(s, 2H, pyrazol-H), 7.93-7.97(d, 2H, $=\text{C}_\beta\text{-H}$, $J=16\text{MHz}$), 7.74-7.76(d, 4H, Ar), 7.64-7.67(d, 5H, Ar), 7.42-7.35(m, 5H, Ar), 7.06-7.1(m, 5H, Ar), 7.08-7.12(d, 2H, $=\text{C}_\alpha\text{-H}$, $J=16\text{MHz}$), 6.48(s, 1H, Ar). ^{13}C -NMR (75 MHz, CDCl_3): δ 190.31(C=O), 157.13(C-OH), 140.02, 137.26, 135.13, 134.52, 131.92, 130.58, 128.34, 128.29, 126.67, 125.14, 122.92, 121.43, 119.54, 117.70, 115.78 and 103.32. MS: m/z 691 [$\text{M}+\text{H}$] $^+$.

(E)-3-[3-(4-Bromophenyl)-1-phenyl-1H-4-pyrazolyl]-1-5-((E)-3-[3-(4-bromo phenyl)-1-phenyl-1H-4-pyrazolyl]-2-propenoyl)-2,4-dihydroxy phenyl)-2-propen-1-one (3g). Yellow solid, mp 256°C. IR (KBr, cm^{-1}) 3418(ν_{OH}), 1636($\nu_{\text{C=O}}$), 1565($\nu_{\text{C=C}}$), 1531. ^1H -NMR (300MHz, CDCl_3): δ 13.82(s, 2H, -OH), 8.17(s, 2H, pyrazol-H), 7.32(d, 2H, $=\text{C}_\beta\text{-H}$, $J=16\text{MHz}$), 7.73(d, 4H, Ar), 7.52(d, 4H, Ar), 7.42-7.50(m, 5H, Ar), 7.28-7.33(m, 5H, Ar), 7.09(d, 2H, $=\text{C}_\alpha\text{-H}$, $J=16\text{MHz}$), 6.78(s, 1H, Ar). ^{13}C -NMR (75MHz, CDCl_3): δ 188.35(C=O), 153.03(C-OH), 139.92, 135.42, 134.19, 130.72, 130.32, 129.08, 128.57, 127.39, 126.23, 126.04, 124.37, 120.33, 119.25, 114.85 and 103.90. MS: m/z 810 [$\text{M}+\text{H}$] $^+$.

(E)-1-(2,4-Dihydroxy-5-((E)-3-[3-(4-nitrophenyl)-1-phenyl-1H-4-pyrazolyl]-2-propenoyl)-phenyl)-3-[3-(4-nitrophenyl)-1-phenyl-1H-4-pyrazolyl]-2-propene-1-one (3h). Yellow solid, mp 251°C. IR (KBr, cm^{-1}) 3420(ν_{OH}), 1632($\nu_{\text{C=O}}$), 1601, 1566($\nu_{\text{C=C}}$), 1531. ^1H -NMR (300MHz, CDCl_3): δ 13.73(s, 2H, -OH), 8.28(s, 2H, pyrazol-H), 8.12(d, 2H, $=\text{C}_\beta\text{-H}$, $J=15\text{MHz}$), 7.78(d, 4H, Ar), 7.72 (d, 4H, Ar), 7.40-7.50(m, 5H, Ar), 7.36-7.38(m, 5H, Ar), 7.18-7.23(d, 2H, $=\text{C}_\alpha\text{-H}$, $J=15\text{MHz}$), 6.78(s, 1H, Ar). ^{13}C -NMR (75MHz, CDCl_3): δ 189.95(C=O), 153.03(C-OH), 138.62, 135.86, 134.03, 133.82, 131.02, 130.78, 129.34, 128.29, 127.47, 125.94, 122.32, 120.53, 119.51, 117.90, 115.75 and 104.45. MS: m/z 745 [$\text{M}+\text{H}$] $^+$.

4. ACKNOWLEDGEMENTS:

The authors thank Head, Department of Chemistry, Central Facilities for Research and development, Osmania University for providing IR and NMR spectral facilities.

REFERENCES:

1. Ananastas P T and Warner J C, *Green Chemistry: Theory and Practice*, 1998, Oxford University press, New York.
2. (a) saini R K, Choudhary A S, Joshi Y C and Joshi P, *E. J. chem.*, 2005, 2(9). (b) Dhar D N, *Chemistry of Chalcones and Related Compounds*; Wiley: N.Y., 1981.
3. Mokle S S, Sayeed M A, Kothawar and Chopde, *Int. J. Chem. Sci.* 2004, 2(1), 96.
4. Hsieh H K, Tsao L T and Wang J P, *J. Pharm. Pharmacol.*, 2000, 52, 163.
5. Viana G S, Bandeira M A. and Matos F, *J. Phytomedicine*, 2003, 10, 189.
6. Zhao L M, Jin H S, Sun L P, Piao H R and Quan Z S, *Bioorg. Med. Chem. Lett*, 2005, 15, 5027.
7. Mukarami S, Muramatsu M, Aihara H and Otomo S, *Biochem. Pharmacol*, 1991, 42, 1447.
8. Liu M, Wilairat P and Go L M, *J. Med. Chem*, 2001, 44, 4443.
9. Francesco E, Salvatore G, Luigi M and Massimo C, *Phytochem*, 2007, 68, 939.
10. Onyilagna J C, Malhotra B, Elder M and Towers G H N, *Can. J. Plant Pathol*, 1997, 19, 133.
11. Nielsen S F, Chen M, Theander T G, Kharazmi A and Christensen S B, *Bioorg. Med. Chem. Lett*, 1995, 5, 449.
12. Miranda C L, Aponso G L M, Stevens J F, Deinzer M L and Buhler D R, *J Agric. Food Chem*, 2000, 48, 3876.
13. Siva Kumar P M, Geetha Babu S K and Mukesh D, *Chem. Pharm. Bull*, 2007, 55(1), 44.
14. Satyanarayana M, Priti Tiwari, Tripathi K, Srivastava A K and Ram Pratap, *Bioorg. Med. Chem*, 2004, 12, 883.
15. Barford L, Kemp K, Hansen M and Kharazmi A, *Int. Immunopharmacol*, 2002, 2, 545.
16. Ko H H, Tsao L T, Yu K L, Liu C T, Wang J P and Lin C N, *Bioorg. Med. Chem*, 2003, 11, 105.
17. Deshpande A M, Argade N P, Natu A A and Eckman, *Bioorg. Med. Chem*, 1999, 7, 1237.
18. Khatib S, Nerya O, Musa R, Shmnel M, Tamir S and Vaya J, *Bioorg. Med. Chem*, 2005, 13, 433.
19. Severi F, Benvenuti S, Costantino L, Vampa G, Melegari M and Antolini L, *Eur. J. Med. Chem*, 1998, 33, 859.
20. Walton et al. 1945.
21. (a) Misra, S. S.; Tewari, R. S. *J Indian Chem. Soc.* 1973, 50, 68. (b) Lafen, L.; Ger. Pp 2010180, 1970; *Chem. Abstr* 1970, 73, 120342s.
22. Ram V J, Saxena A S, Srivastava S and Chandra S, *Bioorg Med Chem Lett.*, 2000, 10, 2159.
23. Chen M, Theander T G, Christenson S B, Hviid L, Zhai L and Kharazmi A, *Antimicrob Agents Chemother*, 1994, 38, 1470.
24. Wu J H, Wang X H, Yi Y H and Lee K H, *Bioorg. & Med. Chem. Lett.*, 2003, 13, 1813.
25. (a) Nam N H, Kim Y, You Y J, Hong D H, Kim H M and Ahn B Z, *Eur. J. Med. Chem.*, 2003, 38, 179. (b) Saydam G, Aydin H H, Sahin F, Kucukoglu O, Erciyas E, Terzioglu E, Buyukkececi F and Omay S B, *Leukemia Res.*, 2003, 27, 57.
26. (a) Migliara, O.; Plescia, S.; Diana, P.; Di Stefano, V.; Camarda, L.; Dall'Olio, R. *Arkivoc* 2004, (v), 44. (b) Daidone, G.; Raffa, D.; Plescia, F.; Maggio, B.; Roccato, A. *Arkivoc* 2002, (xi), 227.
27. Tewari, A.K.; Mishra, A. *Bioorg. Med. Chem.*, 2001, 9, 715-718.
28. Wiley, R.H.; Wiley, P. John Wiley and Sons: New York, 1964.
29. Pimerova, E.V.; Voronina, E.V. *Pharm. Chem. J.*, 2001, 35, 18-20.
30. Janus, S.L.; Magdif, A.Z.; Erik, B.P.; Claus, N. *Monatsh. Chem.*, 1999, 130, 1167-1174.
31. Park, H.J.; Lee, K.; Park, S.; Ahn, B.; Lee, J.C.; Cho, H.Y.; Lee, K.I. *Bioorg. Med. Chem. Lett.*, 2005, 15, 3307-3312.
32. Bouabdallah, I.; M'barek, L.A.; Zyad, A.; Ramadan, A.; Zidane, I.; Melhaoui, A. *Nat. Prod. Res.*, 2006, 20, 1024-1030.
33. Michon, V.; Du Penhoat, C.H.; Tombret, F.; Gillardin, J.M.; Lepagez, F.; Berthon, L. *Eur. J. Med. Chem.*, 1995, 147-155.
34. Yildirim, I.; Ozdemir, N.; Akcamur, Y.; Dincer, M.; Andaç, O. *Acta Cryst.*, 2005, E61, 256-258.
35. Bailey, D.M.; Hansen, P.E.; Hlavac, A.G.; Baizman, E.R.; Pearl, J.; Defelice, A.F.; Feigenson, M.E. *J. Med. Chem.*, 1985, 28, 256-260.
36. Chu, C.K.; Cutler, J. *J. Heterocycl. Chem.*, 1986, 23, 289-319.

**UGC Sponsored Two Day National Seminar on
GREEN CHEMISTRY FOR SUSTAINABLE DEVELOPMENT (GCSD -2017)
April 06 - 07, 2017 at Government Degree College,
Jammikunta, Karimnagar, Telangana State, India**

Novel three-component one-pot synthesis of 1,2-dihydro-1-aryl-naphtho[1,2-e] [1,3]oxazin-3-one derivatives catalyzed by Cu(II)-NaY Zeolite and their Evaluation of biological activity

K. Sudhakar^{*1}, Y. Hemasri², Y. Jayaprakash Rao³, K. Arundhathi⁴ & Thota Anupama Yadav⁵

^{1, 2, 3, 4} Department of Chemistry, Osmania University, Hyderabad, Telangana-500007, India.

⁵Organic and Biomolecular Chemistry Division, CSIR-Indian Institute of Chemical Technology, Hyderabad 500 007, India

Email - ¹ksudhakarou@gmail.com; ²hemay2@yahoo.com

Abstract: A simple and efficient route for the synthesis of naphtho[1,2-e][1,3]oxazin-3-one derivatives via one-pot condensation of aromatic aldehyde, β -naphthol and urea using Cu(II)-NaY zeolite is as a heterogeneous catalyst reported. The salient features of this zeolite are economical, cost-effective, reusable with easy work up and high-yield protocol are aerobic conditions, and milder reaction conditions without any additives. All these compounds have been characterized by modern spectral techniques such as IR, ¹H NMR, Mass etc. Evaluation of synthesized compounds for antimicrobial activity against specific bacterial strains like 1) *Bacillus pumilis* 2) *Bacillus subtilis* 3) *Echerichia coli* 4) *Protius vulgaris*, along with antifungal activity against 1) *Aspergillus niger*, 2) *Rhizopus oryzae* and 3) *Aspergillus flavus*.

Keywords: Naphthoxazinones, heterogeneous catalyst, Cu(II)-NaY Zeolite, Multi-component reactions (MCR), Green chemistry, Antimicrobial activity.

1. INTRODUCTION

Aromatic and naphthalene condensed oxazinone derivatives are known to possess interesting pharmacological¹⁻³ and anti-microbial properties⁴⁻⁸. These compounds have also been used in the preparation of chiral amino phosphine ligands for asymmetric catalysis⁹. Even though a large number of methods¹⁰⁻¹⁴ were reported for the preparation of intermediate compounds (amidoalkyl naphthols), reports for the synthesis of naphthoxazinone derivatives, which includes acidic catalyst¹⁵, pyridiniumbased ionic liquid¹⁶, wet cyanuric chloride, and using ZnO nanoparticles¹⁷⁻¹⁸. This has stimulated significant interest and there is always considerable demand in exploring more milder, convenient, practical and benign reagents for their synthesis using multi-component reactions (MCR). Therefore, the development of simple, convenient and practical procedures for the synthesis of naphtho[1,2-e][1,3]oxazin-3-one derivatives continue to be a challenging endeavor in synthetic organic chemistry.

In recent years, there has been increasing emphasis on the use of environmentally friendly solid catalysts to reduce the amount of toxic waste. Zeolites are very useful catalysts in a large variety of reactions, from acid to base and redox catalysis. They contain large number of Brønsted and Lewis acidic sites and transition metal ion supported zeolites act as bifunctional catalysts and more useful in synthetic organic chemistry. Recently Metal exchanged-mediated zeolites attracted much attention due to their higher catalytic activity in a variety of organic transformations¹⁹⁻²⁰. To the best of our knowledge, no report has been made about the use of heterogeneous catalyst, Cu(II)-NaY zeolite for the synthesis of these compounds. Herein, we report an extremely efficient three-component one-pot reaction of β -naphthol, aldehydes and urea in the presence of Cu(II)-NaY as a recyclable green catalyst for the synthesis of 1,2-dihydro-1-aryl-naphtho[1,2-e][1,3]oxazine-3-one derivatives (Scheme 1). All the synthesized compounds have tested in vitro for their antibacterial (*Bacillus pumilis*, *Bacillus Subtilis*, *Echerichia coli*, *Protius vulgaris*) and antifungal (*Aspergillus niger*, *Rhizopus oryzae*, *Aspergillus flavus*) activities. Compounds 4b, 4c, 4f, and 4g, were showed most potent in vitro activity against bacterial and fungal strains. However, to the best of our knowledge, there are no earlier reports on the preparation of 1-Oxo-1,2, 3,4,9,10-hexahydroanthene derivatives using Cu(II)-NaY zeolite to date.

2. RESULTS AND DISCUSSION

Thus heating a mixture of β -naphthol (1), benzaldehyde (2) and urea (3) in the presence of Cu(II)-NaY in

CH₃CN/DMF at 120⁰C for 1.5 h afforded the corresponding naphthoxazinone 4a in 81% yield (Scheme 1). Encouraged by this result, we turned our attention to various substituted aromatic aldehydes (4b-4m). In all cases, the reaction proceeded efficiently and completed within 1-5 h under similar conditions. It is important to note that the reaction proceeds efficiently with the aldehydes having electron-withdrawing and electron releasing substituents, which is contrary to Bazgir et al.²¹ procedure. The known compounds were compared with authentic samples and also were characterized by spectral data. The new products (Table1, entries 4h, 4i, 4l and 4m) were characterized by their physical and spectral analysis. Para substituted aldehydes gave higher yields in short reaction times when compared to ortho and meta substituted aldehydes (Table1, entries 4b, 4c, 4d, 4e, 4f, 4g, 4h, 4i). This may be attributed to the steric hindrance. The scope and generality of this process is illustrated with respect to various aldehydes and the results are summarized in Table 1. The recovered catalyst was recycled up to three times without observation of appreciable lost in catalytic activity. The results of the first experiment and subsequent experiments were almost consistent in yields (80, 78 and 75%). These results clearly show the advantage of this method over existing procedures. The synthesis could not be achieved in the absence of the catalyst.

Since a number of 1,2-dihydro-1-aryl-naphtho[1,2-e][1,3]oxazin-3-one derivatives reported to possess biological activities like antibacterial and anti-fungal activities; it is thought worthwhile to screen them for these activities.

2.1 Antibacterial Activity

“All the synthesized naphtho[1,2-e][1,3]oxazine-3-one derivatives (Table 2, Figure 1), 4a-m were screened for their antibacterial activity against different types of bacterial strains”, they are “Gram positive bacterial strains of *Bacillus pumilis* and *Bacillus subtilis*, Gram negative bacterial strains of *Escherichia coli* and *Protius vulgaris*”²², at a concentration of 10 µg/mL. The results of these evaluation have been compared by taking Ampicillin (10 µg), as the standard.

Some of the synthesized compounds showed high activity and some showed moderate activity compared to standard drug Ampicillin at a concentration of 10 µg/mL. The antibacterial activity of compound 4b (R₃ = -Cl), 4c (R₃ = -F), 4e (R₃ = -OCH₃), and 4f (R₃ = -CH₃) showed good zone of inhibition against *Bacillus pumilis*, *Bacillus Subtilis*, *Echerichia coli*, and *Protius vulgaris* compared to the standard drug at a concentration of 100 µg/ mL. Whereas the compounds 4a, 4f, 4g, and 4h were showing moderate activity against all the bacterial strains when compared to standard drug Ampicillin at a concentration of 100 µg/ mL. Compounds 4d, 4i, and 4j weren't showing activity against all bacteria. It leads us to conclude that from Table 2 and Figure 1, Electron donating groups at Para positions like methoxy, Chloro, Fluoro, and methyl substituted compounds showed higher zone of inhibition when compared with other compounds. Furthermore, substitutions like -C(CH₃)₃, CH(CH₃)₂, and CH₃ did not provide any significant change in the levels of activity against *P. vulgaris* bacterial strains. All the compounds showed less activity compared to Ampicillin.

2.2 Antifungal Activity

The antifungal activity of naphtho[1,2-e][1,3]oxazine-3-one derivatives have been evaluated (Table 3, Figure 2) 4a-m against *A. niger*, *R. oryzae* and *A. flavus* by employing Clotrimazole (10 mg) as the standard drug by the cup plate at a concentration of 100 µg/mL. The antifungal activity of compounds like the electron donating groups at para position 4b (R₃ = -Cl), 4c (R₃ = -F), 4f (R₃ = -OMe), and 4h (R₃ = -CH(CH₃)₂) showed inhibitory activity against *Aspergillus niger*, *Rhizopus. Oryzae*, *Aspergils flavus*, however the activity is mild compared to clotrimazole standard. Compounds 4a (R₃ = -H), 4d (R₃ = -Br), 4g (R₃ = -CH₃), and 4i (R₃ = - C(CH₃)₃) showed inhibitory activity against *Aspergillus niger* and *Rhizopus oryzae*, except *Aspergillus flavus*. Compounds 4e (R₃ = -OH), 4j (R₁ = -Cl), and 4m (R₂ = -OH), did not showed any inhibitory activity.

The electron donating groups such as methoxy, methyl and halogens substituted groups showed better antifungal activity and which could seen in the case of 4b, 4c, 4f, and 4g against The antifungal activity. However the other substitution at ortho and meta positions did not provide any significant change in the levels of activity against fungi.

Scheme 1 :

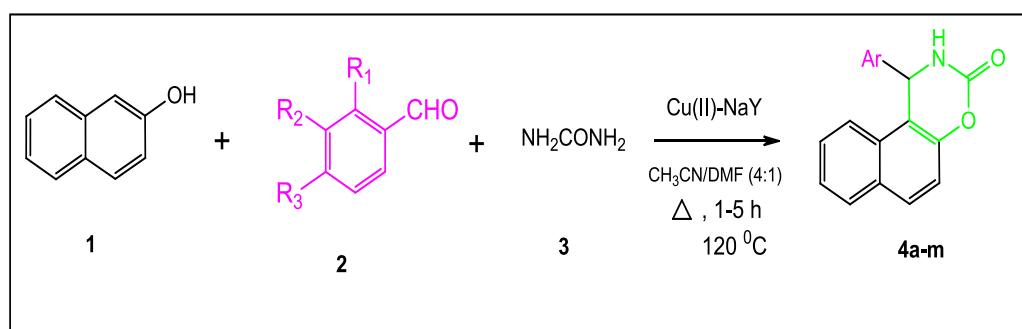
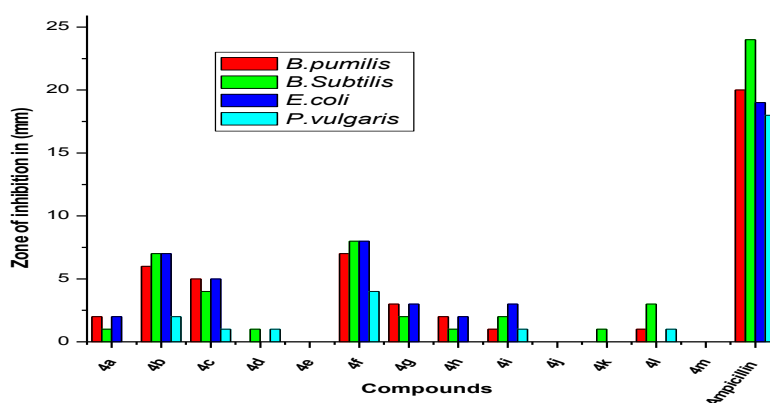


Table 1: Cu(II)-NaY zeolite catalyzed synthesis of naphtho[1,2-e][1,3]oxazin-3-ones (4)^{a,b}

Entry	R ¹	R ²	R ³	Time (h)	Yield (%)	MP (°C)
4a	H	H	H	1.5	81	219 (218-220) ¹⁹
4b	H	H	Cl	1.2	86	208 (208-210) ¹⁹
4c	H	H	F	1.0	89	203 (202-204) ¹⁹
4d	H	H	Br	1.6	83	221 (220-223) ¹⁹
4e	H	H	OH	2.1	90	182 (180) ¹⁹
4f	H	H	OMe	1.1	81	187 (185-188) ¹⁹
4g	H	H	Me	1.6	94	166 (166-168) ¹⁹
4h	H	H	CH(Me) ₂	2.1	84	172
4i	H	H	C(Me) ₃	1.7	81	178
4j	Cl	H	H	3.0	68	249 (251-253) ²⁰
4k	H	Br	H	2.5	67	225 (226-228) ²⁰
4l	H	OMe	H	4.0	69	172
4m	H	OH	H	5.0	71	189

^a all products were characterized by spectral data and known compounds were compared with authentic samples^b isolated Pure products**Table 2: Antibacterial activity of naphtho[1,2-e][1,3]oxazin-3-ones (4a-m)**

Compound	Zone of Inhibition (mm)			
	<i>B. pumilis</i>	<i>B. subtilis</i>	<i>E. coli</i>	<i>P. vulgaris</i>
4a	2	1	2	-
4b	6	7	7	2
4c	5	4	5	1
4d	-	1	-	1
4e	-	-	-	-
4f	7	8	8	4
4g	3	2	3	-
4h	2	1	2	-
4i	1	2	3	1
4j	-	-	-	-
4k	-	1	-	-
4l	1	3	-	1
4m	-	-	-	-
Ampicillin (10 µg/mL)	20	24	19	18



Concentration of the test compound: 100 µg/ mL

Figure 1: Antibacterial activity of compounds **4a-m** against *Bacillus pumilis*, *Bacillus Subtilis*, *Echerichia coli* and *Protius vulgaris*. Micro organism were screened using potato dextrose agar with *Bacillus pumilis*, *Bacillus subtilis*, *Echerichia coli* and *Protius vulgaris* are showing zone of inhibition (mm) with different concentration of compound.

Table 3: Antifungal activity of naphtho[1,2-e][1,3]oxazine-3-ones (4a-m)

Compound	Zone of inhibition in (mm)		
	<i>B. pumilis</i>	<i>B. subtilis</i>	<i>E. coli</i>
4a	1	1	-
4b	3	4	2
4c	3	2	1
4d	1	1	-
4e	-	-	-
4f	5	7	4
4g	3	2	-
4h	2	1	2
4i	1	2	-
4j	-	-	-
4k	-	1	-
4l	-	2	-
4m	-	-	-
Clotrimazole (10 µg/ml)	20	18	16

Concentration of the test compounds : 100 µg/ mL

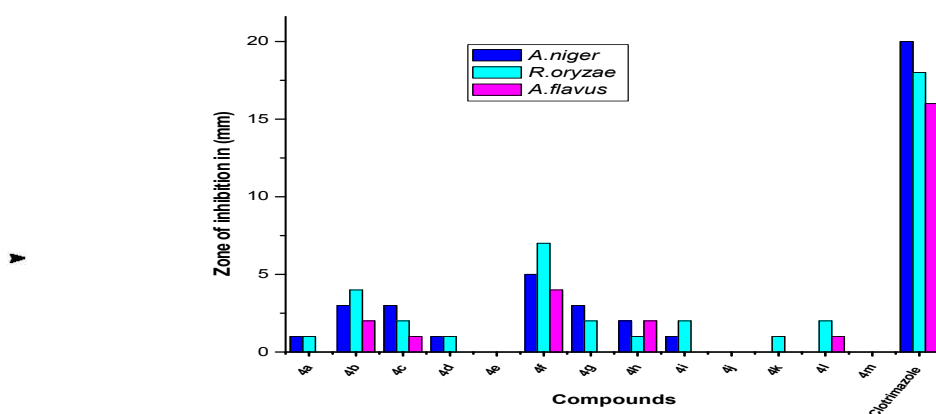


Figure 2: Anti fungal activity of compounds **IIIa-m** against *Aspergillus niger*, *Rhizopus oryzae* and *Aspergillus flavus*. Micro organism were screened using potato dextrose agar with *Aspergillus niger*, *Rhizopus oryzae* and *Aspergillus flavus* are showing zone of inhibition (mm) with different concentration of compound.

3. EXPERIMENTAL SECTION:

Melting points were recorded on Buchi R-535 apparatus and are uncorrected. IR spectra were recorded on a Perkin-Elmer FTIR 240-c spectrophotometer using KBr optics. ¹H NMR spectra were recorded on Varian-unity 300 spectrometer in DMSO-d₆ using TMS as internal standard. Mass spectra were recorded on a Finnigan MAT 1020 mass spectrometer operating at 70 eV.

3.1 Preparation of Cu(II)-NaY Catalyst:

All chemicals and solvents were of analytical grade and used as received without further purification. Cu(II)-NaY zeolite was prepared by ion-exchange of zeolite NaY (10 g) with a solution of copper(II)acetate (2.86 g, 15.75 mmol in deionized water 150 mL) for 24h at room temperature. The material was recovered by centrifugation, dried (110°C) and calcined (550°C) in a flow of air. The obtained Atomic absorption spectroscopy analysis showed that the zeolite contains 6.84 wt% of Cu.

3.2 General Procedure For The Synthesis Of Naphthoxazinones:

To a mixture of 1eq. of β-naphthol, 1eq. of aromatic aldehyde and 1.5 eq. of Urea in acetonitrile/dimethyl formamide solvent (6ml:1.5ml; 4:1) was added a catalytic amount of Cu(II)-NaY zeolite and stirred at 120°C. After

completion, ethyl acetate was added to the reaction mixture and the catalyst was recovered by filtration, washed with acetone and dried at 80°C. Ethyl acetate (filtrate) was washed with water, dried and evaporated. The residue was purified by silica gel column chromatography (ethyl acetate: hexane, 1:9).

3.3 Spectral Data:

Compound **4a**: mp 219 °C. ¹H NMR (300 MHz, DMSO): 6.12 (d, *J* = 2.26 Hz, 1H, CH), 7.24-8.12 (m, 3H, ArH), 8.88 (brs, 1H, NH). IR (KBr): 3296, 1721, 1517, 720 cm⁻¹. ESI MS : *m/z* 275 (M⁺).

Compound **4b**: mp 208 °C. ¹H NMR (300 MHz, DMSO): 6.21 (s, 1H, CH), 7.26-8.10 (m, 10H, ArH), 8.92 (brs, 1H, NH). IR (KBr): 3229, 3142, 1734, 1517, 747 cm⁻¹. ESI MS : *m/z* 310 (M⁺⁺¹).

Compound **4c**: mp 203 °C. ¹H NMR (200 MHz CDCl₃): 6.23 (s, 1H, CH), 7.31-8.02 (m, 10H, ArH), 8.94 (brs, 1H, NH). IR (KBr): 3126, 1751, 1509, 736 cm⁻¹. ESI MS : *m/z* (%) 293 (M⁺).

Compound **4d**: mp 221 °C. ¹H NMR (200 MHz DMSO): 6.21 (s, 1H, CH), 7.20-8.13 (m, 10H, ArH), 8.90 (brs, 1H, NH). IR (KBr): 3229, 3146, 1730, 1515, 723 cm⁻¹. ESI MS : *m/z* 377 (M^{++Na}).

Compound **4e**: mp 182 °C. ¹H NMR (300 MHz DMSO): 5.6 (s, 1H, CH), 7.32-8.20 (m, 10H, ArH), 8.55 (brs, 1H, NH), 11.10 (s, 1H, OH). IR (KBr): 3673, 3215, 1701, 1551, 746 cm⁻¹. ESI MS : *m/z* 291 (M⁺).

Compound **4f**: mp 187 °C. ¹H NMR (200 MHz DMSO): 3.76 (s, 3H, OCH₃), 6.24 (s, 1H, CH), 7.20-8.01 (m, 10H, ArH), 8.65 (brs, 1H, NH). IR (KBr): 3149, 2942, 1733, 1607, 1510, 842, 723 cm⁻¹. ESI MS : *m/z* 305 (M⁺).

Compound **4g**: mp 166 °C. ¹H NMR (300 MHz DMSO): 2.03 (s, 3H, CH₃), 6.26 (s, 1H, CH), 7.26-8.05 (m, 10H, ArH), 8.86 (brs, 1H, NH). IR (KBr): 3148, 2921, 1735, 1512, 723 cm⁻¹. ESI MS : *m/z* 289 (M⁺).

Compound **4h**: mp 172 °C. ¹H NMR (300 MHz DMSO): 1.25 (s, 6H, 2CH₃), 2.56 (m, 1H), 6.01 (d, *J* = 2.86 Hz, 1H, CH), 7.24-8.08 (m, 10H, ArH), 8.82 (brs, 1H, NH). IR (KBr): 3281, 2924, 1729, 1513, 830 cm⁻¹. ESI MS : *m/z* 317 (M⁺).

Compound **4i**: mp 178 °C. ¹H NMR (200 MHz, DMSO): 1.24 (s, 6H, 2CH₃), 1.31 (s, 3H, CH₃), 6.30 (s, 1H, CH), 7.40-8.19 (m, 10H, ArH), 8.92 (brs, 1H, NH). IR (KBr): 3203, 2959, 1727, 1515, 828, 740 cm⁻¹. ESI MS : *m/z* (%) 332 (M⁺⁺¹).

Compound **4j**: mp 199 °C. ¹H NMR (300 MHz, DMSO): 6.13 (s, 1H, CH), 7.21-8.06 (m, 10H, ArH), 8.92 (brs, 1H, NH). IR (KBr): 3220, 3142, 1729, 1513, 820, 748 cm⁻¹. ESI MS : *m/z* 309 (M⁺).

Compound **4k**: mp 222 °C. ¹H NMR (200 MHz, DMSO): 6.20 (s, 1H, CH), 7.18-8.06 (m, 10H, ArH), 8.91 (brs, 1H, NH). IR (KBr): 3252, 3140, 1730, 1512, 823, 758 cm⁻¹. ESI MS : *m/z* 355 (M⁺⁺¹).

Compound **4l**: mp 172 °C. ¹H NMR (200 MHz, CDCl₃): 3.78 (s, 3H, OCH₃), 6.12 (s, 1H, CH), 7.03-8.06 (m, 10H, ArH), 8.93 (s, 1H, NH). IR (KBr): 3149, 1733, 1510, 814, 743 cm⁻¹. ESI MS : *m/z* 306 (M⁺⁺¹).

Compound **4m**: mp 191 °C. ¹H NMR (200 MHz, DMSO): 6.01 (d, *J* = 3.38 Hz, 1H, CH), 6.98-8.01 (m, 10H, ArH), 8.56 (brs, 1H, NH). IR (KBr): 3423, 3299, 1730, 1515, 812, 743 cm⁻¹. ESI MS : *m/z* 292 (M⁺⁺¹).

4. CONCLUSION:

In summary, we have described a simple, convenient and efficient protocol for the synthesis of naphthoxazinones using Cu(II)-NaY zeolite as a cost-effective reusable and heterogeneous catalyst. The notable features of this method are simplicity in operation, cleaner reaction profiles and reusability of the catalyst, which make it an attractive and very useful process for the synthesis of naphthoxazinones of biological importance. We believe this methodology is superior to remaining methodologies for the synthesis of 1-oxo-hexahydroxanthene.

The in vitro antibacterial, antifungal evaluation showed that most of the synthesized naphthoxazinones derivatives exhibited moderate to good zone of inhibition. From the results of antibacterial and antifungal activity of naphthoxazinones it is interesting to note that substituents like methoxy, methyl and halogens at para substituents shows better antibacterial and antifungal activity compared to other substituted compounds. Noticeably, compound **4b**, **4c**, **4e**, and **4g**, were most potent compound in vitro activity against bacterial and fungal strains. These findings demonstrated that naphtho[1,2-*e*][1,3]oxazine-3-one have biological significance; further optimization of this series as well as preparation of new, 1-oxo-hexahydroxanthenes derivatives are ongoing in our laboratory.

5. ACKNOWLEDGMENT: KS thank DST-SERB, New Delhi, for the award of fellowship.

REFERENCES:

1. Banzatti C, Torre A D, Melloni P, Pieraccioli D, and Salvadori P, *J. Heterocycl. Chem* **1983**, 20, 139.
2. Cabiddu S, Floris C, Melis S, Sotgiu F, and Cerioni G, *J. Heterocycl. Chem.*, **1986**, 23, 1815.
3. Butler R C M, Chapleo C B, Meyers P L, and Welbourn A P, *J. Heterocycl. Chem.* **1985**, 22, 177.
4. Yoshida K, Minami Y, Azuma R, Saeki M, and Otani T, *Tetrahedron Lett.* **1993**, 34, 2637.
5. Thuillier G, Laforest J, Bessin P, Bonnet J, and Thuillier J, *Eur. J. Med. Chem. Chim. Ther.* **1975**, 10, 37.
6. Wheeler K W, *J. Med. Chem.* **1962**, 5, 1383.
7. Rekka J E, Refsas S, Dimpoulos V J, and Kouounakis P N, *Arch. Pharm.* 53, **1989**, 323.
8. Sridhar D R, Gandhi S S, and Srinivasa Rao K, *Synthesis* 11, **1982**, 987.
9. Wang Y, Ding X Li K, *Tetrahedron Asymmetry* 13, **2002**, 1291.

10. Shaterian H R, Yarahmadi H, Ghashang M, *Tetrahedron* 64, **2008**, 1269.
11. Srihari G, Nagaraju M, Murthy M M, *Helv. Chim. Acta* 90 (8), **2007**, 1504.
12. Rahul N R, Devanand S B, *Chinese. J. Chem.* 25 (11), **2007** 1714.
13. Das B, Laxminarayana K, Ravikanth B, and Rama Rao B, *J. Mol. Cat.* 261, **2007**, 183.
14. Kantevari S, Vuppalapati SVN, Nagaraju L, *Catal. Commun* 8 **2007**, 1857.
15. Sabitha G, Aurandhathi K, Sudhakar K., Sastry B S, *J.Heterocyclic. Chem.*, **2010**, 47, 272.
16. Dong F, Li-fang Y, Jin-ming Y, *Res. Chem. Intermed*, **2013**, 39, 2505.
17. Nemati F, Beyzai A, *Journal of Chemistry*, **2013**, 2012
18. Dharma Rao G. B, Kaushik M P, Halve A K, *Tetrahedron Lett.*, **2012**, 53, 2741. b) Dabiri M, Delbari A S, Bazgir A, *Syn. Lett.* 5, **2007**, 821.
19. Rama V, Kanagaraj K, Pitchumani K., *J. Org. Chem.* **2011**, 76, 9095.
20. Esakkidurai T, Pitchumani K, *J. Mol. Cat. A.* **2002**, 185, 309.
21. Dabiri M, Delbari A S, and Bazgir A, *Heterocycles*, **2007**, 71, 543.
22. Amol H K, Swapni S S, Rajkumar U P, Atul H K, Bapurao B S, Muralidhar S S, *Bull. Korean Chem. Soc.* **2010** 31(6) 1657.

**UGC Sponsored Two Day National Seminar on
GREEN CHEMISTRY FOR SUSTAINABLE DEVELOPMENT (GCSD -2017)**

April 06 - 07, 2017 at Government Degree College,
Jammikunta, Karimnagar, Telangana State, India

A Structure-Based Qsar And Docking Studies On Donepezil Derivatives As Selective Ache Inhibitors

Dr. B. Venkateshwarlu

Department of Chemistry, K.N.M G.D.C, Miryalaguda, T.G. INDIA –508207.

Email - venkateswarlu.bolisetty@gmail.com

1. INTRODUCTION:

Donepezil Derivatives marketed under the trade name Aricept and now sold as a generic by multiple suppliers, is a centrally acting reversible acetylcholinesterase inhibitor. Its main therapeutic use is in the palliative treatment of Alzheimer's disease. Donepezil Derivatives should be used with caution in people with cardiac disease. The precise mechanism of action of Donepezil Derivatives as selective Antagonist in patients with Alzheimer's disease [42]. Certainly Alzheimer's disease involves a substantial loss of the elements of the cholinergic system and it is generally accepted that the symptoms of Alzheimer's disease are related to this cholinergic deficit, particularly in the cerebral cortex and other areas of the brain. Donepezil and their derivatives binds and inactivates reversibly the cholinesterases, thus inhibiting hydrolysis of acetylcholine. This results in an increased acetylcholine concentrations at cholinergic synapses. Acetylcholinesterase (AChE) inhibitors are the main drugs used in the treatment of AD [3-6]. In this work, docking studies have been performed in order to understand the interaction between inhibitor and AChE. The increase observed in the calculated binding affinities between inhibitor and AChE, reflect the experimental inhibitory activity expressed in terms of the half maximal inhibitory concentration ($IC_{50} = 0.0092$ to $36.8 \mu\text{M}$) of the above inhibitor. The AM1 and PM3 semi-empirical methods are used to estimate the predictive power of final QSAR equations. QSAR and molecular docking studies indicated that, (1-benzylpiperidyl)5,6-dimethoxy,2,3-dihydro indene-1-one derivative of Donepezil showed the highest percentage of concentration and can become a potential lead for treating Alzheimer's disease. The loss of memory is directly correlated with the abridged cholinergic neurotransmission, caused by the pronounced diminish in the levels of the neurotransmitter [7-9]. AChE abnormal activity of human acetylcholinesterase (hAChE), the enzyme responsible for hydrolysis of AChE, was attributed to the reduced level of AChE. Treating AD was achieved through inhibiting the anomalous action of AChE by various specific AChE inhibitors such as

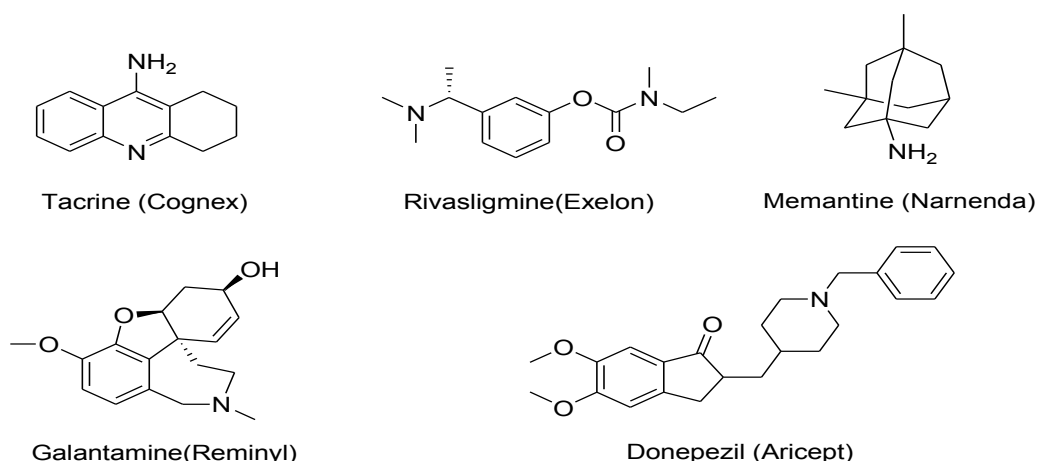


Fig1: Marketed drugs for the treatment of Alzheimer's disease.

Donepezil Derivatives is reversible acetylcholinesterase inhibitors that readily crosses the blood-brain barrier to reduce the breakdown of acetylcholine is too basic heterocyclic compound. It is a raw material used for the production of dyes and some valuable drugs. Many Donepezil Derivatives also have antiseptic properties. Donepezil Derivatives and related derivatives bind to DNA and RNA through intercalation mode [10-12].

2. MATERIALS AND METHODS

2.1 Bioassay: In the present investigation bioassay of 15 derivatives of Donepezil found in the literature [39] whose IC_{50} values are known. The criteria for selection of molecules are

- 1) Against same target.
- 2) Which have available biological activity data.
- 3) Molecules possessing Donepzil Derivatives scaffold.

15 molecules were selected based on the above set criteria. More than 11 molecules showed IC_{50} below 1_Micro_molar concentration. These were further supported by docking studies using GOLD and Argus Lab 4.0.1 Software.

2.2 Structural Skeleton of Donepzil

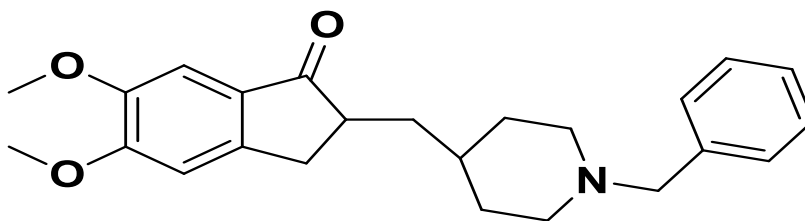
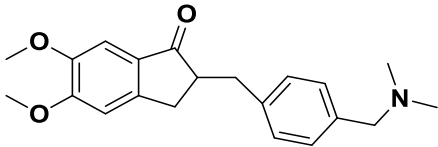
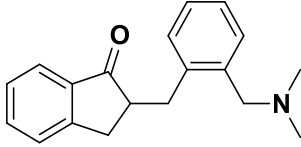
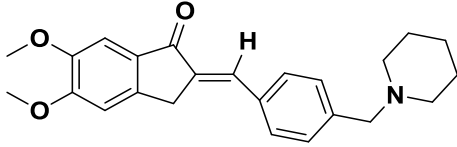
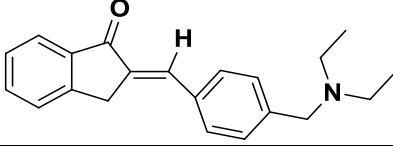
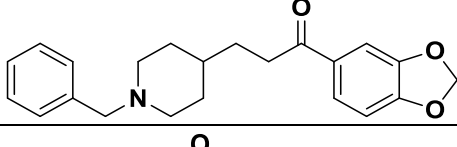
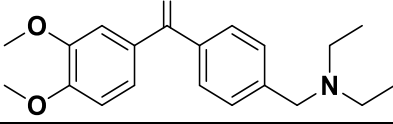


Fig 2: Donepzil

Table 1: DONEPZIL DERIVATIVES with IC_{50} values

COMPOUND	STRUCTURE	$IC_{50}(\mu M)$
1		0.0092
2		0.0116
3		0.12
4		0.66
5		0.25
6		0.29
7		1.48
8		0.38
9		0.69

10		1.38
11		3.74
12		0.1
13		0.035
14		0.041
15		36.8

3. COMPUTATIONAL CALCULATIONS

3.1 Molecular Structure Building

A series of 15 compounds tested for inhibitory activity were selected for the present study from pubchem [1], and Hyperchem software [2] were used in modeling studies. The molecules were generated and the geometry optimization was performed using molecular modeling programme (Force Field).

3.2 Data Set and Validation of QSAR Models

QSAR technique was applied to the Donepezil analogues that were varied at the positions of different substituent's from structure to structure shown in Table 1. The appropriate descriptors or parameters for the identified compounds viz; vertical ionization potentials (IPV's), electron affinity (EA), electro negativity (χ), hardness (η), softness (S), electrophilicity index (ω), partition coefficient (LOGP), polarisability (POL) and hydration energy (HE) were used as independent variables for deciding in AChE inhibitory activity.

4. CHEMICAL DESCRIPTORS

4.1 Semi Empirical Methods

Quantum chemical calculations at the DFT/RB3LYP/631G* (restricted B3LYP), RHF/6-31G* (restricted Hartree-Fock), AM1 and PM3 semi empirical theory levels, are employed for full optimization of the selected neutral compounds [17-19]. The geometrical structures of the radicals studied are optimized independently from the neutral molecules prior to the calculation of energies, treated as open shell systems [20-22]. All calculations are performed by using the program of Hyperchem software Inc.

The calculated vertical ionization potential (IPV's) and electron affinity (EA) are corrected for zero-point energy, assuming a negligible error and thus saving computer-time. The IPV are calculated as the energy differences between a radical cation and the respective neutral molecule; IPV ($E_{\text{cation}} - E_{\text{neutral}}$)_{DFT} and Koopmans's theorem (IPV = $-\epsilon_{\text{HOMO}}$). The EA are computed as the energy differences between a neutral form and the anion molecule; EA = $E_{\text{neutral}} - E_{\text{anion}}$. The AM1 reactivity descriptors are obtained from Eqs.(1)&(2) [23-25].

4.2 Correlation Analysis

The window version software SPSS [26] was used in the regression analysis. A relation between biological activity, expressed as Log (1/IC₅₀), and the physicochemical parameters and QSAR was analyzed statistically by fitting

the data to correlation equations consisting of various combinations of these parameters. The statistical optimization was used to propose the best correlation model.

The matrix correlation uses the Pearson product moment correlation to measure the degree of linear relationship between two variables. The coefficient assumes a value between -1 and +1. If one variable tends to increase the other decreases, the correlation coefficient is negative. Conversely, if the two variables tend to increase together the correlation coefficient is positive. We obtained the correlation matrix between inhibitory activity and respective calculated properties for eight Donepezil derivatives. The more relevant regression models were selected: The correlation coefficient (R), the Fisher ratio values (F) and the standard deviations(s), standard error estimate (SEE), percentage of effective variable(%EV) and R^2 adjusted (Adj R^2).

The best equation was also tested for their predictive power using a cross-validation procedure. The cross-validation is a practical and reliable method for testing this significance. In principle, the so-called "leave-one-out" approach consists in developing a number of models with one sample omitted at the time [27].

After developing each model, the omitted data is predicted and the differences between actual and predicted reduction potential (y) values are calculated. The sum of squares of these differences is computed and finally the performance of the model (its predictive ability) is given by PRESS (Predictive Sum of Squares) and S_{PRESS} (Standard deviation of cross validation). The predictive ability of the model was also quantified in terms of the Q^2 .

4.3 Docking Studies and Validation

GOLD and Argus lab 4.0.1 are Molecular Docking software. This helps in computational virtual screening to find the lead compounds. Molecular docking started with Fischer's lock and key theory, where, every receptor has its unique ligand to catalyze the reaction [28-30]. Now-a-days docking is frequently to predict the binding orientations of small molecules of drug candidates to their protein targets in order to predict the affinity of the small molecules.

The GOLD Score was calculated by defining the site using the list of atom numbers and retaining all the other default parameters. The 3D structure of AChE was retrieved from Protein Data Bank (PDB ID 1EVE) [31] with an X-ray resolution of 2 Å. Docking poses were obtained by applying Gold score, fitness functions available for scoring. All the results reported in the present paper are referred to the ChemScore and GOLD fitness functions. These complexes were prepared for docking studies by adding hydrogen atoms, removing water molecules and co-crystallized inhibitors and refined by using the DeepView/SwissPdbViewer3.7(SP5)(Guex N, Peitsch MC).

Swiss Model and the Swiss Pdb-Viewer: DeepView/Swiss PdbViewer3.7 (SP5) Enzyme- inhibitor interactions within a radius equal to 10 Å centered on reported bound inhibitors were taken into account. As a conclusive part of docking we expect, generated results should yield RMSD values below 1.5 Å. Successful docking has been performed for the selected set of Donepezil derivative inhibitors and their corresponding Chemscore with their RMSD have been produced in the Table 2.

Table 2: Energy, ChemScore and gold fitness values of the docked ligands.

Compound	Activity(IC ₅₀ in μ m)	GOLD Software		ArgusLab (Energy Values in k.cal/moles)
		CHEMSCORE	FITNESS	
1	0.0092	28.21	-824.48	0
2	0.0116	25.54	-698.51	0
3	0.12	38.29	72.59	-11.2631
4	0.66	-1.19	-1354.89	0
5	0.25	33.52	-485.83	0
6	0.29	-8.17	-1853.91	-9.72916
7	1.48	16.71	-994.78	0
8	0.38	-13.71	-1632.48	-10.3238
9	0.69	30.02	-337.25	-9.13203
10	1.38	26.27	-662.66	-10.269
11	3.74	30.03	-336.30	-7.46565
12	0.1	15.88	-1295.08	0
13	0.035	22.17	-1626.47	0
14	0.041	4.32	-1933.45	-10.0251
15	36.8	-19.90	-1698.39	-8.59288

5. RESULTS AND DISCUSSIONS:

5.1 Simple linear regression model

The biological activity data and the physicochemical properties IPV, IP, EA, EI, EN, Hardness, Softness, LOGP, HE and POL of the Donepezil derivatives are given in Table 3. The data from this table was subjected to regression analysis [32-35]. The Correlation matrices were generated with 15 analogs (Table 4). The term close to 1

indicates high co-linearity, while the value below 0.5 indicates that no co-linearity exist between more than the two parameters.

The perusal of correlation matrix (**Table 5**) indicates that and HE are the predicted parameters from AM1 method. POL and Hardness were found to be explainable variable from regression methods backward, forward, removed and stepwise.

$$\text{Predicted Activity} = (-1.617 \cdot \text{Hardness}) + (0.205 \cdot \text{POL}) \rightarrow (1)$$

N=15; R=0.968; R²=0.937; AdjR²=0.927; %EV=93.7; SEE = 0.73251; F= 96.338; Q=1.32148;

In addition, the plot of observed activity versus predicted activity was not found to be satisfactory. Hence, the predictive ability of the model is not good. **Eq.1** shows that the values of %EV are less and to improve its value, outliers were sought and eliminated.

After the elimination of the outlier (**3, 6, 8, 9, 10, 11, 14 and 15**), a second model was developed. Overall, there is an increase in R and %EV (93.6-100) values, and a decrease in SEE (0.73251-0.09821).

$$\text{Predicted Activity} = (-1.172 \cdot \text{Hardness}) + (-16.177 \cdot \text{Softness}) + (0.216 \cdot \text{POL}) \rightarrow (2)$$

N=8; R=1.000; R²=0.999; AdjR²=0.999; %EV=99.99; SEE=0.09821; F=2080.487; Q=10.18226;

Eq.2 is an improved model since it explains the biological activity to the extent of 99.99%. In this way, the predictive molecular descriptors Hardness, Softness and POL were considered as variables.

In an attempt to investigate the predictive potential of proposed models, the cross-validation parameters (q²_{cv} and PRESS) were calculated and used. The predictive power of the equations was confirmed by cross-validation method where, compounds are deleted one after another and prediction of the activity of the deleted compound is made based on QSAR model. The cross-validation evaluates the validity of a model by how well it predicts the data rather than how well it fits the data. The cross-validation parameter, q²_{cv}, is mentioned in the respective equations (**Table 6**).

$$q_{cv}^2 = \frac{(\text{SD} - \text{PRESS})}{\text{SD}}$$

Where the PRESS (predictive residual sum of squares) and SD (standard deviation) values are obtained as

$$\text{PRESS} = \sum (\text{property}_{\text{observed}} - \text{property}_{\text{predicted}})^2$$

$$\text{SD} = \sum (\text{property}_{\text{observed}} - \text{property}_{\text{mean}})^2$$

The PRESS, SD, q²_{cv} values for the fifteen Donepezil derivatives (AM1 method) is given by

$$\text{PRESS}=6.9634, \text{SD}=13.0769, q_{cv}^2=0.4675.$$

The PRESS, SD, q²_{cv} values for the seven donepezil derivatives (AM1 method) is given by

$$\text{PRESS}=0.0502, \text{SD}=2.784, q_{cv}^2=0.9819.$$

From the above observations, AM1 method gave a good q²_{cv} values, which should be always smaller than %EV. A model is considered to be significant when q²_{cv}>0.3.

Another cross-validation parameter, PRESS which is the sum of the squared differences between the actual and that predicted when the compound is omitted from the fitting process, also supports the predictive ability of **Eq.2**. Its value decreases from **Eq.1**.

The quality factor Q, is defined as the ratio of regression constants (R) to the standard error estimation (SEE), i.e. Q = R/SEE. This indicates that the higher the value of R, and the lower the value of SEE, the higher is the magnitude of Q and the better will be the correlation. In present case, Q increases from 1.32148 to 10.18226 (Eq. 1 & 2).

5.2 Docking Analysis

The compounds were then docked in to protein active site using docking software [226]. The ChemScore and GOLD fitness of two docking software's are presented in **Table 2**. The binding energies obtained in Argus Lab ranged from -7.465 to -11.26kJ/mol. The results of CCDC GOLD can be analyzed both in terms of energy values ranging from -1933.45 to 72.59 and -1.19 to 38. 29

The docking simulation of the most active Donepezil derivatives **15** towards AChe (PDB ID 1EVE) showed that the enzyme-inhibitor complex was stabilized by hydrophobic interactions occurring between the aromatic moieties of the ligand and lipophilic residues of the binding site [36-39]. The compounds 3, 6, 8, 9, 10, 11, 14 and 15 were oriented towards the hydrophobic region lined by SER200A, TRP84A, TYR130, ASP72, ARG289, PHE290 and HIS440. Result of docking studies has proved that the molecule numbered 3 shows Chemscore, Gold fitness and RMSD values as 38.29, 72.59 and 1.5 Å respectively (Table2). The molecule 8 has been reported with appreciable IC₅₀ values of 0.12µM. All the poses of molecule 3 (chosen as best in docking studies) and its interactions in the active pocket of AChe have been illustrated in Figure 4.

Table 3: Values obtained for the AM1 computational method.

Compound	IPV	EA	EN(μ)	Hardness(η)	Softness(S)	EI(ω)	ACT	HE	LOGP	POL(A°3)
1	8.49	0.87	4.68	3.81	0.13	2.88	4.04	-4.08	1.31	43.28
2	8.98	1.45	5.22	3.77	0.13	3.61	3.94	-3.25	2.76	48.29
3	8.42	1.11	4.76	3.66	0.14	3.1	2.92	-2.67	1.13	43.28
4	8.53	1.2	4.87	3.67	0.14	3.23	2.18	-2.67	1.13	43.28
5	8.8	1.15	4.98	3.82	0.13	3.24	2.6	-3.54	0.44	42.7

6	8.45	1.1	4.77	3.67	0.14	3.1	2.54	-2.47	1.09	42.22
7	8.55	1.19	4.87	3.68	0.14	3.23	1.83	-2.35	1.09	42.22
8	8.39	1.16	4.77	3.61	0.14	3.15	2.42	-2.71	0.75	40.38
9	8.55	1.19	4.87	3.68	0.14	3.22	2.16	-2.69	0.75	40.38
10	8.45	1.11	4.78	3.67	0.14	3.11	1.86	-3.11	0.41	38.55
11	8.55	1.19	4.87	3.68	0.14	3.22	1.43	-3.12	0.41	38.55
12	8.2	1.25	4.73	3.48	0.14	3.21	3	-6.87	-0.1	43.72
13	8.53	1.32	4.93	3.61	0.14	3.36	3.46	-2.47	0.89	42.02
14	8.9	1.14	5.02	3.88	0.13	3.25	3.39	-5.96	1.68	39.61
15	8.74	0.36	4.55	4.19	0.12	2.47	0.43	-9.14	0.51	38.67

*IPV→Vertical Ionization Potential, *EA→Electron Affinity, *EN→Electro Negativity, *EI→Electrophilicity Index,
 *ACT→Observed Activity, *HE→Hydration Energy, *LOGP→Partition Coefficient, *POL→Polarizability

Table 4: Correlation matrix between the selected variables, by using AM1 method.

		IPV	EA	EN	η	S	EI	ACT	HE	LOGP	POL
IPV	Pearson Correlation	1	-.030	.632	.658	-.686	.185	.109	-.164	.635	.163
	Sig. (2-tailed)		.917	.011	.008	.005	.510	.699	.558	.011	.562
	N	15	15	15	15	15	15	15	15	15	15
EA	Pearson Correlation	-.030	1	.756	-.772	.746	.976	.536	.662	.288	.480
	Sig. (2-tailed)	.917		.001	.001	.001	.000	.039	.007	.297	.070
	N	15	15	15	15	15	15	15	15	15	15
EN	Pearson Correlation	.632	.756	1	-.167	.129	.877	.487	.405	.639	.479
	Sig. (2-tailed)	.011	.001		.551	.648	.000	.066	.134	.010	.071
	N	15	15	15	15	15	15	15	15	15	15
η	Pearson Correlation	.658	-.772	-.167	1	-.998	-.617	-.334	-.603	.187	-.258
	Sig. (2-tailed)	.008	.001	.551		.000	.014	.223	.017	.506	.354
	N	15	15	15	15	15	15	15	15	15	15
S	Pearson Correlation	-.686	.746	.129	-.998	1	.588	.309	.558	-.223	.247
	Sig. (2-tailed)	.005	.001	.648	.000		.021	.262	.031	.424	.375
	N	15	15	15	15	15	15	15	15	15	15
EI	Pearson Correlation	.185	.976	.877	-.617	.588	1	.541	.597	.418	.520
	Sig. (2-tailed)	.510	.000	.000	.014	.021		.037	.019	.121	.047
	N	15	15	15	15	15	15	15	15	15	15
ACT	Pearson Correlation	.109	.536	.487	-.334	.309	.541	1	.255	.555	.671
	Sig. (2-tailed)	.699	.039	.066	.223	.262	.037		.358	.032	.006
	N	15	15	15	15	15	15	15	15	15	15
HE	Pearson Correlation	-.164	.662	.405	-.603	.558	.597	.255	1	.232	.226
	Sig. (2-tailed)	.558	.007	.134	.017	.031	.019	.358		.405	.417
	N	15	15	15	15	15	15	15	15	15	15
LOGP	Pearson Correlation	.635	.288	.639	.187	-.223	.418	.555	.232	1	.591
	Sig. (2-tailed)	.011	.297	.010	.506	.424	.121	.032	.405		.020
	N	15	15	15	15	15	15	15	15	15	15
POL	Pearson Correlation	.163	.480	.479	-.258	.247	.520	.671	.226	.591	1
	Sig. (2-tailed)	.562	.070	.071	.354	.375	.047	.006	.417	.020	
	N	15	15	15	15	15	15	15	15	15	15

Table 5: Correlation matrix between the selected variables, by using AM1 method.

		IPV	EA	EN	η	S	EI	ACT	HE	LOGP	POL
IPV	Pearson Correlation	1	.572	.957	.885	-.878	.773	.475	.364	.722	.546
	Sig. (2-tailed)		.139	.000	.003	.004	.024	.234	.375	.043	.162
	N	8	8	8	8	8	8	8	8	8	8
EA	Pearson Correlation	.572	1	.785	.124	-.110	.962	.814	-.303	.649	.805
	Sig. (2-tailed)	.139		.021	.770	.796	.000	.014	.465	.082	.016
	N	8	8	8	8	8	8	8	8	8	8
EN	Pearson Correlation	.957	.785	1	.712	-.701	.924	.647	.168	.774	.697
	Sig. (2-tailed)	.000	.021		.048	.053	.001	.083	.692	.024	.055
	N	8	8	8	8	8	8	8	8	8	8
η	Pearson Correlation	.885	.124	.712	1	-.999	.389	.113	.613	.505	.204
	Sig. (2-tailed)	.003	.770	.048		.000	.340	.791	.106	.202	.629

	N	8	8	8	8	8	8	8	8	8	8
S	Pearson Correlation	-.878	-.110	-.701	-.999	1	-.376	-.098	-.640	-.513	-.187
	Sig. (2-tailed)	.004	.796	.053	.000		.359	.817	.088	.194	.657
	N	8	8	8	8	8	8	8	8	8	8
EI	Pearson Correlation	.773	.962	.924	.389	-.376	1	.788	-.113	.742	.805
	Sig. (2-tailed)	.024	.000	.001	.340	.359		.020	.789	.035	.016
	N	8	8	8	8	8	8	8	8	8	8
ACT	Pearson Correlation	.475	.814	.647	.113	-.098	.788	1	-.260	.696	.987
	Sig. (2-tailed)	.234	.014	.083	.791	.817	.020		.535	.055	.000
	N	8	8	8	8	8	8	8	8	8	8
HE	Pearson Correlation	.364	-.303	.168	.613	-.640	-.113	-.260	1	.444	-.243
	Sig. (2-tailed)	.375	.465	.692	.106	.088	.789	.535		.270	.562
	N	8	8	8	8	8	8	8	8	8	8
LOGP	Pearson Correlation	.722	.649	.774	.505	-.513	.742	.696	.444	1	.697
	Sig. (2-tailed)	.043	.082	.024	.202	.194	.035	.055	.270		.055
	N	8	8	8	8	8	8	8	8	8	8
POL	Pearson Correlation	.546	.805	.697	.204	-.187	.805	.987	-.243	.697	1
	Sig. (2-tailed)	.162	.016	.055	.629	.657	.016	.000	.562	.055	
	N	8	8	8	8	8	8	8	8	8	8

Table 6: Observed Activity and Predicted Activity values of DONEPZIL derivatives by using AM1 equations.

Compound	Observed Activity	Equation(1)		Equation(2)	
		Predicted	Residual	Predicted	Residual
1	4.04	2.71	-1.33	-	-
2	3.94	3.81	-0.13	3.87	-0.07
3	2.92	2.96	0.04	2.85	-0.07
4	2.18	2.94	0.76	-	-
5	2.6	2.57	-0.03	2.63	0.03
6	2.54	2.72	0.18	2.61	0.07
7	1.83	2.71	0.88	-	-
8	2.42	2.43	0.01	2.25	-0.17
9	2.16	2.32	0.16	2.21	0.05
10	1.86	1.97	0.11	1.82	-0.04
11	1.43	1.95	0.52	-	-
12	3	3.34	0.34	3.04	0.04
13	3.46	2.78	-0.68	-	-
14	3.39	1.85	-1.54	-	-
15	0.43	1.16	0.73	-	-

6. CONCLUSIONS

Quantitative structure–activity relationship studies (QSAR) and molecular docking were performed on fifteen DONEPZILDERIVATIVES as AChE inhibitors to find out the structural relationship with the activity. The best predictive AM1 model resulted in cross-validated R^2 value of 1.000, $\text{Adj}R^2$ value of 1.000 and standard error of estimate 0.05969 (AM_1). Similarly the best predictive PM3 model was derived with R^2 of 0.999, $\text{Adj}R^2$ of 0.999 and standard error of estimate of 0.12754, comprising softness, hydration energy, hydrophobic and hydrogen bond donor fields. These models were able to predict the activity of test set molecules efficiently (best molecules 3, 6, 8, 9, 10, 11, 14 and 15) within an acceptable error range. GOLD and Argus lab docking software were employed to dock the inhibitors into the active site of AChE and these docking studies revealed the vital interactions and binding conformation of the inhibitors.

Therefore, the present study showed that the QSAR studies and the docking approach of DONEPZILDERIVATIVES as AChE inhibitors can be successfully modeled using the parametric equations. The Eq.2 from AM1, semi empirical calculations reveal EA, Hardness, Softness, EI, LOGP, POL and HE cause the

inhibitory activity. Higher values of EA, Hardness, Softness, EI, LOGP, POL and HE were responsible for higher inhibitory activity nature for AChE enzyme. The linear dependence of inhibitory nature on Softness and HE were evident from Figure 3.

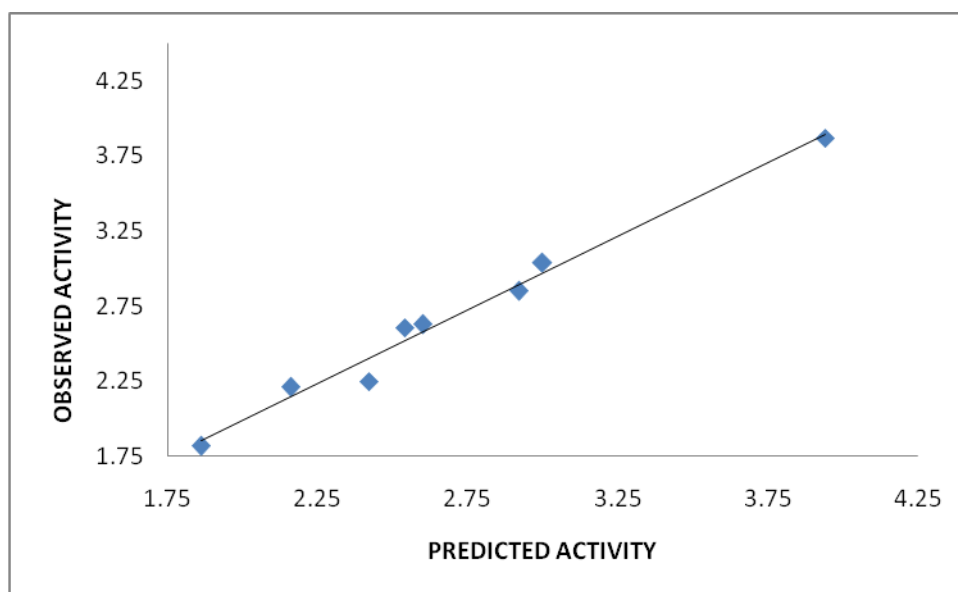


Fig 3 Plot of Observed Verses Predicted activity (AM1 Method)

The most active compounds docked successfully into the active site of the inhibited enzyme. Inhibitory activity of the most potent compounds was explained mostly by hydrophobic interactions.

The compounds 3, 6, 8, 9, 10, 11, 14 and 15 were found to present high antibacterial activity and significant inhibitory activity on AChE. The information rendered by QSAR models and the docking interactions may afford valuable clues to optimize the lead and design of new potential inhibitors [41-42].

The order of the more effective and the higher activity of the remaining eight compounds 15, 14, 11, 10, 9, 8, 6 and 3. Best pose of the more effective and the higher activity of the Donepezil derivatives compound 3 is as follows

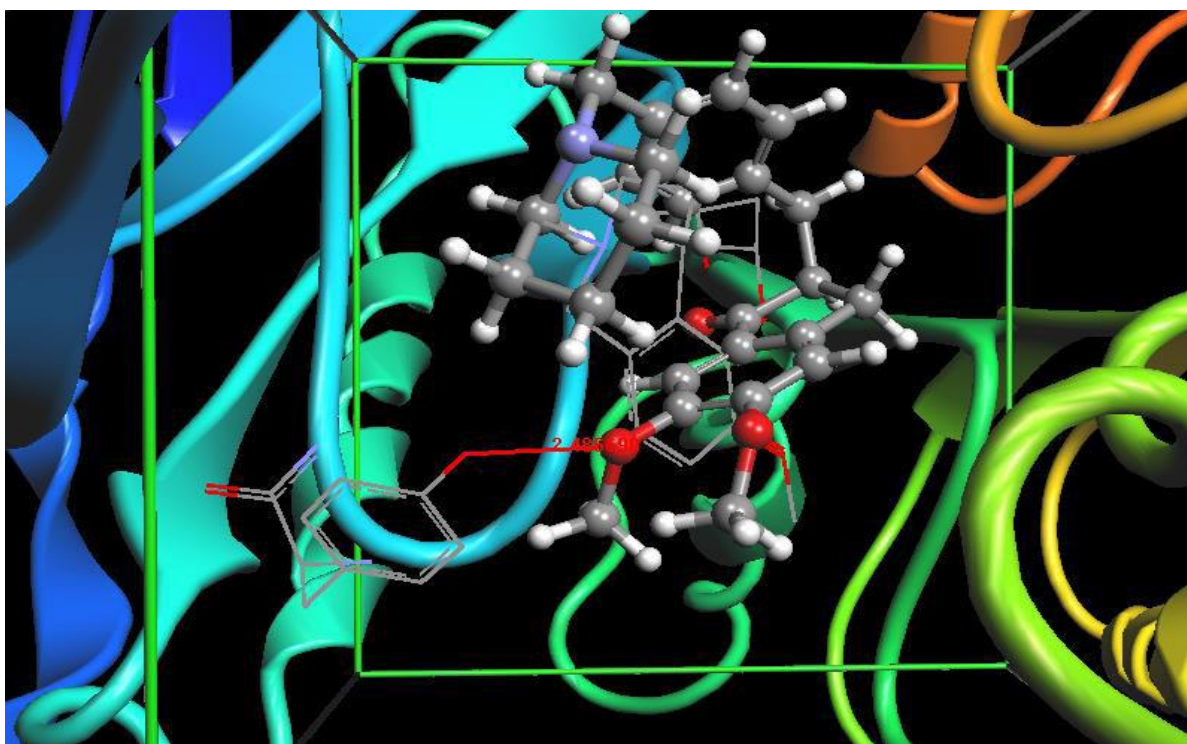


Fig 4 Best pose of molecule 3 and secondary structure of AChE (PDB ID 1EVE).

REFERENCES:

- Goedert M, Spillantini MG: **A Century of Alzheimer's Disease**. *Science* **2006**, **314**:777-781.
- Cummings JL, Morstorf T, Zhong K. Alzheimer's disease drug-development pipeline: Few candidates, frequent failures. *Alzheimer Res Therapy* **2014**; **6**:37.
- Camps P, Formosa X, Galdeano C, Muñoz-Torrero D, Ramírez L, Gómez E, Isambert N, Lavilla R, Badia A, Clos MV, Bartolini M, Mancini F, Andrisano V, Arce MP, Rodríguez-Franco MI, Huertas Ó, Dafni T, Luque FJ: **Pyrano[3,2-c]quinoline-6-chlorotacrine hybrids as a novel family of acetyl cholinesterase and beta amyloid directed anti-Alzheimer compounds**. *J Med Chem* **2009**
- Schmidt R, Neff F, Lampl C, Benke T, Anditsch M, Bancher C, Dal-Bianco P, Reiskecker F, Marksteiner J, Rainer M, Kapeller P, Dodel R: **Therapy of Alzheimer's disease: current status and future development**. *Neuropsychiatr* **2008**,
- Koji Hori, Kimiko Konishi, Masayuki Tani, Hiroi Tomioka, Ryo Akita, Yuka Kitajima, et al. (2014) Serum Anticholinergic Activity: A Possible Peripheral Marker of the Anticholinergic Burden in the Central Nervous System in Alzheimer's Disease.
- Racchi M, Mazzucchelli M, Porrello E, Lanni C, Govoni S: **Acetyl cholinesterase inhibitors: novel activities of old molecules**. *Pharmacol Res* **2004**,
- Carlier PF, Han YF, Chow ESH, Li CPL, Wang H, Lieu TX, Wong HS, Pang YP: **Evaluation of short-tether Bis-THA AChE inhibitors. A further test of the dual binding site hypothesis**. *Bioorg Med Chem* **1999**,
- Pang YP, Quiram P, Jelacic T, Hong F, Brimijoin S: Highly potent, selective, and low cost bis-tetrahydroacminacrine Inhibitors of Acetyl cholinesterase. Steps toward novel drugs for treating Alzheimer's disease. *J Biol Chem*, **1996**,
- Marco JL, delos Ríos C, Carreiras MC, Baños JE, Badía A, Vivas NM: Synthesis and acetylcholinesterase/butrylcholinesterase inhibition activity of new tacrine-like analogues, *Bioorg Med Chem*, **2001**
- Suresh reddy j, Vobalaboina Venkateswarlu, Novel drug delivery systems for drug targeting to the brain, *Drugs Fut*, **29** (1):63-83, (2004).
- Brown, E.G. Ring Nitrogen and Key. "Biomolecules. Kluwer" *Academic Press*, **1998**.
- Pozharskii, A.F, et al. "Heterocycles in Life and Society". *John Wiley & Sons*, **1997**.
- Katritzky A. R.; Rees. "Comprehensive Heterocyclic Chemistry", **1984**, **5**, 469-498.
- Tetko IV, Luik AI, Poda GI: Applications of neural networks in structure-activity relationships of a small number of molecules, *J. Med. Chem* **1993**,
- Duchowicz PR, Castro EA, Fernández FM, González MP: A new search algorithm of QSPR/QSAR theories: normal boiling points of some organic molecules. *Chem. Phys Lett*, **2005**
- Moreau G, Broto P: Auto-correlation of molecular structures, application to SAR studies. *Nouv J Chim* **1980**, **4**:757-764.
- Consonni V, Todeschini R, Pavan M, Gramatica P: Structure/Response Correlations and Similarity/Diversity Analysis by GETAWAY Descriptors. 2. Application of the novel 3D molecular descriptors to QSAR/QSPR studies. *J Chem Inf Model* **2002**, **42**:693-705.
- Akula NL, Lecanu J, Greeson V: 3D QSAR studies of AChE inhibitors based on molecular docking scores and CoMFA. *Bio-org Med Chem Lett* **2006**, **16**:6277-6280.
- Marco JL, delos Ríos C, Carreiras MC, Baños JE, Badía A, Vivas NM: Synthesis and acetyl cholinesterase /butryl cholinesterase inhibition activity of new tacrine-like analogues. *Bio-org Med Chem* **2001**,
- "AM₁ study on the conformation of 6-aminopencillanic acid" Bojja Rajeshwar Rao, *Indian J. Chem.*, **41**(B), 1697-1701, **2002**.
- Selassie, C.D. "History of quantitative structure-activity relationships". *Medicinal Chemistry and Drug Discovery*. **2003**, **1**, 1-48.
- Reis M, Lobato B, Lameira J, Santos AS, Alves CN "A theoretical study of phenolic compounds with antioxidant properties". *E J Med Chem.*, **2007**, **42**:440-446
- Roothan, C.C. J. "New Developments in Molecular Orbital Theory". *Rev. Mod. Phys.*, **1951**, **23**, 69.
- Pople, J.A.; Nesbet, R.K.; "Self consistent Orbitals for Radicals". *J. Chem. Phys.*, **1954**.
- McWeeny, R.; Dierksen, G. "Interpolating functionals in relation to the transition state and transition operator methods". *J. Chem. Phys.*, **1968**, **49**, 4852.
- Dewar, M.J.S.; Zebisch, E.G.; Healy E.F.; Stewart J.J.P. "The development and use of quantum mechanical molecular models". 76. AMI: a new general purpose quantum mechanical molecular model; *J. Am. Chem. Soc.*, **1985**, **107**, 3902.
- Stewart, J.P. "Optimization of parameters for semi empirical methods" *J. Comput. Chem.* **1989**
- Kohn, W.; Becke, A.D.; Parr, R.G. "Density Functional Theory of Electronic Structure". *J. Phys. Chem.*, **1996**, **10**, 12974.
- Parr, R.G.; Pearson, R.G.; "Hardness, softness, and the Fukui function in the electronic theory of metals and catalysis". *J. Am. Chem. Soc.* **1983**, **105**, 7512.

30. SPSS Software. Consult <http://www.spss.com>.
31. Senba Y., Nishita T., Stopped flow and spectrophotometric studies on radical scavenging by Tea catechins and the model compounds, *Chem.Pharm.Bull.*,**1999**,47,1369-1374.
32. Jones, G.; Willet, P.; Glen, R.C. "Molecular recognition of receptor sites using a genetic algorithm with a description of desolvation". *J mol boil*, **1995**, 245, 43.
33. Pogliani, L.; "Structure property relationships of amino acids and some dipeptides". *Amino Acids*.**1994**, 6, 14.
34. Schulz-Gasch, T.; Stahl, M.; "Scoring functions for protein–ligand interactions": a critical perspective. *Drug Discovery.Today*.**2004**, 1 (3), 231-239.
35. Guex, N.; Peitsch, MC. Swiss Model and the Swiss Pdb-Viewer: An environment for comparative protein modeling. *Deep View/SwissPdbViewer3.7 (SP5) Electrophoresis*, 18, 2714-2723.
36. Chatterjee, S.; Hadi.A.S; Price.B; "Regression Analysis by Examples", *3rd Ed Willy: New York*. **2000**.
37. Thompson & Mark, A. "Argus Lab 4.0.1" www.arguslab.com Planaria Software LLC, Seattle

WEB REFERENCES:

- <http://pubchem.ncbi.nlm.nih.gov>.
- <http://www.warezdestiny.com/free-hyp>
- <http://www.nia.nih.gov/Alzheimers/Publications/CaringAD/other/medicines.htm>

UGC Sponsored Two Day National Seminar on GREEN CHEMISTRY FOR SUSTAINABLE DEVELOPMENT (GCSD -2017)

April 06 - 07, 2017 at Government Degree College,
Jammikunta, Karimnagar, Telangana State, India

Novel Method Development Of Ertapenem By Spectrophotometric Determination In Bulk And Injection Formulations By Cobalt Thio Cyanate

N. Aruna kumari¹ and A.Vasundhara²

¹Associate Professor, Department of HBS GIET, Rajahmundry India

²Reader and HOD SKR College for Women, Rajahmundry

Email - drsidvi@gmail.com

Abstract: A simple and cost effective spectrophotometric method was described for the determination of Ertapenem in pure form and in pharmaceutical formulations. The method is based on the formation of colored chromogen when the drug reacts with Cobalt thio cyanate in presence of a buffer prepared by mixing potassium chloride solution (0.2M) and HCl (0.2M) having pH 2.0 and nitrobenzene. This method was applied for the determination of drug contents in pharmaceutical formulations and enabled the determination of the selected drug in microgram quantities (0.5 to 3.0 mL). No interferences were observed from excipients and the validity of the method was tested against reference method. The colored species has an absorption maximum at 625 nm for Ertapenem and obeys beer's law in the concentration range 5 – 30 µg/mL of Imipenem. The apparent molar absorptivity was 151×10^5 and sandell's sensitivity was 175×10^{-3} . The slope is 0.2114 ± 0.0022 , the intercept of the equation of the regression line is 0.0042 ± 0.0039 . The optimum experimental parameters for the reaction have been studied and the validity of the described procedure was assessed. Statistical analysis of the results has been carried out revealing high accuracy and good precision. The proposed method was successfully applied for the determination of Ertapenem in pharmaceutical formulations.

Keywords- Ertapenem, Cobalt thio cyanate, Molar absorptivity, sandell's sensitivity, Spectrophotometry.

1. INTRODUCTION

Due to counterfeiting, the drug quality has become a source of major concern worldwide, particularly in many developing countries. The most commonly counterfeited drugs are anti-infectives or antibiotics. Use of poor quality antibiotics bears serious health implications such as treatment failure, adverse reactions, drug resistance, increased morbidity, and mortality¹. Among antibiotics, penems are much recently introduced, widely prescribed and costlier. Therefore, incentive to produce their counterfeits because of profit margin increases considerably.

Ertapenem² is an ultra-broad spectrum injectable antibiotic used to treat a wide variety of infections. It is a beta-lactam and belongs to the subgroup of carbapenem, similar to imipenem and ertapenem. In contrast to other beta-lactams, it is highly resistant to degradation by beta-lactamases or cephalosporinases.

Ertapenem (Fig:1) is a carbapenem antibiotic marketed by Merck as Invanz. It is structurally very similar to meropenem including its stability to dehydropeptidase-1. ERP is a new carbapenem of beta-lactam-type antibiotics with an exceptionally broad spectrum of activity. It has antimicrobial activity against many Gram-positive and gram-negative aerobes and anaerobes and is resistant to nearly all beta-lactamases, including extended-spectrum beta-lactamases.

Drug Profile

Name	Ertapenem (ERP)
Chemical Name	(4R,5S,6S)-3-[(3S,5S)-5-[(3-carboxyphenyl)carbamoyl]pyrrolidin-3-yl]sulfanyl-6-(1-hydroxyethyl)-4-methyl-7-oxo-1-azabicyclo[3.2.0]hept-2-ene-2-carboxylic acid
Structure	:

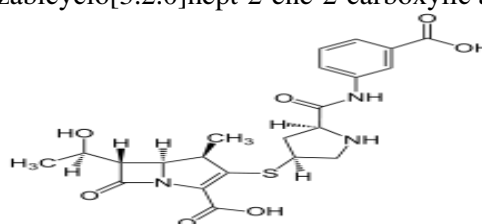


Fig 1

Molecular formula	$_{25}N_3O_7S$
Empirical formula	$C_{12}H_{17}N_3O_4S \cdot H_2O$
Molecular weight	475.51 g/mol
Color	Off-white
	3.37
Solubility	Soluble in water and slightly soluble in methanol.
Pharmacodynamic /	Antibacterial Agent
Chemotherapeutic category	

2. Literature Survey on the Analytical Methods for ERP:

Ertapenem acts by interfering with their ability to form cell walls, and therefore the bacteria break up and die. It is a broad spectrum antibiotic with activity against many aerobic and anaerobic gram-positive and gram-negative organisms. In contrast to other beta-lactams, it is highly resistant to degradation by beta-lactamases or cephalosporinases.

Literature survey reveals that the drugs were determined by using HPLC and some spectrophotometric methods³⁻⁸. According to literature survey there is no method reported for Ertapenem with CTC reagent by visible spectrophotometry. Hence an attempt was made to develop simple and sensitive spectrophotometric method for the estimation of the above drug in pure and in pharmaceutical formulations. The method uses the well known charge transfer complex formation reaction between the reagent and Ertapenem resulting in the formation of a coloured chromogen that could be measured at 520 nm for Ertapenem. In the present study, Ertapenem has estimated in pharmaceutical dosage forms and in biological samples using UV spectrophotometry.

3. EXPERIMENTAL

3.1 Instruments used

All spectral characteristics and absorbance measurements were made on Perkin Elmer, LAMBDA 25 double beam UV-Visible spectrophotometer with 10 mm matched quartz cells. A systronics digital pH meter 361 was used for pH measurements.

3.2 Preparation of standard drug solution

The stock solution (1mg/mL) of drug was prepared by dissolving 100 mg of ERP in 100 mL of distilled water. A portion of this stock solution was diluted stepwise with the distilled water to obtain the working standard solution of 100 µg/mL in the proposed methods.

In the present study, Ertapenem has estimated in pharmaceutical dosage forms and in biological samples using UV spectrophotometry⁹⁻¹⁰.

3.3 Apparatus

All spectral characteristics and absorbance measurements were made on Perkin Elmer, LAMBDA 25 double beam UV-Visible spectrophotometer with 10 mm matched quartz cells. All chemicals used were of analytical reagent grade and double distilled water was used throughout.

3.4 Preparation of reagents:

Cobalt thiocyanate Solution ($2.50 \times 10^{-1}M$)	:	Prepared by dissolving 7.25 g of cobalt nitrate (BDH) and 3.8 g of ammonium thiocyanate (BDM) in 100 mL of distilled water.
Nitrobenzene (Qualigens)	:	Used as it is
Buffer pH 2.0 Solution	:	Prepared by mixing 25 mL of potassium chloride solution (0.2M) and 13 mL of HCl (0.2M) and made upto 100 mL Distilled water and the pH was adjusted to 2.0

3.5 General procedure

Into a series of 125 mL separating funnels, different aliquots of working standard solution (0.5 to 3.0 mL) of ERP were transferred to provide final concentration range of 5 – 30 µg/mL. Then 3.0 mL of pH 2.0 buffer solution and 7.0 mL of CTC solution ($2.50 \times 10^{-1}M$) were added and the total volume of aqueous phase in each funnel was adjusted to 15.0 mL with distilled water. To each separating funnel, 10 mL of nitrobenzene was added and the contents were shaken for 2 min. The two phases were allowed to separate and the absorbance of the separated nitrobenzene layer was measured immediately at 625 nm against a similar reagent blank. The colored species was stable for 1 h. The amount of ERP present in sample solution was calculated from its calibration graph.

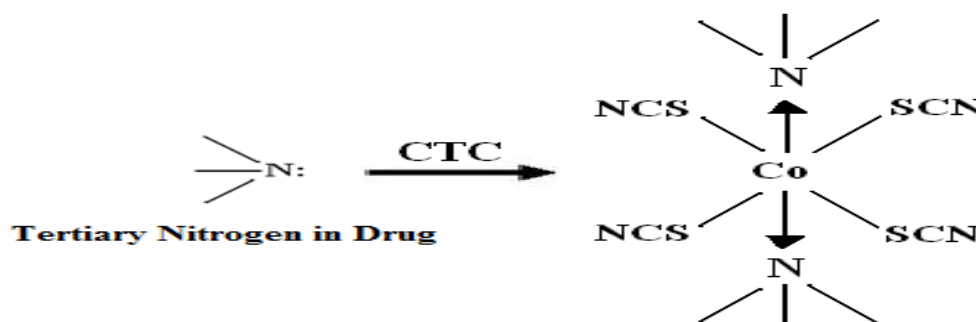
3.6 Procedure for Injections

An amount of powder equivalent to 100 mg of Ertapenem was weighed into a 100 mL volumetric flask, 50 mL of distilled water was added and shaken thoroughly for about 10 min, then the volume was made up to the mark with the distilled water, mixed well and filtered. Further dilutions were made and the assay of injections was completed according to general procedure.

4. RESULTS AND DISCUSSION

Cobalt thiocyanate CTC formed by combination of ammonium thiocyanate and cobalt nitrate is a valuable chromogenic reagent for the detection and determination of tertiary amino compounds and drugs. The colored species formed is the coordination complex of the drug (electron donor) and the central metal atom of cobalt thiocyanate, which is extractable into nitrobenzene from aqueous solution.

In the present investigation, Ertapenem possess tertiary amino group in β -lactum undergo a colored complex formation with CTC was observed. The reaction path way has given in Scheme.



4.1 Optimization of the conditions on absorption spectrum of the reaction product

The condition under which the reaction of Ertapenem with Cobalt thio cyanate fulfills the essential requirements was investigated. All conditions studied were optimized at room temperature ($32 \pm 2^\circ\text{C}$).

4.2 Selection of reaction medium

To find a suitable medium for the reaction, different acids have been used. The best results were obtained when nitrobenzene was used. Addition of 10.0 mL of nitrobenzene is necessary for proceeding the reaction. Larger volumes had no significant effect on the absorbance of the colored species.

4.3 Effect of order of addition of reactants

Few trials were performed to ascertain the influence of order of addition of reactants on the color development and the results are presented in Table 1. The order of addition of serial number (i) is recommended for Ertapenem

Tab: 1. Effect of order of addition of reactants on color development

S.No.	Drug		Order of Addition	Absorbance	Recommended order of Addition
		i	D+Buffer+CTC	0.199	
1.	Ertapenem ^a	ii	D+CTC+Buffer	0.112	i
		iii	CTC+Buffer+D	0.04	

^aFor 40 $\mu\text{g/mL}$ of Drug sample

4.4 Effect of Cobalt thio cyanate concentration

Several experiments were carried out to study the influence of CTC concentration on the color development by keeping the concentration of drug and Buffer to constant and changing reagent concentration (1.0-8.0). It was apparent that 7.0 mL of CTC gave maximum color for Ertapenem. Volume above 7.0 mL gave high optical densities in blanks (>7.0), which resulted in deviations from Beers law.

4.5 Effect of Buffer concentration

Several experiments were carried out to study the influence of Buffer in the present investigation keeping the drug and CTC concentration to constant and changing the concentration of Buffer to 1.0 – 4.0 and it is observed that to speed up the reaction stage in color development 3.0 mL of buffer was found necessary for maximum color development.

4.6 Reaction time and stability of the colored species

The color reaction was not instantaneous. Maximum color was developed within 5 minutes of mixing the reactants and was stable for 60 minutes thereafter.

Tab: 2 RESULTS OF METHOD OPTIMISATION FOR ERTAPENEM – COBALT THIO CYANATE

Parameter	Range of study	Optimised condition in procedure	Remarks
λ_{\max} (nm)	450-750	623	
Effect of volume of CTC required for complex formation (mL)	1.0-8.0	6.0	Volume above 6.0 mL gave high optical densities in blanks (>7.0), which resulted in deviations from Beers law.
Effect of volume of Buffer (mL)	1.0 - 4.0	3.0	To speed up the reaction in color development, 3.0 mL of buffer was found necessary for maximum color development.
Effect of volume of nitrobenzene (mL)	10.0	10.0	Addition of 10.0 mL of nitrobenzene is necessary for proceeding the reaction
Effect of reaction time (min)	15-30	30	The minimum time required for complete reaction was found to be 30 min.
Effect of temperature ($^{\circ}\text{C}$) for complex formation	20-40	32 ± 2 Lab. Temp	At low temperatures ($<30^{\circ}\text{C}$) the reaction time was found to be more and at high temperatures ($>34^{\circ}\text{C}$) no added advantage was found.
Standing time (min)	1-3	2	A minimum amount of time, i.e., 2 min was necessary for undergoing complex formation and beyond 3 min results in low sensitivity.
Stability period after final dilution (min)	5-40 min	40 min	The absorbance of the colored product decreases slowly with time after 40 min.

4.7 Absorption spectrum and calibration graph

Absorption spectrum of the colored complex was scanned at 350-650 nm against a reagent blank. The reaction product showed absorption maximum at 623 nm for Ertapenem. Calibration graph was obtained according to the above general procedure. The linearity replicates for six different concentration of Ertapenem was checked by a linear least - squares treatment. All the spectral characteristics and the measured or calculated factors and parameters were summarized in Table 3.

Fig 2. Calibration graph of Ertapenem
MRP (0.5-3mL)+buffer (3mL) + CTC(6mL)

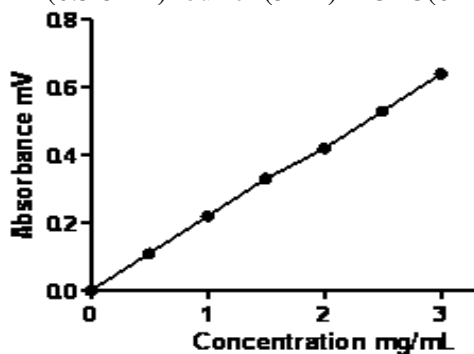
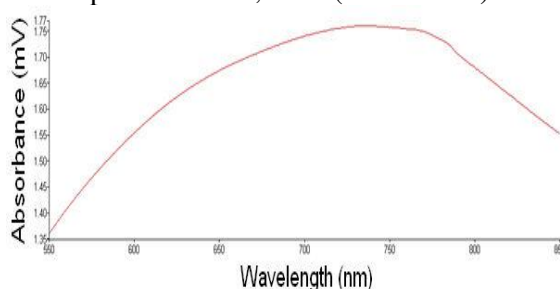


Fig 3 Absorption spectra of Ertapenem
pH 2.0 Buffer, CTC ($2.50 \times 10^{-1}\text{M}$)



4.8 Sensitivity, accuracy and precision

Sandell's sensitivity, molar absorptivity, precision and accuracy were found by performing eight replicate determinations containing $3/4^{\text{th}}$ of the amount of upper Beer's law limits. The measured standard deviation (S.D),

relative standard deviation (RSD), and confidence limits (Table 3) were considered satisfactory.

Interference

These substances are seldom present in the reagents and used in the pharmaceutical formulations. Hence, the method is devoid of error due to above substances.

Tab: 3 Optical and regression characteristics of the proposed method for Ertapenem

PARAMETER	VALUE
λ_{\max} nm	623
Beer's law limits, $\mu\text{g/mL}$	2 - 12
Molar absorptivity, L/mol.cm	101×10^{-5}
Sandell's sensitivity $\mu\text{g/cm}^2/0.001$ absorbance unit	175×10^{-3}
Regression equation ($Y = a + bc$)	
Slope(b)	0.2193 ± 0.0021
Standard deviation of slope (Sb)	0.0057
Intercept	0.0067 ± 0.0039
r^2	0.9995
Limit of Detection	0.0065
Limit of Quantification	0.0194
Standard deviation of intercept (Sa)	0.0024
Standard error of estimation (Se)	0.0024
Correlation coefficient ®	0.9998
Relative standard deviation (%)*	0.0190
% Range of error (Confidence limits)*	
Precision	
0.05 level	0.2251
0.01 level	0.3144
Accuracy	
Bulk sample	Amount found (μg)
50	49.79
75	74.86
100	99.89

Application to formulation

The proposed procedure was applied for the determination of Ertapenem in commercially available injections. Table 4 summarized the results.

Tab: 4 Results of analysis of injection formulations containing Ertapenem

Injection	Ertapenem
Company Name	Troika Pharma
Formulation	Inj
Labeled amount, mg	1000
% Recovery	99.9

5. CONCLUSION:

The proposed method was found to be simple, rapid and inexpensive, hence can be used for routine analysis of Ertapenem in bulk and in injection formulations.

6. ACKNOWLEDGEMENTS:

We wish to thank Aurobindo labs, Hyd. for providing gifted samples of Penems; Research lab, Dept., of Engineering chemistry, AUCE(A), Visakhapatnam, India, Dept., of Analysis, GIET School of Pharmacy, Rajahmundry, India.

REFERENCES

1. United States Pharmacopeia Drug Quality and Information Program. 2004. A review of drug quality in Asia with focus on anti-infectives, United States Pharmacopoeia, Drug Quality and Information Program 1-46.
2. Sean C. Sweetman, Martindale Extra Pharmacopoeia, **2009**, 36(1), 286.
3. Forsyth R J and Ip DP, , "Determination of Imipenem and Cilastatin sodium in Primaxin by first order derivative ultraviolet spectrophotometry", *J Pharm Biomed Anal*, **1994**, 12(10), 1243-8,.
4. Gravallesse D A, Musson D G, Pauliukonis L T, Bayne W F,. "Determination of Imipenem (N-formimidoylthienamycin) in human plasma and urine by high-performance liquid chromatography, comparison with microbiological methodology and stability", *J Chromatography*, **1984**, 14(1), 71-84.
5. Myers C M and J L Blumer J L, "Determination of Imipenem and Cilastatin in serum by high-pressure liquid chromatography", *Antimicrob Agents Chemother*, 1984, 26(1), 78-81.
6. Garcia- Capdevila L, López-Calull C, Arroyo C, Moral M A, Mangues M A and Bonal J, "Determination of Imipenem in plasma by high-performance liquid chromatography for pharmacokinetic studies in patients", *J Chromatogr B Biomed Sci Appl*, 1997, 25(1), 127-132.
7. Irene A, Miguel A B, Manuel C, and Juan C J, "Liquid chromatographic method for the simultaneous determination of Imipenem and sulbactam in Mouse Plasma". *J. chromatography Sci*. 2006, 44, 548-551.
8. Chaudhary A K, Ankushrao W S, Yadav S, Chandrashekhar T G and Vandana S, "Validated Reverse Phase HPLC method for the determination of DEHP content in reconstituting diluents and in reconstituted solutions of Imipenem and Cilastatin for Injection", *E-J. Chem.*, **2010**, 7(2), 501-513.

UGC Sponsored Two Day National Seminar on GREEN CHEMISTRY FOR SUSTAINABLE DEVELOPMENT (GCSD -2017)

April 06 - 07, 2017 at Government Degree College,
Jammikunta, Karimnagar, Telangana State, India

Solvent effects in the reaction between allyl bromide and thioacetamide

B. Ramesh¹, B. Kavitha², D. Vijaya Bharathi² and P. Manikyamba²

¹Department of Chemistry, Government Degree College, Jammikunta - 505 122, India

²Department of Chemistry, Kakatiya University, Warangal 506 009-India

Email - ¹drbodduramesh@gmail.com; ²drkavithachem@gmail.com

Abstract: The reaction between allyl bromide and thioacetamide has been studied in 16 different protic and aprotic solvents. The reaction is overall second order with first order dependence of rate on each reactant. Correlation of rate data with different solvent parameters indicates that the reaction rate is influenced simultaneously by polarity, polarisability, electrophilicity of the solvent. From the regression analysis, the information about the mode of solvation of the reactants and the transition state is obtained. The reaction has also been studied at different temperatures and thermodynamic parameters ΔH^\ddagger , ΔS^\ddagger , ΔG^\ddagger are computed.

Keywords: linear solvation energy relationship, allyl bromide, thioacetamide, solvent parameters, regression analysis.

1. INTRODUCTION

A solvent influences the rate of a reaction by solvating the reactants and the transition state due to dipolar effects[1]. The solvent-solute interactions are of two types, namely, specific and nonspecific[2]. The specific solvent-solute interactions primarily occur when a solvent interacts with the solute by accepting or donating an electron pair or by forming hydrogen bonds. These are short range interactions and are chemical in nature. The intensities of these interactions are measured in terms of electrophilicity(E)[3] nucleophilicity (B)[3], hydrogen bond donor acidity (α)[4], and hydrogen bond acceptor basicity (β)[4] of the solvent. In addition to these interactions, all solvents are able to interact with the reactants and transition state non-specifically. These are long range interactions and the intensities of these interactions are measured in terms of polarity (Y)[5] and polarisability (P)[5] which depend on dielectric constant ($Y = \epsilon - 1/\epsilon + 2$) and refractive index ($n^2 - 1/n^2 + 2$) of the solvent. The term solvent polarity means the overall solvation ability of the solvent due to either all or some of the above properties of the solvent. Solvation always stabilizes the solute i.e., the reactants and the transition state and hence the rate is dependent on the extent and mode of solvation. According to the linear solvation energy relationship proposed by Koppel and Palm any solvent dependent property can be represented as[6]

$$\log k = \log k_0 + xX + yY + zZ + \text{-----}$$

where k is the rate constant in any solvent, k_0 is the rate constant in an inert solvent which does not solvate the solute at all, X , Y and Z are different solvation parameters which are the measures of the solvation abilities of the solvent due to different properties. x , y and z are coefficients which describe the susceptibility of k towards different solvation properties. By studying the rate of reaction in different solvent parameters one can get an insight into nature of solvation of reactants/transition state and relative contribution of solvent property in solvating them. With this end in view the authors have studied the effect of sixteen different solvents on the rate of the reaction between allyl bromide and thioacetamide. The rate constants are correlated with different solvent parameters. From the results of this correlation analysis, a solvation model [7-20] is proposed with the help of the LSER obtained.

2. EXPERIMENTAL

Allyl bromide (Merck) and thioacetamide (ALDRICH) were used without any further purification as their boiling and melting point determined coincided with the literature values. The solvents methanol, ethanol, n -propanol, i -propanol n -butanol, sec -butanol, i -butanol, t -butanol were Sd-fine samples. Acetone, ethyl methyl ketone, cyclohexanone, dimethyl formamide, dimethyl sulphoxide, formamide, acetonitrile, benzyl alcohol are (Merck) samples. These solvents were used after distillation following literature methods[21]. The stock solutions of the nucleophile, thioacetamide were prepared by dissolving the required weighed quantities in appropriate solvents. The solution of the substrate, allylbromide in appropriate solvent was prepared ten minutes before the reaction to avoid solvolysis of allylbromide. The preliminary study of the reaction indicated that HBr was produced as one of the

products of the reaction. Therefore, the progress of the reaction was studied by noting the conductance of the reaction mixture from time to time using a digital conductivity bridge and a glass conductivity cell of cell constant 0.987 cm^{-1} . Temperature of the reaction mixture was maintained constant using a thermostat (INSREF) with an accuracy of $\pm 0.5^\circ\text{C}$. The reaction was initiated by mixing the thermally equilibrated solutions of the substrate and the nucleophile at the required temperature. The course of the reaction was followed by measuring the conductance of the reaction mixture at different time intervals, (C_t) and after the completion of the reaction (C_∞). The reaction was studied using 0.02 mol dm^{-3} allylbromide and 0.1, 0.2 and 0.3 mol dm^{-3} thioacetamide. And the rate constant (k) was determined applying following relation

$$k_I = \frac{2.303}{t} \log \frac{(C_\infty - C_t)}{(C_\infty)} \quad \dots\dots\dots(1)$$

In each case the plot of $\log (C_\infty - C_t / C_\infty)$ against time is linear. C_t and C_∞ are the conductances of the reaction mixture at time t and after completion of the reaction. This indicates that the reaction is first order with respect to concentration of allylbromide. The pseudo first order rate constants k_I determined from the slopes of these linear plots ($k_I = \text{slope} \times 2.303$) were found to be directly proportional to the concentration of thioacetamide suggesting that the reaction is first order with respect to the nucleophile also.

As the reaction is overall second order it was studied using 0.02 mol dm^{-3} allyl bromide and 0.02 mol dm^{-3} thioacetamide in 16 different protic and aprotic solvents in the temperature range 303-318K. The second order rate constants (k_{II}) were computed using the following equation

$$k_{II} = \frac{1}{at} \frac{C_t - C_o}{C_\infty - C_t} \quad \text{-----}(2)$$

where a is the initial concentration of the reactants. The plots of $(C_t - C_o / C_\infty - C_t)$ against t were linear with positive slopes. From these slope values the second order constants k_{II} were determined. A typical plot is shown in fig.1.

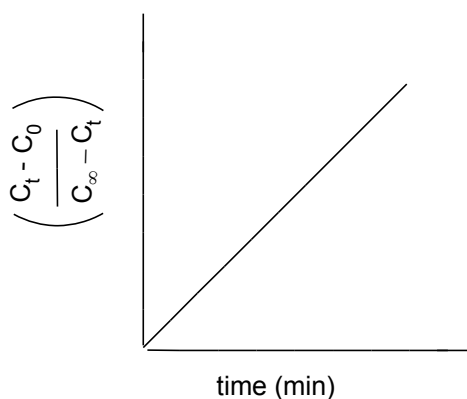


Fig.1.

The rate constants thus determined were found to be reproducible within $\pm 5\%$ error. The possibility of allyl bromide undergoing simultaneous solvolysis was checked by conducting an independent study in similar experimental conditions. This solvolysis rate constant is found to be nearly 100 times less than the substitution rate constant. Hence the spontaneous solvolysis was neglected while determining the substitution rate constants. The rate data is analysed using linear multiple regression analysis and the linear solvation energy relationship (LSER) is derived. Regression analysis is carried using statistical package which is a part of MS Excel with the help of Acer PC. F-test and Student t-test are applied to test the validity of the LSER derived[22]. The product separated from methanol has a melting point of $116 \pm 2^\circ\text{C}$. The IR spectrum (with KBr) shows absorption bands at 2720 cm^{-1} and 1400 cm^{-1} indicating the presence of S-CH₂ group (literature values[23] are $2,700\text{-}2,600 \text{ cm}^{-1}$ and 1420 cm^{-1}). Another band at 700 cm^{-1} confirms the presence of the C-S-C group (thioether link). These data tentatively suggest the formation of S-allyl thioacetamide.

3. RESULTS AND DISCUSSION:

The second order rate constants (k_{II}) determined in 16 different protic and aprotic solvents in the temperature range 303-318K are presented in Table-1. These $\log k_{II}$ values are correlated with different solvent parameters namely, polarity (Y), polarisability (P), solvent electrophilicity (E), solvent nucleophilicity (B), hydrogen bond donor

acidity (α), hydrogen bond acceptor basicity (β) and specific polarization (π^*). These parameters used are presented in Table-2. To know the influence of each parameter on rate, $\log k_{II}$ values are correlated independently with each parameter i.e., Y, P, E, B, α , β and π^* . The corresponding correlation coefficients (r) are 0.748, 0.431, 0.185, 0.360, 0.089, 0.085 and 0.527 respectively. These poor correlation coefficients suggest that any of these single parameters cannot totally explain the solvent effect on rate. Then the rate data is analysed using two parameters simultaneously. The results of these analyses are presented in Table-3.

A glance at these data indicates that, there is an improvement in the strength of correlation with the introduction of second parameters as indicated by the multiple regression coefficient. To enhance the strength of the relation further, a third parameter is added and the analysis is extended. These results are also included in Table-3.

Thus a better correlation is observed when Y, P and E are used. The corresponding correlation is

$$\log k_{II} = -11.420 + 15.258Y + 8.452P + 0.016E \quad ; \quad R = 0.949 \dots\dots(3)$$

$$(0.907) \quad (1.785) \quad (1.465) \quad (0.005)$$

The values in the parentheses are standard errors of the coefficients.

The validity of this equation is confirmed by subjecting the statistical data to the following tests

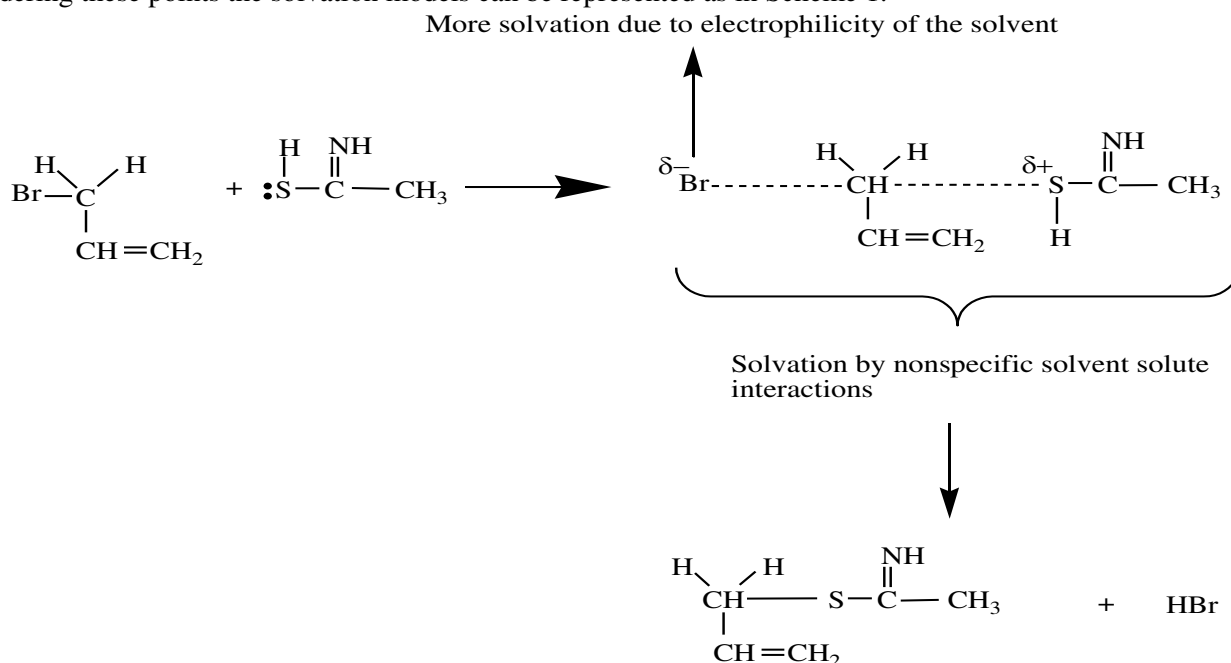
1. Correlation of $\log k_{II}$ (observed) with $\log k_{II}$ (calculated) is excellent with a slope value of 0.982 and correlation coefficient of $r = 0.998$.
2. F-test : The F_{cal} is very high (36.77) compared to the Table value ($F_{table} = 4.77$) at 1% level of significance[24]. This suggests that this LSER is not a chance correlation.
3. t-test : The significance of the individual parameters was tested by comparing t_{cal} with t_{table} . This comparison indicates that the parameters Y, P and E parameters are significant at 99.9%, 99.5% and 99% confidence levels[25].

Thus $\log k_{II}$ correlates well with Y, P, and E with a correlation coefficient, $R = 0.949$. This shows that 90% of the experimental results can be explained by the above relation. The above linear solvation energy relationship (LSER) (Eqn-3) indicates that the rate of this reaction is influenced by polarity parameter, Y, polarisability parameter, P and electrophilicity parameter, E. The positive sign of all the coefficients in the above LSER suggests that the transition state is more solvated than the reactants.

The contributions of these parameters towards total solvation are estimated by normalisation[26] of the coefficients. These values are found to be

$$Y = 50\%, P = 33\%, E = 17\%$$

Considering these points the solvation models can be represented as in Scheme 1.



Scheme 1

Thus it can be concluded that in the present system, the transition state is strongly solvated by non-specific solvent-solute interactions extensively, than the reactants. This is indicated by large positive coefficients of Y and P. The positive E coefficient indicates that the transition state, especially the $Br^{\delta-}$, is more solvated by donating electrons.

From the temperature effect on rate, different thermodynamic parameters ΔH^\ddagger , ΔS^\ddagger and ΔG^\ddagger are evaluated and presented in Table-1. The entropy of activation ΔS^\ddagger values are all negative ranging from -2 to -67 JK⁻¹ mol⁻¹ suggesting that the overall solvation of the transition state is more than the reactants. The free energy of activation ΔG^\ddagger is nearly constant in all the solvents (87.65 ± 3.55 kJmol⁻¹) suggesting the operation of a unified mechanism in all the solvents used. The differential free energy of activation $\delta\Delta G^\ddagger$ calculated taking methanol as reference solvent using the equation $\delta\Delta G^\ddagger = \Delta G^\ddagger_{\text{solvent}} - \Delta G^\ddagger_{\text{methanol}}$ are also presented in Table 1. There are all positive except in n-butanol, benzyl alcohol, dimethyl formamide and formamide. The sign of this differential free energy indicates the relative stability of the transition state due to change of solvent. The negative sign of this term in the above four solvents suggests that the transition state is more stabilized in these solvents than in methanol. While in all other solvents it is less stabilized.

4. CONCLUSION:

In the present kinetic study of allylation of thioacetamide the mode of solvation of the reactants and the transition state is investigated by studying the reaction in different protic and aprotic solvents. This indicates that the role of the solvent in these reactions is not simply to provide a medium, but it is interacting with specific suitable centres of the reactants and the transition state.

REFERENCES:

1. E. S. Amis, J. F. Hinton, *Solvent Effects on Chemical Phenomena*: Academic Press, New York, Vol.1., **1973**.
2. C. Reichardt, *Angew Chem.*, **1979**, 18, 98.
3. I. A. Koppel, A. I. Paju, *Org. React. (Tarter)*, **1974**, 11, 137.
4. R. W. Taft, J. L. M. Abboud, M. J. Kamlet, M. H. Abraham, *J. Org. Chem.*, **1983**, 48, 2877.
5. M. H. Aslam, G. Collier, J. Shorter, *J. Chem. Soc: Perkin Trans. 2*, **1981**, 1572.
6. I. A. Koppel, V. A. Palm, *Advances in linear free energy relationship*, edited by Chapman, N. V., Shorter, J. : Plenum Press, New York, **1972** 222.
7. K. Ohkata, T. Nagai, A. Tomaru, T. Hanafusa, *J. Chem. Soc. Perkin Trans.2*, **1986**, 43.
8. R. D. Martinez, P. M. E. Mancini, L. R. Voltero, N. S. Nudleman, *J. Chem. Soc. Perkin Trans. 2*, **1986**, 1427.
9. P. Manikyamba, *Indian J. Chem.*, **1992**, 31A, 959.
10. T.M.Krygowski, J.G. Radomski, A. Rzeszowiak, P.K. Wrona, *Tetrahedron*, **1981**, 37, 119.
11. L. Fernandobanez, J.G. Santos, *J.Chem.Soc, Perkin Trans. 2*, **1984**, 1323.
12. Y. Zhuzhong, E. Samcheng, K. Hante, *J.Chem.Soc, Perkin Trans. 2*, **1985**, 929.
13. T. Compino, J.G. Santos, F. Ibaniz, *J.Chem.Soc, Perkin Trans. 2*, **1986**, 1021.
14. P. Manikyamba, E. V. Sundaram, *Int J. Chem. Kinet.*, **1990**, 22, 1153.
15. M.R. Gholami, A.H. Yangjeh, *J.Chem.Research(s)*, **1999**, 226.
16. A.M. Yangjeh, M.R. Gholami, R. Mastaghim, *J. Physical.Org.Chem.*, **2001**, 14, 884.
17. P. Kalyani, P. Manikyamba, *Indian.J.Chem.*, **2003**, 42A, 75.
18. S. Ranga Reddy, P. Manikyamba, *Indian.J.Chem.*, **2004**, 43A, 1092.
19. S. Ranga Reddy, P. Manikyamba, *Indian.J.Chem.*, **2005**, 44A, 1831.
20. D. Gary Christian, *Analytical Chemisry* (John Wiley and Sons), New York., **1994**, 36, .
21. Wiley, Jhon and Sons, *Vogel's text book of Practical Organic Chemistry*. 4th edn, **1978**.
22. Announcement by the International Group for correlation Analysis in Organic Chemistry, *Quant Structure Activity Relationships*, **1985**, 4, 29.
23. K.Nakanishi, P.M. Solomon, *Infrared Absorption Spectroscopy*, Holden-day Inc., **1977**, 50.
24. J. Shorter, *Correlation, Analysis of Organic Reactivity* (John Wiley and Sons.), Research studies Press, **1982**, 107.
25. M.S. Charles, D. Hodgman, *Standard Mathematical Tables*, 12th edn., **1959**, 251.
26. M. Ezekiel, K.A. Fox, *Methods of correlation and Regression Analysis*, 3rd edn, Wiley, New York, **1959**, 204.

Table. 1 Second order rate constants and thermodynamic parameters at 303K
= 2.00 x 10⁻² moldm⁻³

[allylbromide] = [thioacetamide]

Solvent	$k_H \times 10^3 \text{ dm}^3 \text{ mol}^{-1} \text{ s}^{-1}$ at TK				ΔH^\ddagger (kJ mol ⁻¹)	ΔS^\ddagger (JK ⁻¹ mol ⁻¹)	ΔG^\ddagger (kJ mol ⁻¹)	$\delta\Delta G^\ddagger$ (kJ mol ⁻¹)
	303	308	313	318				
Methanol	3.52	6.35	10.83	18.37	83.64	-15	88.50	0.00
Ethanol	2.97	5.92	9.45	15.89	83.97	-16	88.97	0.47
<i>n</i> -propanol	2.12	3.96	6.65	10.42	80.45	-30	89.78	1.28
<i>i</i> -propanol	2.62	4.44	7.12	10.65	70.90	-60	89.25	0.75
<i>n</i> -butanol	2.34	4.06	6.43	9.86	72.37	-56	86.55	-1.95
2-butanol	1.91	3.69	5.88	8.47	75.08	-49	90.03	1.53
<i>i</i> -butanol	2.92	4.25	7.15	11.38	69.35	-64	88.97	0.47
<i>t</i> -butanol	1.25	2.29	3.68	5.05	70.62	-67	91.19	2.69
Benzyl alcohol	3.67	7.43	13.79	18.68	84.15	-14	88.42	-0.08
N,N-dimethyl formamide	4.04	7.61	12.65	20.98	83.22	-16	88.15	-0.35
Dimethyl sulphoxide	8.05	13.86	25.65	42.22	85.00	-5	86.40	2.10
Acetone	2.65	5.53	8.82	-	88.61	-2	89.24	0.74
Ethylmethyl ketone	2.08	4.17	6.88	9.23	75.86	-46	89.90	1.40
Cyclohexanone	1.69	3.05	4.39	7.98	76.30	-47	90.46	1.96
Acetonitrile	1.97	3.39	6.26	10.63	86.20	-12	90.03	1.53
Formamide	20.02	30.26	50.12	72.08	65.52	-61	84.10	-4.40

Table – 2 : Solvent parameters of different solvents used in the present study

Solvent	ϵ	Y	P	B	E	α	β	π^*
Methanol	32.6	0.477	0.169	119	14.94	0.93	0.62	0.60
Ethanol	24.3	0.470	0.181	124	11.57	0.83	0.77	0.54
<i>n</i> -propanol	20.1	0.464	0.190	120	10.60	0.77	0.82	0.51
<i>i</i> -propanol	18.3	0.462	0.187	128	8.73	0.76	0.95	0.48
<i>n</i> -butanol	17.1	0.459	0.195	160	10.30	0.71	0.88	0.43
<i>Sec</i> -butanol	17.1	0.459	0.194	158	9.05	0.66	0.96	0.92
<i>i</i> -butanol	15.8	0.454	0.193	161	13.24	0.66	0.96	0.97
<i>t</i> -butanol	12.2	0.442	0.191	132	5.15	0.68	1.01	0.41
Benzyl alcohol	13.1	0.444	0.239	117	10.91	0.43	0.50	0.98
Acetone	20.7	0.466	0.180	123	2.13	0.08	0.48	0.71
Ethyl methyl ketone	18.5	0.460	0.188	109	2.00	0.06	0.48	0.67
Cyclohexanone	18.3	0.455	0.213	118	0.51	0.06	0.53	0.76
Acetonitrile	37.5	0.480	0.174	103	5.21	0.19	0.31	0.75
Dimethylformamide	48.9	0.484	0.221	193	3.20	0.00	0.76	1.00
Dimethylsulphoxide	36.7	0.480	0.204	166	2.60	0.00	0.69	0.88
Formamide	111.5	0.498	0.211	140	14.59	0.71	0.69	0.97

Table-3: Statistical data of results of correlation analysis

S.No.	Y	P	B	E	α	β	π^*	$\log k_0$	R
1.					0.060	0.166		-2.437	0.097
2.		**4.986	0.003					-3.928	0.480
3.			0.004	0.018				-3.272	0.492
4.						0.082	0.777	-3.149	0.557
5.					0.240		0.922	-3.308	0.609
6.	14.392							-9.312	0.758
7.	13.721		0.002					-9.273	0.777
8.	15.869	8.578						-11.602	0.915
9.		5.648	0.002	0.021				-4.193	0.592
10.					0.303	-0.172	0.923	-3.216	0.618
11.	13.168		0.002	0.013				-9.141	0.823
12.	15.677	7.872	0.004					-11.420	0.909
13.	15.258	8.452		0.016				-11.420	0.949

** coefficients of solvent parameters in the LSER

R : correlation coefficient of linear multiparametric equation.

UGC Sponsored Two Day National Seminar on GREEN CHEMISTRY FOR SUSTAINABLE DEVELOPMENT (GCSD -2017)

April 06 - 07, 2017 at Government Degree College,
Jammikunta, Karimnagar, Telangana State, India

Synthesis of Multifunctional nanocomposites of superparamagnetic (Fe_3O_4) /SiO₂ nanoparticles

K.Anjaneyulu¹, Gundu.Mallikarjun²

¹Government Degree College Mancherla and ²Government Degree College Siddipet
Email - gundumallikarjun8@gmail.com

Abstract: Silica coated magnetite ($\text{Fe}_3\text{O}_4@\text{SiO}_2$) core-shell nanoparticles (NPs) with controlled silica shell thicknesses were prepared by ultrasonic irradiation using 10 nm oleylamine stabilised Fe_3O_4 NPs as seeds. The core-shell nanoparticles were characterized by X-ray diffraction (XRD), transmission electron microscopy (TEM), high-resolution TEM (HRTEM), selected area electron diffraction (SAED), Thermogravimetric analysis (TGA) and X-ray photoelectron spectroscopy (XPS). The results imply that NPs consist of a crystalline magnetite core and an amorphous silica shell. The silica shell thickness can be controlled from 2 nm to 6 nm by varying the TEOS concentration and the reaction is accelerated many-fold in the presence of ultrasonic field. These core-shell $\text{Fe}_3\text{O}_4@\text{SiO}_2$ NPs show superparamagnetic properties at room temperature. Fluorescent dye was

1. INTRODUCTION:

Super paramagnetic iron oxide nanoparticles with appropriate surface chemistry can be used for numerous *in Vivo* applications, such as MRI contrast enhancement^{1,2,3}. All of these biomedical applications require that the nanoparticles have a size smaller than 100 nm, chemical stability, biocompatibility, strong magnetization, and low coercivity. Although strategies for synthesizing Fe_3O_4 NPs have been fully developed, a few reports were capable of producing Fe_3O_4 NPs that meet all the requirements above right after synthesis. In particular, a high local concentration of metal cations resulting from the dissolution of surface Fe cations is toxic to organisms and the aggregation of Fe_3O_4 NPs resulting from incompatible surface chemistry in liquid media weakens the specific targeting. Therefore, it is necessary to add a coating to Fe_3O_4 NPs that is expected to offer an inert surface layer with compatible surface chemistry to help magnetic NPs survive *in vivo* and work well in specific targeting.

In recent years magnetic nanoparticles have been coated with different materials like noble metals, metal oxides and inorganic silica^{4,5,6}. Silica is found to be very promising among these coating materials since the silica shell may prevent Fe_3O_4 cores from oxidation, chemical contact with Corrosive liquids and most importantly chemistry of a silica shell is compatible with various chemicals and molecules for bio-conjugations. Taking these advantages of silica, it has been proved experimentally that the silica surface works well with various coupling agents to covalently attach to specific ligands and to deliver ligands to target organs through antibody-antigen recognition¹¹ (Ulman, Chem. Rev., 1996, 96, 1533–1554).

A number of reports have been devoted to silica coating of Fe_3O_4 nanoparticles by aqueous classical methods such as Stöbers synthesis⁷, use of silane coupling agents⁸ and the sodium silicate water-glass methodology⁹. The $\text{Fe}_3\text{O}_4@\text{SiO}_2$ NPs prepared by the Stöber process usually contain multiple Fe_3O_4 cores even under optimal conditions. Further detailed studies of Fe_3O_4 NPs coating using TEOS¹⁰ revealed the high sensitivity of this process to experimental conditions such as ethanol/water ratio, concentration of ammonia and TEOS, and temperature, etc. Moreover, the coating of Fe_3O_4 NPs with silica using TEOS was found to be a very slow process: from 12 to 48 h of mechanical stirring at room temperature is necessary to obtain uniform silica shell on the surface of magnetite NPs. Heating of the reacting mixture causes formation of big magnetite silica aggregates with irregular morphology. To improve the homogeneity of silica-coated iron oxide NPs and to increase the limiting concentration of NPs in reaction medium several authors used a modified Stöber process in reverse micro emulsion conditions¹¹. However, this method also requires at least 20–24 h of aging to obtain the final product and much effort to separate core shell NPs from the large amount of surfactants associated with the micro emulsion system.

This paper reports that the sonochemical approach provides a resolution of several important problems in the synthesis of $\text{Fe}_3\text{O}_4@\text{SiO}_2$ NPs by the Stöber process related to the necessity of silicate pretreatment, the slow kinetics, and the risk of aggregates formation. In this paper, we report the use of ultrasonic irradiation for the rapid synthesis of water-soluble, monodisperse core-shell $\text{Fe}_3\text{O}_4@\text{SiO}_2$ NPs with tunable properties using the modified Stöber process. Oleylamine stabilized 10 nm Fe_3O_4 NPs were used as core materials. By varying the concentration of TEOS in the presence of Fe_3O_4 NPs, the thickness of the silica shell was controlled from 2 to 6 nm. This control leads to a further manipulation of the composition, morphology and magnetic properties of the core-shell. The core-shell

nanoparticles were tagged with the commonly used fluorescent dye FITC (Fluorescein Iso Thio Cyanate) and observed under the fluorescence microscope for dispersibility and cellular internalization in CHO cells

2. MATERIALS

Iron (III) acetyl acetonate (97%), Oleylamine (70%), Tetraethyl ortho silicate (TEOS, 98%), amino propyloxy silane (APS), fluorescein-5-isothiocyanate (FITC) were purchased from sigma Aldrich. Ethanol (99.7 to 100% w/v). all reagents were used without further purification.

3. CHARACTERIZATION.

The structure, phase and crystallinity of the iron oxide have been evaluated by X-ray diffraction using a Seimens (Cheshire, UK) D5000 diffractometer over a 2θ range from 2° to 80° using $\text{CuK}\alpha$ ($\lambda = 1.5406 \text{ \AA}$) radiation at 40 kV and 30 mA by scanning at step time 13.6 sec. The formation of silica over iron oxide was confirmed by FT-IR spectroscopy. FT-IR spectra of the samples were recorded on a Bruker alpha spectrometer with DTGS KBr detector at a resolution of 4 cm^{-1} in the range of 4000 cm^{-1} to 400 cm^{-1} . The sample was dried overnight at 80°C in a vacuum oven and then ground and mixed with KBr to form the pellets used in the measurements. The HRTEM images were collected on a JEOL TEM 2010 microscope operating at 200 kV. The synthesized nanoparticles were dispersed in ethanol by ultrasonication prior to loading onto a carbon-coated copper grid. Thermogravimetry scans were obtained on TGA Q500 (TA Instruments) in the temperature range of 30 – 800°C at a heating rate of 10°C/min under nitrogen atmosphere. X-ray photoelectron spectroscopy studies were carried out on a Kratos system with $\text{MgK}\alpha$ X-ray source. Magnetic studies of the samples were carried out with a MICROSENSE vibrating sample magnetometer at different temperatures in the applied magnetic field sweeping from -60 to 60 kOe . A FAST CLEAN ultrasonicator operating at 100W power and 35 kHz frequency was employed to carry out sonochemical reaction. The core-shell nanoparticles were tagged with the commonly used fluorescent dye FITC (Fluorescein Iso Thio Cyanate) and observed under the fluorescence microscope for dispersibility.

Cellular Uptake Studies: Chinese Hamster Ovary Cells (CHO) maintained in DMEM with 10% FCS at 37°C and 5% CO_2 in a humidified incubator were plated on cover slips taken in a 6-well dish. Cells were then incubated with 50 ug/ml and 100 ug/ml FITC- $\text{Fe}_3\text{O}_4@ \text{SiO}_2$ nanoparticles in DMEM and in plain DMEM at 37°C for 3 hrs and 6 hrs. After the specified time intervals cells were washed with fresh medium and PBS and then fixed in 3.7% formaldehyde in PBS and mounted on glass slides using Vectashield containing DAPI (nuclear stain). These slides were scanned on Leica TCS SP5 Confocal Microscope with a $63\times 1.4 \text{ NA}$ oil objective. This system uses 405 and 488 lasers for excitation of DAPI and FITC respectively and emissions were collected with 405-475BP and 500-550BP filters. Optical sectioning was done at $0.35 \text{ }\mu\text{m}$ intervals and central 5 sections were projected using LAS AF software

4. EXPERIMENTAL

4.1 Synthesis of $10 \text{ nm Fe}_3\text{O}_4$ nanoparticles.

Iron oxide nanoparticles were prepared using an adaptation of the procedure reported by Sun et al. In a typical synthetic procedure 3 mmol of $\text{Fe}(\text{acac})_3$ was dissolved in 15 ml of oleyl amine. The solution was dehydrated at 110°C for 1 hour under nitrogen atmosphere, then quickly heated to 300°C . The solution was aged at this temperature for one hour with magnetic stirring. The solution was allowed to cool down to room temperature after the completion of reaction. The black product was collected by magnetic separation and washed several times under sonication with ethanol and dispersed in various organic solvents. The amine group of each oleylamine molecule coordinately bonds to the surface iron oxide nanoparticles, resulting in a hydrophobic capping layer to enable excellent dispersibility in organic media

4.2 Synthesis of $\text{Fe}_3\text{O}_4@ \text{SiO}_2$ nanoparticles.

5 mg of iron oxide nanoparticles and 5 ml ethanol were taken in a sample vial. This mixture was intensely sonicated for 20 minutes, after then $5 \text{ }\mu\text{L}$ of tetra ethyl ortho silicate was added and sonicated for further 20 mins. The above procedure was repeated by taking 10 and 15 μL of TEOS. The nanoparticles were collected by a magnet and washed three times with ethanol.

4.3 Synthesis of FITC tagged $\text{Fe}_3\text{O}_4@ \text{SiO}_2$ nanoparticles.

0.5 ml APS and 0.4 mg FITC dye were added to 5 ml ethanol. This solution was degassed for 30 minutes and stirred at room temperature for 24 hours under nitrogen atmosphere. 50 mg of $\text{Fe}_3\text{O}_4@ \text{SiO}_2$ nanoparticles dispersed in 10 ml ethanol were mixed with APS- FITC solution and this mixture was stirred for 24 hours. The products were separated by a magnet and washed three times with ethanol.

5. RESULTS AND DISCUSSION:

Iron oxide nanoparticles were prepared by reductive decomposition of $\text{Fe}(\text{acac})_3$. In this synthesis, Oleyl amine acts both as a reducing agent and stabilizer. The crystal structure of nanoparticles was studied by XRD analysis.

Fig. 1 represents the XRD pattern of synthesized iron oxide nanoparticles (A) and silica coated iron oxide nanoparticles (B). The peaks appearing at 2θ values 2.96, 2.53, 2.43, 1.71, 1.61 and 1.42 in curve A refer to (111), (220), (311), (400), (422), (511) and (440) planes of cubic inverse spinel Fe_3O_4 , respectively. The results are in good agreement with the XRD patterns of Fe_3O_4 nanoparticles reported previously. The crystallinity of nanoparticles was revealed by well resolved diffractions peaks. The average crystallite size estimated by applying scherrer equation to the major diffraction peak is 9.74 nm which is consistent with particle size determined from TEM data (10 nm). This indicates that the particles are single-crystalline and the crystallinity of Fe_3O_4 cores persists after SiO_2 coating. The lattice parameter calculated from our data $a = 8.381 \text{ \AA}$ is quite close to standard lattice parameter of magnetite (8.396 \AA). XRD pattern of silica coated iron oxide nanoparticles is similar to that of uncoated nanoparticles; this indicates the coated silica is in amorphous form and particles retain their crystallinity even after coating. The presence of amorphous silica shell can be observed as a broad peak in 20 to 30 degrees range in the curve B.

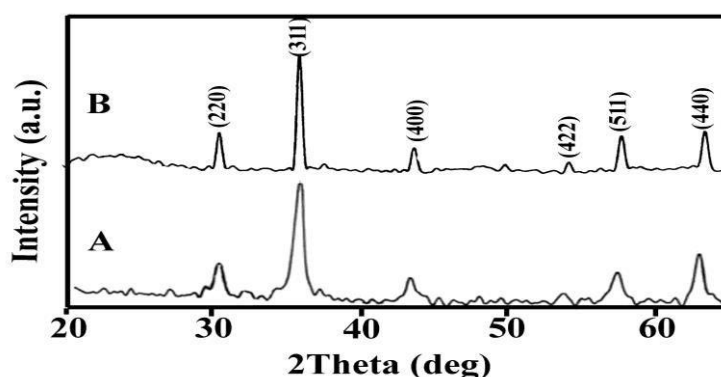


Fig.1 XRD pattern of Iron oxide nanoparticles.

Fig2. Illustrates the FT-IR spectrum of iron oxide (B) and silica coated iron oxide nanoparticles (A). The band at 580 cm^{-1} refers to Fe-O deformation in octahedral and tetrahedral sites and the band at 420 cm^{-1} refers to Fe-O deformation in octahedral sites for spinel structured iron oxide. Other bands in $1330\text{--}1650 \text{ cm}^{-1}$ are due to $-\text{NH}_2$ bending mode and the bands around 2920 cm^{-1} and 2850 cm^{-1} are due to methyl stretching modes of surface bound oleylamine^{12, 13}. Silica shell formation on nanoparticles was confirmed by the appearance of band around 1080 cm^{-1} and 805 cm^{-1} due to Si-O and Si-O-Si stretching modes respectively¹⁴. The stretching band at 1615 cm^{-1} shows the presence of residual physisorbed water molecules.

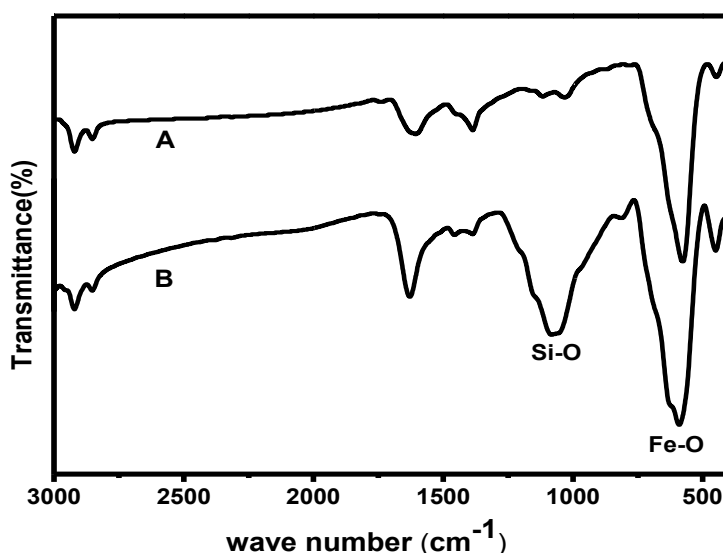


Fig2. FT-IR spectrum of and iron oxide nanoparticles (A) silica coated iron oxide (B).

The particle size of iron oxide nanoparticles and silica shell formation on nanoparticles was investigated by TEM analysis. Fig 3 corresponds to TEM images of iron oxide nanoparticles. Fig A is TEM image of iron oxide nanoparticles while Figs B, C and D are TEM images of silica coated iron oxide nanoparticles with different silica shell thickness. The average particle size of the nanoparticles was found to be around 10 nm while that of silica coated nanoparticles ranged from 12- 16 nm. The thickness of silica shell was 2nm, 4nm and 6nm when $5 \mu\text{l}$, $10 \mu\text{l}$ and $15 \mu\text{l}$ of TEOS were used respectively to coat the magnetic particles with silica.

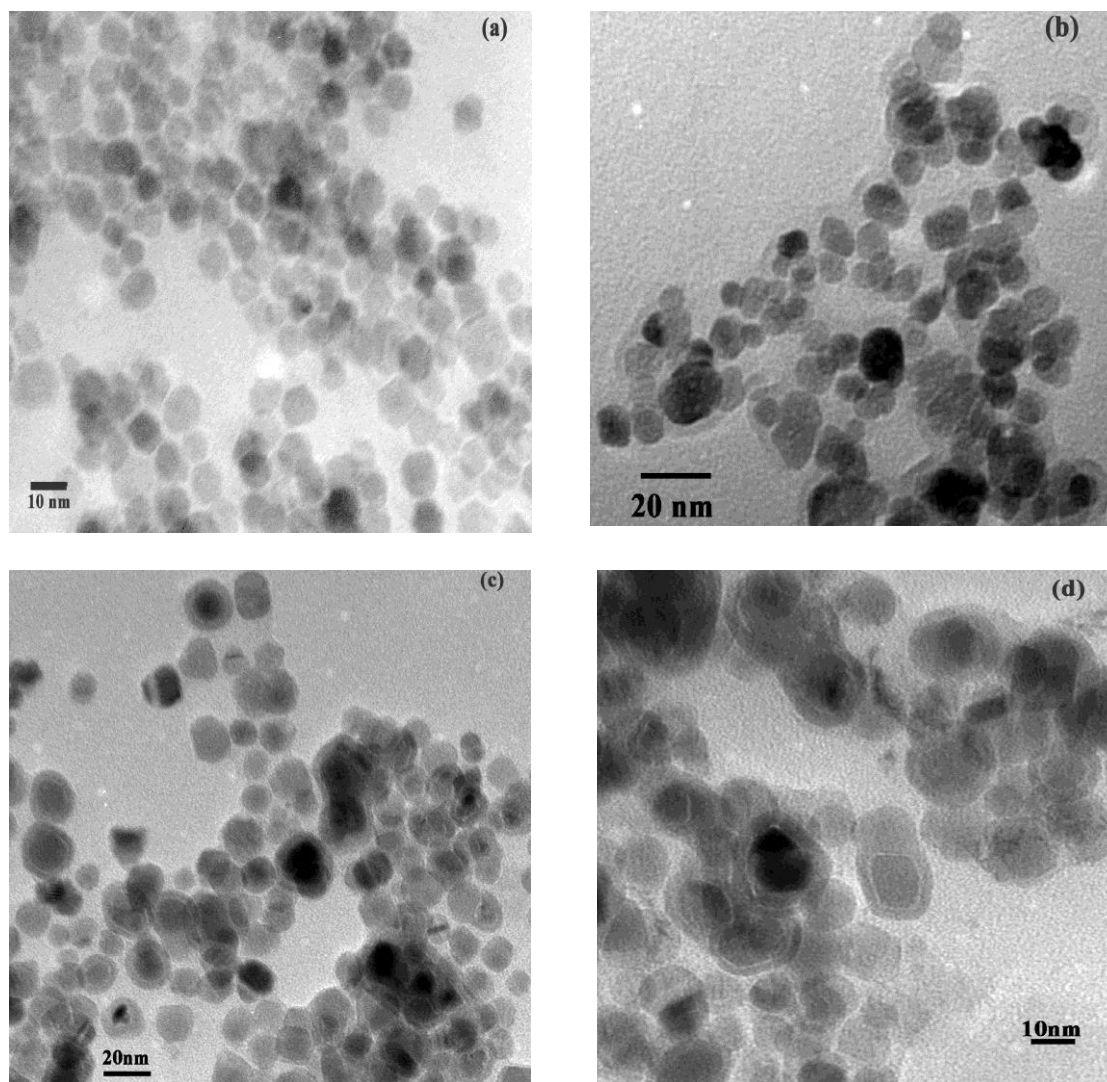
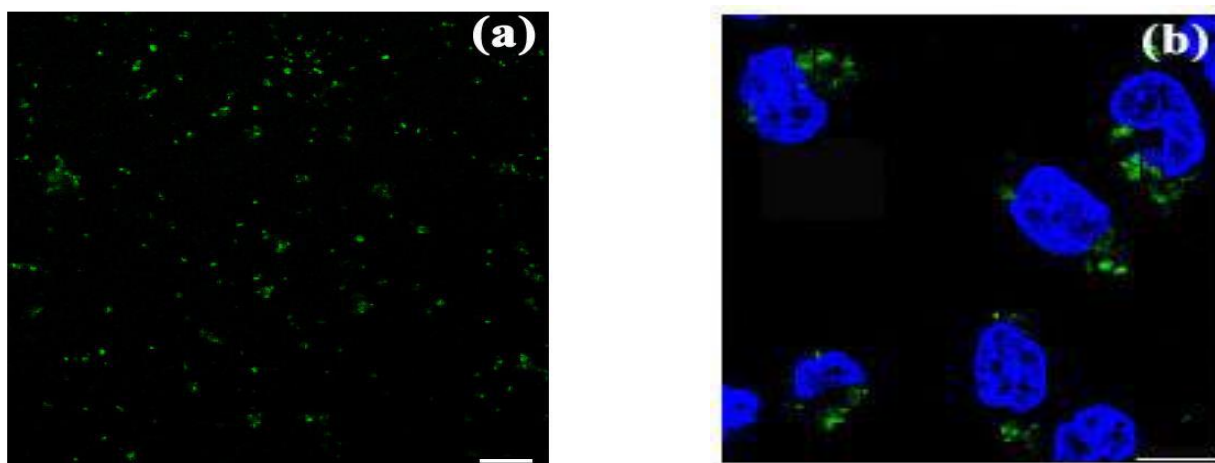


Fig 3 TEM images of iron oxide nanoparticles FO (a) and silica coated iron oxide nanoparticles FS5 (b), FS10 (c), FS15 (d).



Confocal microscopic images showing the dispersibility of FITC tagged $\text{Fe}_3\text{O}_4@\text{SiO}_2$ nanoparticles in water (a) and their uptake of (50 $\mu\text{g}/\text{ml}$) by CHO cells (b). Fluorescence image of nano particles alone showed their dispersibility in water.

As seen from the confocal images (Fig. 7) of the as synthesized FITC tagged $\text{Fe}_3\text{O}_4@\text{SiO}_2$ nanoparticles, they were well dispersed in water and efficiently internalized in CHO cells within 3 hrs of incubation at a concentration of 50 $\mu\text{g}/\text{ml}$ and were localized mostly around the nucleus.

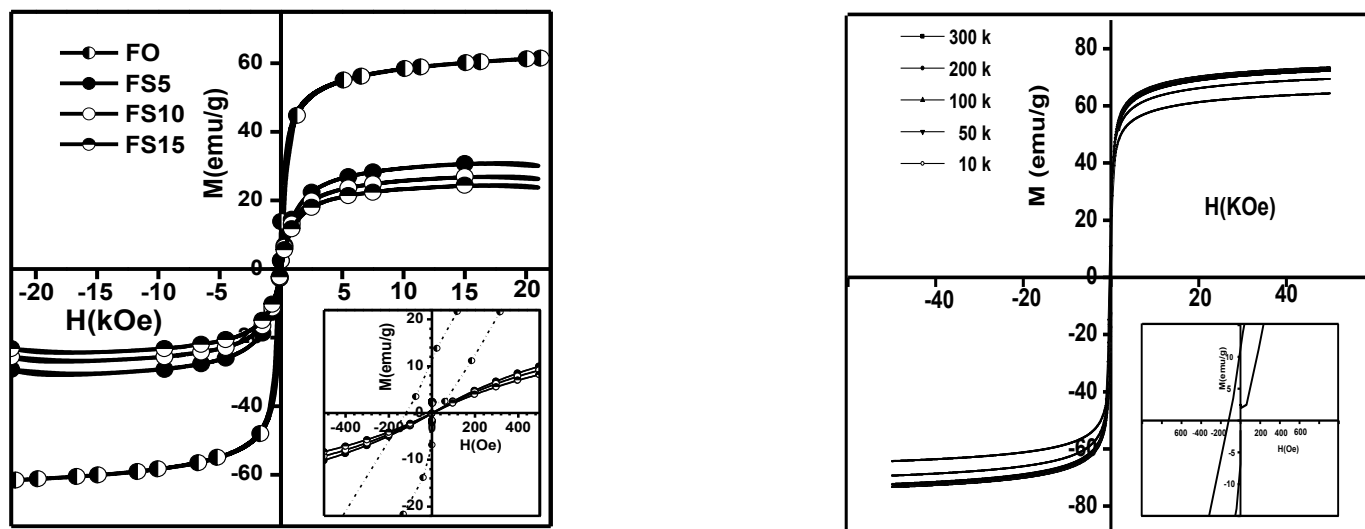


Fig .4 Magnetization (M) vs.magnetic field (H)curves of silica coated iron oxide nanoparticles.

The magnetic properties of nanoparticles were studied by VSM at different temperatures. The Saturation magnetization value (M_s) of nanoparticles is 60.2emu/g. The smaller magnetization values of nanoparticles compared to their bulk counterparts are due to the existence of surfactant layer with reduced magnetization, and some diamagnetic contribution from the surfactant shell. The M_s Values of nanoparticles increases with decrease in temperature. The magnetic behavior of silica coated nanoparticles was investigated as comparison to uncoated iron oxide nanoparticles. The saturation magnetization of silica coated nanoparticles FS5, FS10 and FS15 was 31.2, 27.2 and 24.2emu/g respectively. The decrease in M_s Values of nanoparticles is due to the diamagnetic contribution from amorphous silica and there is also a progressive decrease in M_s Values of nanoparticles with increase in thickness of silica¹⁵

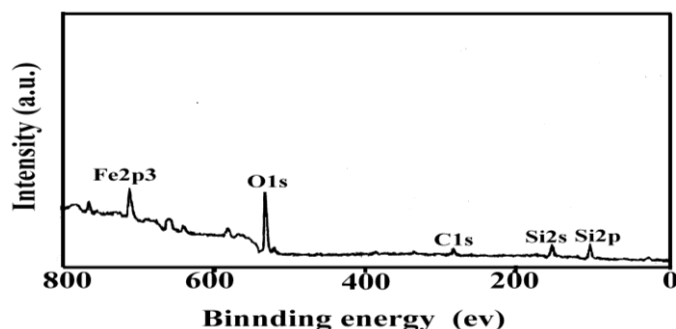


Fig.5XPS survey of silica coated iron oxide nanoparticles.

The formation of silica over magnetic nanoparticles is further confirmed by XPS analysis. Fig.5 Represents XPS survey of silica coated iron oxide nanoparticles. The peaks at binding energies 711 eV and 103 eV corresponds to Fe 2p_{3/2} and Si 2p core electrons¹⁶

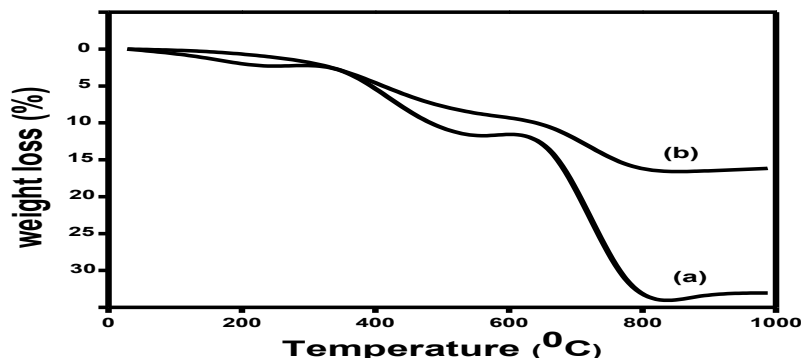


Fig.6TGA curve of oleylamine capped iron oxide nanoparticles.

Fig.6 shows the TGA data of oleylamine capped iron oxide nanoparticles. The TGA pattern of iron oxide

nanoparticles prepared by oleylamine shows a weight loss of 11.75% with two weight loss steps, one at $\sim 230^{\circ}\text{C}$, another at 560°C . This pattern is close to that observed for the oleylamine capped nanoparticles¹⁷ but with different weight loss. The weight loss of 11.75% is attributed to the degradation of oleylamine. Thermo gravimetric analysis (TGA) was used to further determine the relative composition of the nanocrystal core and the organic monolayer shell. With an average particle size of 10 nm and iron oxide density 5.196 g/cm^3 , an average of 720 oleylamine molecules are expected to attach to the surface of one iron oxide nanoparticles. The ligand coverage observed for oleylamine stabilized iron oxide nanoparticles is in good agreement with values reported in literature¹⁸

It has been shown that it is relatively easy to replace one molecule with the other by using an excess of new molecule providing enough heat or sonication in a ligand exchange reaction¹⁹. The same principle applies to iron oxide surfaces and molecules containing amine groups, the interactions between which have been investigated by means of IR spectroscopy. In our experiment the oleylamine molecules are detached from iron oxide surface while sonicating and participated in the hydrolysis of TEOS.

6. CONCLUSION:

In summary, ultrasonic treatment was employed for the simple synthesis of $\text{Fe}_3\text{O}_4@\text{SiO}_2$ core/shell nanoparticles. This work provides an alternative way to prepare $\text{Fe}_3\text{O}_4@\text{SiO}_2$ core/shell nanoparticles with different silica shell thickness by tuning the concentration of TEOS. The magnetic core-shell nanoparticles synthesized by this method are dispersible, biocompatible and can be further functionalized for specific biomedical applications.

REFERENCES

1. Bulte, J. W. *Methods Mol. Med.*, **2006**, 124, 419.
2. Modo, M.; Bulte, J. W., *Mol. Imaging*, **2005**, 3, 143.
3. Boutry, S.; Laurent, S.; Vander Elst, L.; Muller, R. N., *Contrast Med. Mol. Imaging*, 2006.
4. Z. C. Xu, Y. L. Hou and S. H. Sun, *J. Am. Chem. Soc.*, **2007**, 129, 8698–8699.
5. Cao and H. B. Jin, *J. Phys. Chem.*, **2009**, 113, 10061–10064.
6. J. P. Ge, Q. Zhang, T. R. Zhang and Y. D. Yin, *Angew. Chem., Int. Ed.*, **2008**, 47, 8924–8928.
7. Stober, W.; Fink, A.; Bohn, E., *J. Colloid Interface Sci.*, **1968**, 1, 62–69.
8. E. P. Plueddemann, in: *Silane Coupling Agents*, Plenum Press, New York, USA, **1991**.
9. Philipse, A. P.; van Bruggen, M. P. B.; Pathmamanoharan, C. *Langmuir*, **1994**, 10, 92–99.
10. Lu, Yu.; Yin, Y.; Mayers, B. T.; Xia, Y. *Nano Letters*, **2002**, 2, 183–186.
11. Santra, S.; Tapecc, R.; N.; Dobson, J.; Hebard, A.; Tan, W., *Langmuir*, **2001**, 17, 2900–2906.
12. Luo, J.; Han, L.; Kariuki, N. N.; Wang, L.; Mott, D.; **Chem. Mater.**, **2005**, 17, 5282.
13. Xie, J.; Xu, C.; Kohler, N.; Hou, Y.; Sun, S. *Adv. Mater.*, **2007**, 19, 3163.
14. Sonia L. C. Pinho, Giovannia A. Pereira, Pierre Voisin, Jinane Kassem, Veronique Bouchaud,
15. Laetitia Etienne, Joop A. Peters, Luis Carlos, Stéphane Mornet, Carlos F. G. C. Geraldes, João Rocha, and Marie-Hélène Delville, *ACS Nano*, **2010**, 4, 5339.
16. Clara Pereira, André M. Pereira, Pedro Quaresma, Pedro B. Tavares, Eulália Pereira, João P. Araújo and Cristina Freire, *Dalton Trans.*, **2010**, 39, 2842–2854.
17. Morel, A. L.; Nikitenko, S. I.; Gionnet, K.; Wattiaux, A.; Lai-Kee-Him, J.; Labrugere, C.; Chevalier, B.; Deleris, G.; Petibois, C.; Brisson, A.; Simonoff, M. *ACS Nano*, **2008**, 2, 847–856.
18. Isojima, T.; Suh, S. K.; Vander Sande, J. B.; Hatton, T. A., *Langmuir*, **2009**, 25, 8292.
19. De Palma, R.; Peeters, S.; Van Bael, M. J.; Van den Rul, H. Bonroy, K.; Laureyn, W.; Mullens, J. Borghs, G.; Maes, G. *Chem. Mater.*, **2007**, 19, 1821–1831.
20. Bain, C. D.; Troughton, E. B.; Tao, Y. T.; Evall, J.; Whitesides, G. M.; Nuzzo, R. G. *J. Am. Chem. Soc.*, **1989**, 111 (1), 321–335.

**UGC Sponsored Two Day National Seminar on
GREEN CHEMISTRY FOR SUSTAINABLE DEVELOPMENT (GCSD -2017)**

April 06 - 07, 2017 at Government Degree College,
Jammikunta, Karimnagar, Telangana State, India

Cellulase Production by *Trichoderma* sp. Under Solid State Fermentation Using Delignified Rice Straw

J Sridevi

Assistant Professor in Microbiology

Government Degree College for Women (Autonomous), Begumpet, Hyderabad, 500016

Email - manikonda.sridevi@gmail.com

Abstract: Alternative substrates to produce useful chemicals such as bioethanol have been attractive. The demand for cellulases is increasing globally because of their application in the production of cellulosic bioethanol. The enzyme cellulase, a multi enzyme complex made up of several proteins, catalyses the conversion of cellulose to glucose in an enzymatic hydrolysis. The fungi belonging to the genera *Trichoderma* and *Aspergillus* are known to be potential cellulase producers. Even in the present scenario, cellulases represent a very significant operational cost. Rice straw, one of the most abundant lignocellulosic agricultural by-products available worldwide can be used as a potential source for bioethanol production. In the present study the feasibility of using pretreated (delignified) rice straw for cellulase production by *Trichoderma* sp. under solid state fermentation (SSF) technique was evaluated to produce cellulase enzyme at a lower cost. The pulverized rice straw was delignified with an alkali. This delignified rice straw was used as carbon source for cellulase enzymes production by the fungus *Trichoderma* sp. Cellulase activity of 17 U/gds was obtained with approximately 85 % (v/w) moisture, pH 5.5 for 5 days incubation at 28±2°C.

Key words: Cellulase, *Trichoderma* sp. lignocellulosic substrates, pretreatment, SSF

1. INTRODUCTION:

Cellulose is the most abundant renewable carbon resource on earth¹. It is synthesized mainly by plants and together with hemicelluloses, lignin and pectin, constitutes most of the plant cell wall material. Huge amount of cellulose yielded annually is subject to degradation by microorganisms like bacteria and fungi to provide themselves with carbon and energy source². In turn the carbon is recycled back into the ecosystem. Lignocellulosic substrates are a promising potential feedstock for bioethanol production. Different non-food lignocellulosic materials such as agricultural residues (corn stover, wheat, rice, sorghum straws, husks and bagasse), alfalfa, switch grass, woody crops, forestry residues, waste paper and other wastes (municipal and industrial) constitute the most abundant renewable feedstock³. Bioethanol production from these feedstocks could be an attractive alternative for disposal of these residues. Lignocellulosic feedstocks do not interfere with food security and contribute energy saving. They are a promising energy source for several reasons. The main reason is that bioenergy contributes greatly to sustainable development^{4,5,6}, can reduce greenhouse gas emissions. One of the lignocellulosic substrates rice straw is the most abundantly available agro waste which can be utilized as a source of cellulose by various fungi for the production of cellulases. Most of the rice straw remains unused, destroyed simply by burning leading to air pollution, which consequently affects public health⁷. Therefore, rice straw is believed to have potential as the preferential feedstock for utilization as cellulose source and subsequently for bioethanol production in Asia⁸. Rice straw contains 25-45% cellulose, 20-30% hemicellulose and 10-15% lignin⁹. To make the process of bioethanol production economical the biomass having cellulose as source of sugars can be hydrolysed by cellulases. The efficient degradation of cellulose is a complex process involving the synergistic action of a number of cellulolytic enzymes¹⁰. Fungi of the genera *Aspergillus* and *Trichoderma* are known to have good potential for cellulase production^{11,12}. Currently, most commercial cellulases, including are produced by *Trichoderma* species and *Aspergillus* species^{13,14}. For effective utilization of the cellulosic fraction of lignocellulosic substrate, delignification, that is lignin removal becomes a necessary step to gain access to cellulosic sugars. The removal of lignin is possible through a process called pretreatment which may include physical, chemical and biological methods. The effect of pretreatment of lignocellulosic materials has been recognized for a long time¹⁵. The purpose of the pretreatment is to remove lignin and hemicellulose, reduce cellulose crystallinity and increase the porosity of the materials so that the hydrolysis of complex cellulosic carbohydrates to monomeric sugars can be achieved more rapidly and with greater yields¹⁶. Solid state fermentation (SSF) using biowaste or agro waste is a potential and attractive process over Submerged fermentation (SmF). SSF technique had been used to get better yields of cellulases which is economical

due to its much lower capital investment and cheaper operating costs¹⁷. Utilization of Lignocellulosic substrates is much economical when compared to pure cellulose¹⁸. To mention about the advantages of SSF processes, it is most often cited that enzyme titers are higher than in SmF^{19,20}.

2. RESULTS AND DISCUSSION:

Microorganism: Based on the size of zones of hydrolysis, one fungal strain (*Trichoderma sp.*) was selected, isolated and cultured onto fresh PDA medium plate (Fig.2). The fungus *Trichoderma sp.* was identified based on its cultural characteristics and microscopic morphology²¹. This strain *Trichoderma sp.* was used for production of cellulase under Solid State Fermentation (SSF).

Pretreatment/Delignification: When rice straw was added with 0.2 M KOH in the ratio of 1:10 to substrate and 0.2 M KOH solution, a maximum removal 65 % of lignin was observed after 2 hrs of reaction at room temperature with a minimum sugar loss of 4.3 %.

Solid State Fermentation: Cellulase production by the isolated *Trichoderma sp.* Is shown in the table: 1. When delignified sterile rice straw was inoculated with spores of *Trichoderma sp.* and incubated for 7 days, at 28±0.5 °C, maximum cellulase yield was observed on 5th day of incubation i.e., 17 FPU/gds.

3. Discussion

Namita Bansal *et al*²², assessed various agricultural and kitchen waste residues for the production of a complete cellulase system by *Aspergillus niger* NS-2 in solid state fermentation and found higher cellulase yields (FPase 17 U/g dry substrate) with NaOH pretreated substrates compared to untreated substrates. In the present study, similar yields were obtained when KOH pretreated rice straw was used for production of cellulase under SSF. FPase was found to be 17 U/gds. An FPase activity of 6.25 U/g was obtained when untreated rice straw was used as a substrate and the organism being *Trichoderma harzianum* SNRS3²³.

4. Experimental

Microorganism

4.1 Screening Of Cellulase Producing Microorganisms

Samples from different environmental sites like damp soil, degrading wood were collected, were transported to the laboratory and stored at 4°C. The samples were subjected to tenfold Serial dilution and were inoculated by spread plate method, onto potato dextrose agar (PDA) plates for the isolation of fungi. After 4 days of incubation at 28°C, morphologically different colonies were picked and sub-cultured onto PDA slants to obtain pure cultures. Stock cultures were maintained on PDA agar slants at 4°C for subsequent use.

Hypercellulase producing fungi were selected based on the growth on phosphoric-acid-swollen cellulose (PASC) containing Mandel's agar medium. Mandel's Medium Composition (g/l): Urea: 0.3, CaCl₂.2H₂O: 0.4, KH₂PO₄: 2, MgSO₄.7H₂O: 0.3, NH₄SO₄: 1.4, Peptone: 1, Tween-80: 0.2, FeSO₄.7H₂O: 0.005, MnSO₄.7H₂O: 0.016, ZnSO₄.7H₂O: 0.014, CoCl₂.6H₂O: 0.2, PSAC: 10, Agar: 17.5, Triton-X 100: 1 ml^{24,25}. PASC was prepared by soaking cellulose powder (Hi media, Mumbai) in 1% Phosphoric Acid overnight. The Mandel's media plates were inoculated with pure cultures and incubated at 28°C for 3 days. The zones of hydrolysis were measured to check for cellulase production in comparison with a standard strain *Trichoderma reesei* NCIM 992. On the 4th day, the plates with growth were flooded with Gram's Iodine and left for 5 min., at 35°C^{26,27}. Zones of hydrolysis were observed around the colonies developed on the plates (Figs: 1,2).

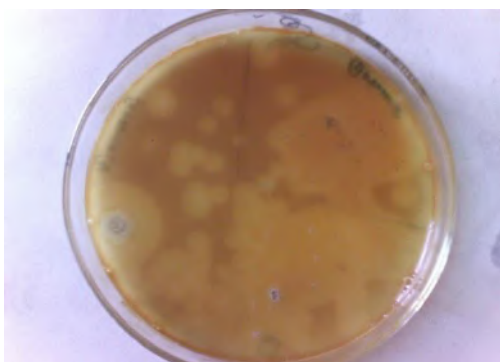


Fig:1 Zones of hydrolysis



Fig:2 *Trichoderma sp.* on PDA slant

4.2 Pretreatment / Delignification of Rice straw for SSF:

Locally procured rice straw was washed thoroughly to remove dust, air dried, pulverised to ≈ 3 mm and stored at room temperature for further use. The Rice straw was added with 0.2 M KOH in the ratio of 1:10 to substrate and 0.2 M KOH solution. and was allowed to stand at room temperature for 2 hrs. The substrate was filtered to remove the liquid portion and washed under tap water until it was neutralized. The substrate was oven dried at 50°C over night to constant weight so as to remove moisture. The delignified rice straw was stored at room temperature for further use.

4.3 Solid State Fermentation:

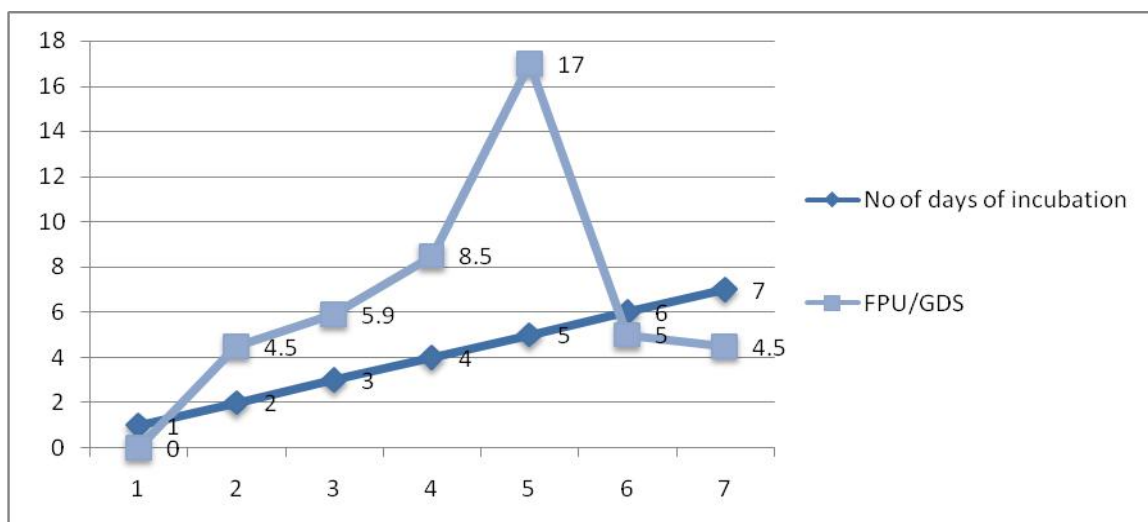
Solid State Fermentation was performed in 250 ml Ehrlenmayer flask using sterile, delignified Rice straw. The substrate was moistened with Mandel's Mineral Medium. The substrate was distributed in 1 cm layer in a 250 ml Ehrlenmayer flask with initial moisture content of 80% and autoclaved at 121°C for 15 min. 2 - 3 ml of spore suspension (1×10^6 spores/ml) of the isolated *Trichoderma sp.* was inoculated into the sterile substrate. The experiment was carried out in duplicates. The flasks were incubated at 28 ± 1 °C, for 7 days in static condition (Fig.3).



Fig: 3 Solid State Fermentation in Ehrlenmeyer flask

	Cellulase Activity in filter paper units per gram dry substrate						
	Day 1	Day 2	Day 3	Day 4	Day 5	Day 6	Day 7
FPU/gds	0.0	4.5	5.9	8.5	17.0	5.0	4.5

FPU/gds: Filter paper units per gram dry substrate



4.4 Sampling and Enzyme extraction

Samples from SSF flasks were collected after every 24 hrs. The substrate was mixed for 5 min prior to sampling process. The sample was used to determine the activity of the enzyme produced Simple contact method was used to extract the enzyme from the fermented substrate^{28,29}. The fermented samples were shaken (150 rpm) with 0.05 M Sodium Acetate buffer (pH4.5) by applying substrate:buffer (S:L 1:20) concentration for 1 h and filtered through Whatman No. 1 filter paper. The filtrates were centrifuged for 20 min at 4°C to remove spores of the organism and the supernatant of crude enzyme extract was used for enzyme assays.

4.5 Enzyme Assays

Cellulase activity (Filter Paper Activity) was analyzed on filter paper, according to Ghose³⁰. One unit of enzyme corresponds to the amount of enzyme necessary to form 1 mole of glucose per ml per minute. The reducing sugars were measured by the dinitrosalicylic acid (DNS) method according to Miller³¹ and concentration of cellulose enzyme was calculated as filter paper units per gram dry substrate (FPU/gds).

5. CONCLUSIONS:

The results indicate the potential and suitability of using lignocellulosic substrates like rice straw as a cheap source and solid substrate for large-scale production of cellulase under solid state fermentation. This also contributes to reduction in the high costs. The process may be further optimized for various parameters for a scale up fermentation.

6. ACKNOWLEDGEMENT:

Author thanks UGC-SERO, Govt. of India, for the financial support to carry out the experimental work under minor research project.

REFERENCES:

1. Monserrate E, Leschine, S B, Canale-Parola, E, *Int J Syst Evol Microbiol*, **2001**,51, 123.
2. Christos Gougoulas, Joanna Clark M & Liz Shaw J, *J Sci Food Agric*, **2014**, 94, 2362.
3. Jitendra Kumar Saini, Reetu Saini & Lakshmi Tewari, *3 Biotech*, **2015**,5, 337.
4. Van den Broek R, **2000**, 215. Sustainability of biomass electricity systems—an assessment of costs, macro-economic and environmental impacts in Nicaragua, Ireland and the Netherlands. Utrecht University.
5. Faith Demirbas M, Mustafa Balat & Havva Balat, *Energy Convers Manage*, **2009**, 50,1746.
6. Monique H, Faaij A, van den Broek R, Berndes G, Gielen D, Turkenburg W, *Biomass Bioenergy*, **2003**, 5 , 119.
7. Lynd L R, *Annu Rev Energy Environ*, **1996**, 21 ,403.
8. Solange M I & Inês R C, *Biotechnol Prog*, **2004**, 20,134.
9. Teng-Chieh H , Gia-Luen G, C Wen-Hua & Wen-Song H , *Bioresource Technology* , **2010**,101,4907.
10. Qiu Zhuo Z & WeiMin C, *Biomass and Bioenergy* , **2008**, 32, 1130.
11. Ryu D D Y & Mandels M, *Enzyme and Microbiol Technology*, **1980**, 2,91.
12. Bhat MK, *Biotechnol Adv*, **2000**, 18, 355.
13. Elad Y, *Crop Protection*, **2000**, 19,709.
14. Cherry J R & Fidantsef A L, *Current Opinion in Biotechnology*, **2003**,14, 438.
15. Kirk O, Borchert T V, & Fuglsang C C, *Curr Opin Biotechnol*, **2002**, 13, 345.
16. Mc Millan J D, Newman M M, Templeton D W & Mohagheghi A, *Appl Biochem Biotechnol*, **1999**, 77,649.
17. Mosier N, Wyman C, Dale B, Elander R, Lee Y Y, Holtzapple M & Ladisch M, *Bioresource Technology*, **2005**, 96,673.
18. Dogaris I, Vakontios G, Kalogeris E, Mamma D & Kekos D, *Ind. Crops and Products*, **2009**, 29 ,404.
19. Robinson T, Singh D & Nigam P, *Appl. Microbiol. Biotechnol*, **2001**, 55,284.
20. Cristobal Noe Aguilar, Gerardo Gutiérrez-Sánchez, PLilia A, Rado-Barragán, Raul Rodríguez-Herrera, José L, Martínez-Hernandez & Juan Contreras-Esquivel C, *Am J Biochem Biotechnol*, **2008**, 4,354.
21. Joseph Gilman C, A manual of soil fungi. Oxford and IBH publishing Co. (Revised second edition).Mandels M, Hontz I, Nystrom J, *Biotechnol Bioeng*, **1974**, 16,1471.
22. Namita Bansal, Rupinder Tewari, Raman Soni, and Sanjeev Kumar Soni, *Waste Management*, **2012**,32, 1341.
23. Nooshin Rahnama, Suhaila Mamat, Umi Kalsam, Md Shah, Foo Hooi Ling, Nor Aini Abdul Rahman & Arbakaria Arif B, *Bioresources*, **2013**, 8, 2881.
24. Montenecourt B S & Eveleigh D E, *Appl Environ Microbiol*, **1977**, 33 , 178.
25. Tansey M R, *Archives in microbiology*, **1971**, 77, 1.
26. Kasana R C, Richa Salwan, Hena Dhar, Som Dutt & Arvind Gulati, *Curr Microbiol*, **2008**, 57, 503.
27. Sridevi Jagavati, Vimala Rodhe Adivikatla, Nirupama Paritala & Venkateswar Rao Linga, *Dyn Biochem Process Biotechnol Mol Biol*, **2012**, 6, 79.
28. Meshram V G, *Intl J BioSciences, Agriculture and Technology (IJBSAT)*, II **2015**,306.
29. Krishna C & Chandrasekaran M, *Appl Microbiol Biotechnol*, **1996**, 46,106.
30. Ghose T K, *Pure Appl Chem*, **1987**, 59, 257.
31. Miller G L, *Anal Chem*, **1959**, 31,426.

UGC Sponsored Two Day National Seminar on GREEN CHEMISTRY FOR SUSTAINABLE DEVELOPMENT (GCSD -2017)

April 06 - 07, 2017 at Government Degree College,
Jammikunta, Karimnagar, Telangana State, India

Insect Growth Regulating Activity of Betulinic Acid in Controlling *Corcyra cephalonica*

N. Sridevi¹, S. Sabita Raja², N. Shilaja Yougander³

¹Asst.Professor of Zoology, Govt. Degree College for Women, Begumpet, Hyderabad,

²Professor, Dept.of Zoology, Entomological Section, Osmania University, Hyderabad.

³Lecturer, Dept.of Zoology, Sarojini Naidu Vanitha Maha Vidhyalaya, Nampally, Hyderabad

Email - sridevinamundla@gmail.com

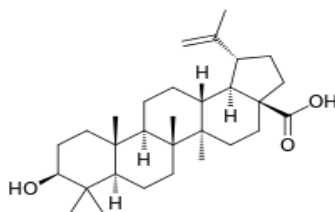
Abstract: Plants possess a variety of Phytochemicals which have been used to cure several diseases and also to control infestations of pests including stored grain pests from time immemorial. Betulinic acid, a terpenoid isolated from the bark of *Ziziphus jujuba*, exhibits Insect growth regulating activity against *Corcyra cephalonica*. The IV and V instar larva of the pest when treated with 0.1, 0.2 and 0.3% concentration of Betulinic acid in solvent Acetone, different morphogenetic abnormalities were observed resulting in formation of permanent larvae, larval-pupal intermediates, pupal-adult intermediates and deformed adults. This shows the interference of Betulinic acid with moulting process and adult eclosion. The resultant forms were ruled out from further development and reproduction. Our results suggest that Betulinic acid inhibits growth and development of the pest, *Corcyra cephalonica* suggesting its potential as an effective Insect growth regulator (IGR) in Integrated pest management modules

Key words: Phytochemicals, Betulinic Acid, *Corcyra cephalonica*, Insect growth regulator (IGR), Morphological Abnormalities.

1. INTRODUCTION:

Since time immemorial plants have been a rich source of variety of chemicals which have been used to cure several diseases related to plants and animals¹. These chemicals are generally referred to as phytochemicals. Several phytochemicals were screened to know their activity as antifeedants, repellants, and insect growth regulators (IGRs), in controlling the pests and to be used as an alternative to chemical insecticides as part of integrated pest management². Research has been carried out to assess the insecticidal properties in plants during last few decades³. Disturbance on growth and reproduction in insects were known as important factors in controlling the pests than antifeedants, fumigants, and repellants^{4, 5}. Several compounds with Juvenile hormone activity have been isolated from plants^{6, 7} and much effort has been made to utilize a variety of biologically active analogues as Insect growth regulators^{8, 9}. Most of the insect growth regulators which have been synthesized and reported with juvenile hormone activity are derived from terpene and sesquiterpenes¹⁰. These induced a variety of reproductive, developmental and morphogenetic effects on insects and are widely used to control pest^{11, 12, 13}. *Corcyra cephalonica*, rice meal moth was believed to be of eastern origin but became a cosmopolitan species spreading throughout the world. This pest mainly attacks rice grains, with secondary infestation seen in wheat, millets, ground nuts, sorghum, corn, maize and other cereals. Adults are pale brown in color, 12 mm long with a wing span of about 15 mm, with no distinct markings, darkened veins, and translucent hind wings. Head bears a projected tuft of scales, nocturnal in nature and short lived (2-4 days). Life cycle includes four stages i.e., egg, larva, pupa, and adult. Eggs are laid on grains, on containers or any surface near grains either singly or clusters. They are whitish, oval in shape, 0.5 mm long and having an incubation period of 4-5 days. Total eggs laid by female is 150-200 eggs in life time. Larvae are creamy white with a prominent head, move actively, feed on broken grains, spins a web to join the grains and become fully grown in 21-41 days, with scattered hairs on the body. After five moults (I, II, III, IV, V instars) pupae are formed. Pupation occurs in the silken cocoon. This is non feeding, immovable stage lasting for 10 days. Immediately after emergence of adults, mating and egg laying occurs. Entire life cycle is completed in 33-52 days. Larvae mainly cause the damage as these are voracious feeders, active and mobile stages. Heavy infestation causes the entire grains into webbed mass which becomes unfit for human consumption. Webbing of grains reduces market value of the grain and can greatly affect the country's economy if the damage is on large scale. To address this problem, the present study is focused on using the phytochemical; Betulinic acid a terpenoid isolated from the bark of *Ziziphus jujuba* to control the pest *Corcyra cephalonica*.

Betulinic Acid :- (3 β)-3-Hydroxy-lup-20(29)-en-28-oic acid



Betulinic acid is naturally occurring pentacyclic triterpenoid found in the bark of several species of plants such as white birch (*Betula pubescens*) and also the Ber tree (*Ziziphus jujuba*). It is well known for its pharmacological activity as anti-retroviral, anti-malarial, anti-inflammatory and anti-cancer. Research has been carried to know its insecticidal activity and very little information is known.

2. RESULTS AND DISCUSSION

The normal life cycle of *Corcyra cephalonica* includes four stages egg, larva, pupa, and adult. (Fig.1 a, b, c, d). Different concentrations of the phytochemical Betulinic acid was applied on IV and V instar larvae and pupae. Several abnormalities were noticed in treated insects (Fig.2 a, b, c, d). The survival rate of the adults decreased as per the increase in concentration.

2.1 Effect of Betulinic acid on IV instar larvae:-

25% of the larvae failed to moult and died within 2-3 days. 7% remained as permanent larvae. 30% moulted into larval-pupal intermediates. These forms suffered from ecdysal failure and their life cycle was terminated. 23% metamorphosed into abnormal pupae and 15% pupated normally (Table 1, Fig. 3).

Figures and Tables



Fig. 1 Life cycle of *Corcyra cephalonica*

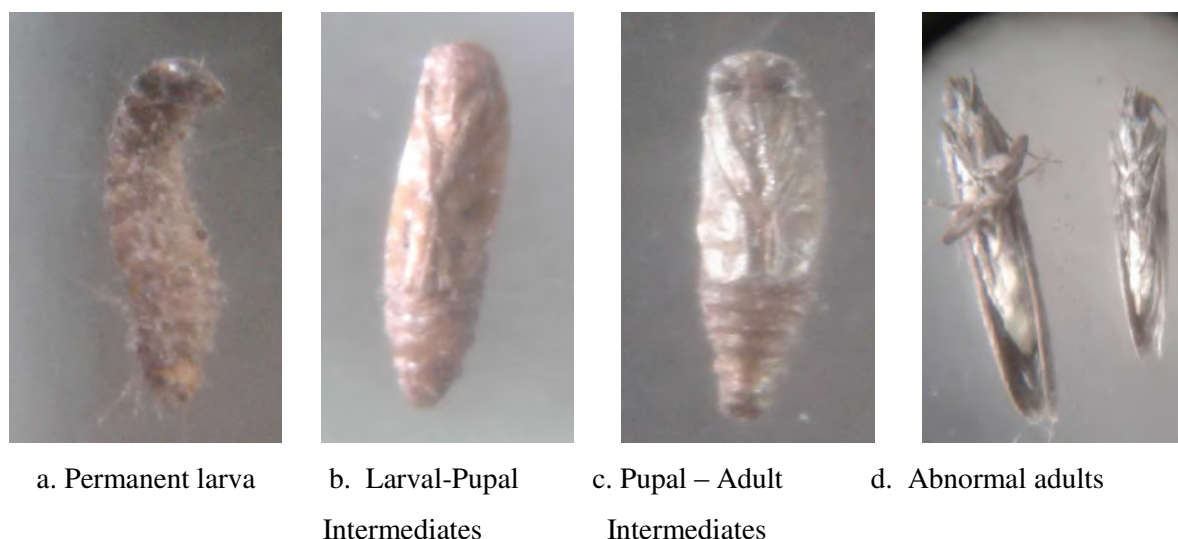


Fig 2. Morphological deformities observed in treated insects

Table 1: Morphogenetic Effects of Betulinic Acid against IV Instar Larvae of *Corcyra cephalonica*

Morphological abnormality produced by Betulinic Acid	% of IV Instar larva affected
Failed To Mould	25 %
Permanent Larvae	7%

Larval Pupal Intermediates	30%
Abnormal Pupae	23%
Normal Pupae	15%

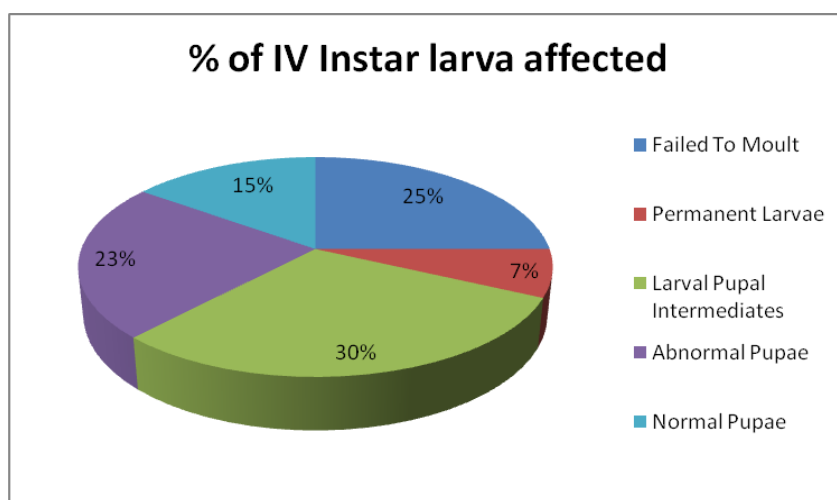


Fig. 3

2.2 Effect of Betulinic acid on V instar larvae:-

30% of the treated insects failed to pupate and finally died. 26% emerged into larval-pupal intermediates. These remained inactive and died after few days. 10% metamorphosed to abnormal pupae and failed to form adults. 15% of them emerged into pupal-adult intermediates. 7% were normal pupae but abnormal adults and 12% pupated normally. (Table 2, Fig. 4)

Table 2: Morphogenetic Effects of Betulinic Acid against V Instar Larvae of *Corcyra cephalonica*

Morphological abnormality produced by Betulinic Acid	% of V Instar larva affected
Failed To Pupate	30%
Larval -Pupal Intermediates	26%
Abnormal Pupae	10%
Pupal - Adult Intermediates	15%
Normal Pupae-Abnormal Adults	19%

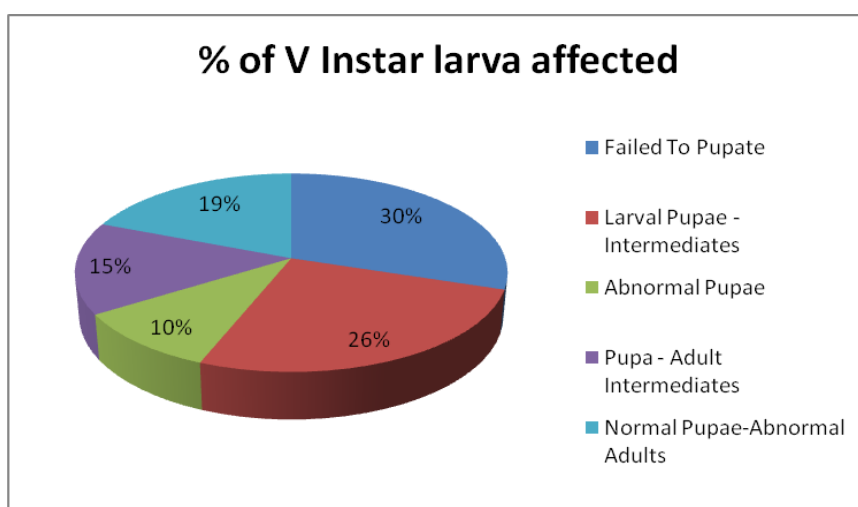


Fig. 4

2.3 Effect of Betulinic acid on Pupae:-

20% pupae failed to metamorphose to adults. 35% moulted into pupal-adult intermediates. These were ruled out from further development. 30% were abnormal adults, with long wings preventing the insects from flying and mating. 15% metamorphosed into morphologically normal adults but could not mate. Betulinic acid induced a decrease in the percentage of adult emergence compared to the controls. (Table 3, Fig. 5)

Table 3: Morphogenetic Effects of Betulinic Acid against Pupae of *Corcyra cephalonica*

Morphological abnormality produced by Betulinic Acid	% of Pupae affected
Failed To Develop into Adults	20 %
Pupal Adult Intermediates	35 %
Abnormal Adults	30 %
Normal Adults	15%

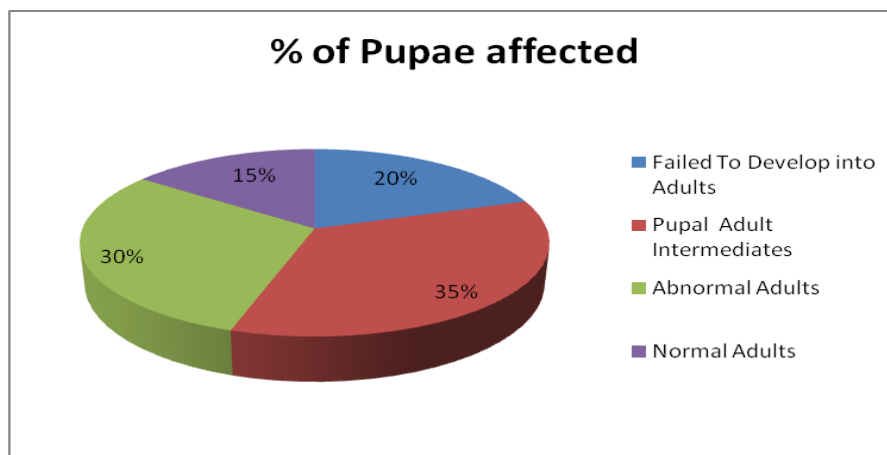


Fig. 5

3. DISCUSSION

The present study shows the effect of different concentrations of the phytochemical, Betulinic acid preventing normal development in stored grain pest, *Corcyra cephalonica*. Betulinic acid exhibits the ecdysis inhibition and the inhibition rate increased as per concentration. Application of lower concentration resulted in the formation of adults that survived only for few hours, failed to mate and oviposit. Treatment with higher concentration resulted in inhibition in pupation, formation of larval-pupal, pupal-adult intermediates, deformed pupae, and deformed adults. Similar morphogenetic effects and IGR activity of several phytochemicals were observed by the researchers. Topical application of different concentrations of neem oil on larvae and maggots of Uzifly *Exorista bombysis* have resulted in several morphogenetic deformities which were dose dependent. The moulting defects produced by the neem oil may be due to its effects on neuroendocrine system of the Uzifly or could be due to higher level of juvenile hormone than normally needed¹⁴. Treatment of *Callasobruchus chinensis* with the Cleistanthin – C influenced larval growth and moulting. The reduced amount of proteins in the ovaries of treated females of *Callasobruchus chinensis* clearly indicates that the Cleistanthin – C caused a lower uptake of proteins by the ovary¹⁵. Similarly the effect of betulinic acid on *Corcyra cephalonica* may be due to its influence on juvenile hormone activity and moulting process, resulting in permanent larvae, larval-pupal intermediates, pupal-adult intermediates and abnormal adults. Few adults which looked normal could not oviposit, which may be due to deformed ovaries by the effect of phytochemical which needs further investigation in future.

4. EXPERIMENTAL

Treatment with Betulinic acid:-

The freshly emerged adults of rice moth *Corcyra cephalonica* were collected and reared in plastic containers with a piece of cotton soaked in honey placed in it. Newly hatched larvae were creamy white in color with brown head and were transferred into a plastic jar containing coarsely crushed sorghum. Different concentrations of Betulinic acid 0.1, 0.2, 0.3% were prepared in acetone. 40 freshly moulted IV, V instar larvae and pupae were separated and 1µl of each concentration was applied topically on the abdominal region with the help of Hamilton micro syringe. The experiment was performed in triplicates. Parallel controls were treated with 1µl of acetone. After a suitable gap of time the treated insects were transferred to the diet. The treated larvae were observed daily to note the changes and the resulting abnormal intermediates were collected from the diet media. The reproductive abnormalities, moulting duration of the larvae and mortality rate of the larvae were recorded.

5. CONCLUSION:

The present investigation gives evidence that the topical application of Betulinic acid on *Corcyra cephalonica* inhibits its growth and development and suggests its potential as an insect growth regulator in integrated pest management modules.

6. ACKNOWLEDGEMENTS:

NS thank UGC-SERO, Govt. of India, for the financial support to carry out the experimental work under minor research project.

REFERENCES:

1. Abayomi Sofowora, Eyitope Ogunbodede & Adedeji Onayade, *Afr J Tradit Complement Altern Med*, **2013**, 10, 210.
2. Erum Iqbal. Kamariah Abu Salim Linda Lim B L, *JKSUS*, **2015**, 27, 224.
3. Safia Z, Aoumeur Baaliouamer, *J Saudi Chem Soc*, **2014**, 18, 925.
4. Adeniyi S A, Orjiekwe C L, Ehiagbonare J E & Arimah B D, *Int J Phys Sci*, **2010**, 5, 753.
5. Jennifer Mordue A & Alasdair Nisbet J, *An Soc Entomol* **2000**, 29 615.
6. Seok-Hee Lee, Hyun-Woo Oh, Ying Fang, Saes-Byeol An, Doo-Sang Park, Hyuk-Hwan Song, Sei-Ryang Oh, Soo-Young Kim, Seonghyun Kim, Namjung Kim, Alexander Raikhel S, Yeon Ho Je & Sang Woon Shin, *Proc Natl Acad Sci U S A*, **2015**, 112,1733.
7. Vaclav Nemecek, *Boll Ist Ent G Grandhi Univ Bologna*, **1993**, 48,67.
8. Graf J F, *Prasitol Today* **1993**, 9, 471.
9. Vardhini D, Raja S S, Varalakshmi K & Quddus K M A, *J Appl Entomol*, **2001**, 125, 479.
10. 10. Ferenc Pallos M, Peter Letchworth E & Julius Menn J, *J Agri. Food Chem*, **1976**, 24 ,218.
11. Jagannadh V & Nair V S K, *Physiol Entomol*, **1992**, 17, 56.
12. 12. Ikbal C, Ben H K & Ben H M, *Commun Agric Appl Biol Sci*, **2006**, 71, 489.
13. Vasudha L, Solanki V R, Amarjit Kaur & Sabita Raja S, *Int J Curr Res*, **2013**, 5, 022.
14. Dr. Appiya Chinnamma C, *Int J Innovative Scie and Res Tech*, **2017**, 2, 2456.
15. Anand K, Sabita Raja, *Journal of Research in Agriculture and Animal Science*, **2014** 2(8), 19-23.